Title
TARGETING DRUG TRANSPORTERS AS A NOVEL APPROACH FOR PLATINUM-BASED ANTICANCER THERAPY

Author
Li, Shuanglian

Publication Date
2010

Peer reviewed|Thesis/dissertation

TARGETING DRUG TRANSPORTERS AS A NOVEL APPROACH FOR PLATINUM-BASED ANTICANCER THERAPY

by

Shuanglian Li

DISSERTATION

Submitted in partial satisfaction of the requirements for the degree of

DOCTOR OF PHILOSOPHY

in

Pharmaceutical Sciences and Pharmacogenomics

in the

GRADUATE DIVISION

ACKNOWLEDGEMENTS

Pursuing Ph.D. training was both as a plan for the future and a commitment to the purpose of my life. Graduate school was quite an adventure for me, it was full of not only excitements, but also some frustrating times. Looking back, I would like to say that the time I spent in the graduate school was well worth it, I have grown professionally and personally. The accomplishment of my graduate study would not have been possible without the contributions of many people who have given me support and devoted their time in training and teaching me.

First and foremost, I would like to thank my advisor, Dr. Kathleen M. Giacomini, who has been a wonderful teacher, mentor, and role model for me during my graduate career. It is her who opened one new knowledge window for me, and helped me develop as a scientist and has offered me the freedom to explore new areas of research. I greatly appreciate the countless hours Kathy has spent with me over the past five years in preparing me for qualifying exams and helping me with my research and my future career. Kathy has also been instrumental in expanding presentation and writing skills. I believe that her mentorship will be a most valuable treasure from which I will benefit for years to come.

I also want to thank my thesis and qualifying exam committees, Dr. Leslie Benet, and Dr. Andrew Ko for their help and advice on my research project and their critical review of my dissertation. I am especially grateful to Dr. Leslie Benet for being a wonderful chair for my oral examination and provided great suggestions to this dissertation. Many thanks to the other members of my oral committee: Dr. Xin Chen, Dr.

Laura Bull for their support and advices on my project. In addition, I also thank Dr. Xin Chen for her friendship and generously providing the experiment materials and technique training.

I thank all members of the Giacomini laboratory, past and present, for their help in the lab, their input on my research, their time and suggestions on my oral examination and for making the lab a fun place to work. In particular, I am grateful to Ying Chen, Shuzhong Zhang and Yan Shu, who were great friends and collaborators in the past and continue to provide me with encouragement and support from different places of the world. I also own my gratitude to James Shima, Sook Wah Yee, Ligong Chen, Swati More, Cheryl Cropps, Alex Ianculescu, Kari Morrissey, Amber Dahlin, Ethan Geier, Par Matsson, and Tsuyoshi Minematsu for technique help, collaboration, and many useful discussions. Moreover, I thank all of them for their friendship and supports throughout the years.

I am indebted to all members of my family for their unconditional support and love during my graduate career. I would like to give special thanks to my parents, who passed away more than fifteen years ago. However, their boundless love and strong spirits are always there with me and supported me though all the up-downs in my life. Special thanks to my parents-in-law, for being very supportive and helpful in taking care of my dearest son, Hongting (Will) Liu. I also thank my son, Will, who is an adorable and lovely kid, and has been brightening my daily life with his purest smiles. My life is full of joy with him.

Finally, I would like to thank my husband, Qing (Jerry) Liu, for his constant love, encouragement and support, for always been there, and always cheering me up. Qing is positive person, without his love, understanding, and support, I would have never made it to this point, including this dissertation.

Shuanglian

April, 2010

ABSTRACT

TARGETING DRUG TRANSPORTERS AS A NOVEL APPROACH FOR PLATINUM-BASED ANTICANCER THERAPY

Shuanglian Li

Tissue specific targeting by design and development of influx transporter targeted compounds represents one effective approach for increasing efficacy and reducing toxicity of drugs. The overall goal of this dissertation research was to test the hypothesis that organic cation transporter 1 (OCT1) can be used as a target to deliver platinum-based chemotherapeutics to tumors with the goal of enhancing the efficacy and reducing the toxicity of these agents.

As a first step in evaluating the potential of OCT1 as a valid drug delivery target we determined the effect of OCT1 on the disposition of pyroplatin (a potent OCT1 substrate) under normal physiological OCT1 expression level *in vitro* and *in vivo*. Studies in primary hepatocytes and *Oct1* knockout mice demonstrated that Oct1 plays a role in mediating the transport of pyroplatin into the Oct1 expressing tissues and accordingly its pharmacokinetics.

The goal of the second part of this dissertation was to determine the role of OCT1 in response to pyroplatin. In particular the role of OCT1 in the toxicity and antitumor effect of pyroplatin was intensively investigated using genetically modified mice. The data supported the concept that by targeting drug influx transporters, off-target toxicities can be greatly spared. Although OCT1 mediated the accumulation of pyroplatin in

hepatocellular carcinoma, a benefit on overall survival of the mice was not observed. Further investigation is needed to elucidate the mechanisms of resistance of hepatocellular carcinoma to pyroplatin and other platinum based chemotherapies.

In the final part of this dissertation, the role of OCT1 in the disposition and drug action of oxaliplatin (a moderate substrate of OCT1) was explored. The minor effects of OCT1 on the pharmacokinetics and tissue accumulation suggested that the Oct1-mediated transport of oxaliplatin is not sufficiently high to remarkably affect its disposition *in vivo*. The increased hepatic platinum levels after multiple dosing in *Oct1*+/+ mice did not result in obvious liver toxicity, indicating that the hepatic toxicity of oxaliplatin observed in humans was not observed under the conditions used in this study and a clear role for Oct1 in oxaliplatin-induced hepatotoxicity could not be established.

TABLE OF CONTENTS

LIST OF TABLES

Chapter 1

Chapter 2

Chapter 4

Chapter 5

LIST OF FIGURES

Chapter 1

Chapter 2

Chapter 3

Chapter 4

Chapter 5

CHAPTER 1

PLATINUM TRANSPORTERS AND DRUG RESISTANCE ASSOCIATED WITH PLATINUM-BASED CHEMOTHERAPY

Introduction

In recent years, a number of important transporters have been cloned, and considerable progress has been made in understanding the molecular characteristics of individual transporters. It has now become clear that some of these are responsible for drug transport in various tissues, and are key determinants of the pharmacokinetic characteristics of many drugs in terms of their absorption, distribution, and elimination properties and ultimately their efficacy and safety [1-3]. One of the main goals in drug development is to select from a diverse array of candidates, drugs with minimal adverse effects. It is also desirable to develop drugs with high selectivity and potency for their therapeutic targets to minimize undesirable off-target effects. By enhancing delivery to their site of action, tissue specific targeting is one effective approach to both increase the selectivity and reduce the potential for side effects of drugs. Recent research has identified many types of transporters that are selectively expressed in the liver, intestine, kidney and other organs. Therefore, transporters with selective expression may be promising candidates for tissue specific drug targeting, which will subsequently lead to targeted therapy.

Cancer accounts for nearly one-quarter of deaths in the United States, exceeded only by cardiac diseases. In 2006, 559,888 deaths in the US were attributed to cancer [4]. Platinum-based drugs are among the most active anticancer agents, and cisplatin

represents one of the three most widely used cancer chemotherapeutics (Figure 1.1) [5]. However, problems with the traditional cytotoxic agents such as cisplatin and doxorubicin are their lack of tumor specificity, and therefore their toxicity to normal tissues (Figure 1.2). In 2002, oxaliplatin, a third generation platinum-based drug, was approved for the treatment of colorectal cancer. Although the platinum-based anticancer drugs cisplatin, carboplatin and oxaliplatin have similar DNA-binding properties, only oxaliplatin is active against colorectal cancer. Differences in the mechanism(s) controlling cellular uptake and efflux of these platinum compounds have gained more attention and are now considered to be among the major mechanisms contributing to their disparate activities. In particular, interactions with organic cation transporters, OCTs, are thought to play a role in both the tumor specificity and the adverse effects of currently available platinum drugs. In this dissertation, the concept of transporter-mediated drug targeting is fully explored by studying oxaliplatin and is extended by studying an emerging platinum analogue, pyroplatin, which has increased selectivity for OCTs.

The introductory chapter is divided into two major sections: **I.** Overview of platinum complexes (Figure 1.1); **II.** Dug transporters associated with tumor resistance to platinum drugs (Figure 1.3). In the first section, major platinum compounds including platinum drugs that were approved for marketing in US and platinum compounds that are under clinical development are described. Initially the major focus of platinum drug development was to improve drug safety. Post carboplatin, the focus has been on agents that circumvent cisplatin resistance (oxaliplatin and picoplatin). The development of an orally administered platinum compound, satraplatin, was aimed to improve patient compliance and quality of life. The alternative to mononuclear platinum compounds

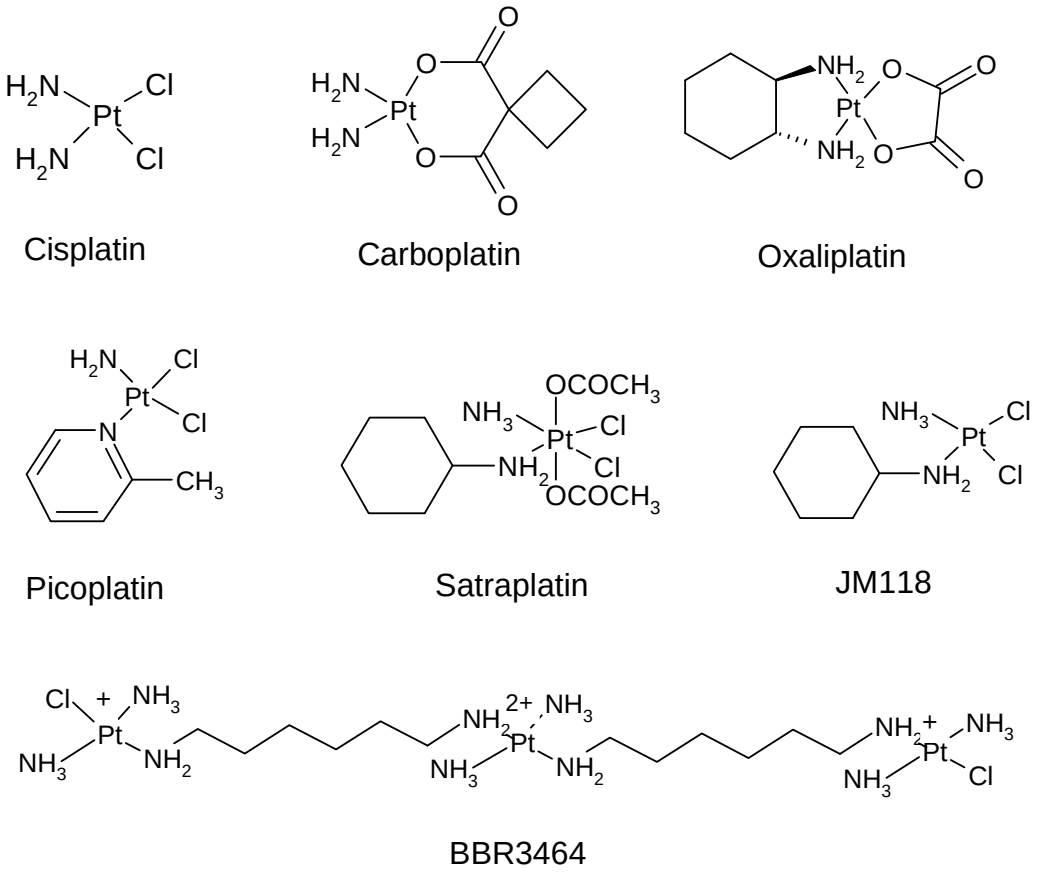

Figure 1.1. Chemical structures of platinum compounds.

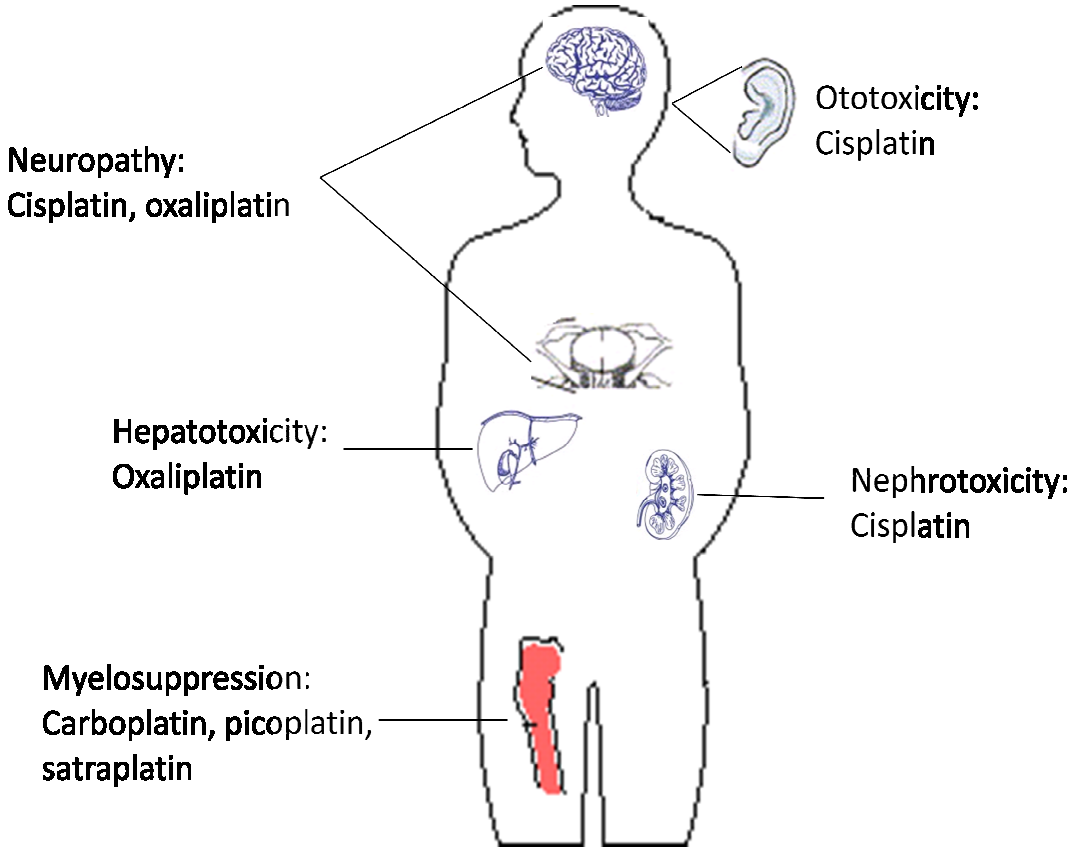

Figure 1.2. Major toxicities associated with treatment with platinum agents.

focused on polynuclear platinum compounds that led to the identification of BBR3464. In the second section, transporters that play a role in resistance and sensitivity to cisplatin, such as copper transporters (CTRs), organic cation transporters (OCTs) and multi-drug resistance related transporters (MDRs), are described (Figure 1.3). These transporters contribute to cisplatin resistance through the reduction of drug accumulation in the cell. Finally, a summary of the major findings in each chapter of this dissertation is presented.

I. Overview of Platinum Complexes

The platinum coordination complex cisplatin, cis-diaminedichloroplatinum(II) (Figure 1.1) was originally synthesized and described in 1845, and was known as Peyrone's chloride. However, its potent antitumor properties were not realized until the late 1960s. Soon after the discovery of its anticancer properties, cisplatin was approved by the US Food and Drug Administration (FDA) in 1978. Since then, cisplatin has played a central role in cancer chemotherapy, especially for testicular cancer, for which the overall cure rate exceeds 90%, and is nearly 100% for early stage disease [6]. However, the drug possesses significant limitations in being markedly toxic to many normal tissues, exhibiting nephrotoxicity, peripheral neurotoxicity and ototoxicity [7]. Moreover, many tumors are either intrinsically resistant or acquire resistance to the antitumor effects of the drug. These limitations have driven intensive synthetic efforts to discover new platinum-based drugs, concentrating on three broad themes: (1) attempts to reduce the severe side effects associated with cisplatin treatment; (2) attempts to find platinum agents that are active against cisplatin-resistant tumors; and (3) attempts to overcome the poor oral bioavailability.

The initial driver for new platinum drug development was to discover a less-toxic analogue that retained anticancer activity. This resulted in the development of carboplatin (Figure 1.1) and its clinical introduction in the mid-1980s [8, 9]. Carboplatin, a second generation platinum analog, was synthesized based on the hypothesis that a more stable leaving group than chloride might lower toxicity without affecting antitumor efficacy. This hypothesis turned out to be correct. One notable distinction between cisplatin and carboplatin is the difference in the spectrum of toxicities. Carboplatin rarely results in nephrotoxicity and peripheral neuropathy, with its major toxicity being myelosuppression principally thrombocytopenia [10].

The second initiative for new platinum drug development was to overcome tumor resistance to cisplatin, these efforts have resulted in the approval of oxaliplatin (Figure 1.1) in Europe in 1999 and in the United States in 2002 [9]. Oxaliplatin (a third generation platinum analog) shows no inheritant cross resistance with both cisplatin and carboplatin; in fact, it is the first platinum analog to demonstrate activity in colon cancer. In combination with infusional 5-fluorouracil/leucovorin (5-FU/LV), oxaliplatin produced significantly higher response rates and increased median time to progression and median survival times [11]. Oxaliplatin shows a very favorable toxicity profile. The drug is essentially devoid of nephrotoxicity, is less toxic to the gastrointestinal tract and less myelotoxic. The most common toxicity associated with oxaliplatin treatment is peripheral neuropathy, which ranges from acute and transient to a cumulative neuropathy. Recently, use of oxaliplatin has been associated with development of hepatic lesions, which include sinusoidal alteration, portal hypertension, increase in transaminases, gammaglutamyl transpeptidase and alkaline phosphatase, and steatohepatitis [12, 13].

Since the development of liver injuries may limit the ability to perform an extensive hepatectomy and can contribute to postoperative patient morbidity and mortality, hepatic toxicity is now included in the list of adverse effects of oxaliplatin.

With the increasing understanding and elucidation of mechanisms of tumor resistance to platinum drugs, a mechanism-directed drug development approach was adopted. A novel class of sterically hindered platinum complex has been designed and synthesized based on the rationale that the increased steric bulk introduced at the platinum center leads to a reduced susceptibility to inactivation by elevated intracellular thiol-containing species such as glutathione, and metallothionein in comparison to cisplatin [9]. Picoplatin (cis-amminedichloro, 2-methylpyridine, platinum (II)) (Figure 1.1), considered a third or even fourth generation platinum drug, emerged from a panel of sterically hindered 'pyridine platinum complexes' due to its reduced reactivity with sulphur ligands, unique DNA binding properties and ability to circumvent several of the major resistance mechanisms that manifest in cisplatin-resistant tumor cell lines [14]. Picoplatin has shown evidence of antitumor activity in phase II trials of platinum-sensitive ovarian cancer and cisplatin-resistant small cell lung cancer. The median time to progression of 180 days and median time to death of 402 days was achieved in a platinum-sensitive ovarian cancer trial. The overall response rate was 15.4% in the cisplatin-resistant second line small-cell lung cancer trial [14]. Based on these data, the sponsoring company, Poniard, conducted a phase III trial of picoplatin in patients with small-cell lung cancer. However, the data analysis showed that the study did not meet its primary endpoint of increasing overall survival in comparison to supportive care without chemotherapy. The data suggested a potential trend toward a survival advantage in

SCLC patients treated with picoplatin and best supportive care compared to best supportive care alone [15]. Currently, picoplatin is in phase-II clinical trials for the treatment of colorectal cancer and castration-resistant prostate cancer. Clinical studies with picoplatin have revealed dose-limiting toxicities similar to those of carboplatin, with reversible thrombocytopenia and neutropenia observed but no marked nephrotoxicity or neurotoxicity [9].

The success of the less toxic cisplatin analog, carboplatin, provided early testimony to the importance of addressing patient quality of life in the chemotherapy of cancer. Both cisplatin and carboplatin are administered by intravenous infusion. For better patient compliance and minimized health care cost, the idea of developing an orally available platinum drug with "carboplatin-like" side effects emerged shortly after the introduction of carboplatin itself into phase I. Satraplatin (bis-acetato-ammine-dichloro-cyclohexylamine platinum(IV)) (Figure 1.1) was originally developed to be an orally active version of carboplatin. It is a fourth-generation platinum analog. The lipophilicity and stability of satraplatin allow its oral administration, making it easier and convenient for the patients. Satraplatin has been generally well tolerated. The most frequent adverse effects were noncumulative myelosuppression such as grade II – III neutropenia, thrombocytopenia and anemia. Among non-hematological events, nausea, vomiting and diarrhea were common. Unlike cisplatin, however, satraplatin was not associated with ototoxicity and nephrotoxicity. Satraplatin has been investigated in numerous clinical trials and appears to have clinical activity against a variety of malignancies such as breast, prostate and lung cancer [16]. However, an FDA-approved indication has not yet been achieved. The only Phase III trial with satraplatin was conducted in pretreated metastatic

castrate-resistant prostate cancer (CRPC), revealing an improvement in progression-free survival but no overall survival benefit [17]. Future development would have to include designing trials in other malignancies where cisplatin is of benefit

In an attempt to find alternatives that show activity in cisplatin-resistant cells and possess broader profile of antitumor activity, polynuclear platinum compounds comprise a further unique class of anticancer agents with distinct chemical and biological properties discrete from their mononuclear counterparts. In 1998, the first drug from this class, BBR3464, entered Phase I clinical trials. BBR3464 (Figure 1.1) is a trinuclear platinum compound, and forms interstrand crosslinks over a much longer range than the "classical" cisplatin compounds. However, the clinical development of BBR3464 was stopped after initial phase II trials showed a relatively poor response rate.

The three approved platinum drugs, cisplatin, carboplatin and oxaliplatin, continue to have a major role in contemporary medical oncology. However armed with newly acquired information concerning mechanisms of action and tumor resistance, it is likely that a mechanism-based drug design will accelerate the production of more promising platinum analogs. In addition, strategies in improving delivery of platinum drugs, co-administration of platinum drugs with pharmacological modulators of resistance mechanisms and combining platinum drugs with new molecularly targeted drugs might also provide future clinical benefits.

II. Drug Transporters Associated with Tumor Resistance to Platinum Drugs.

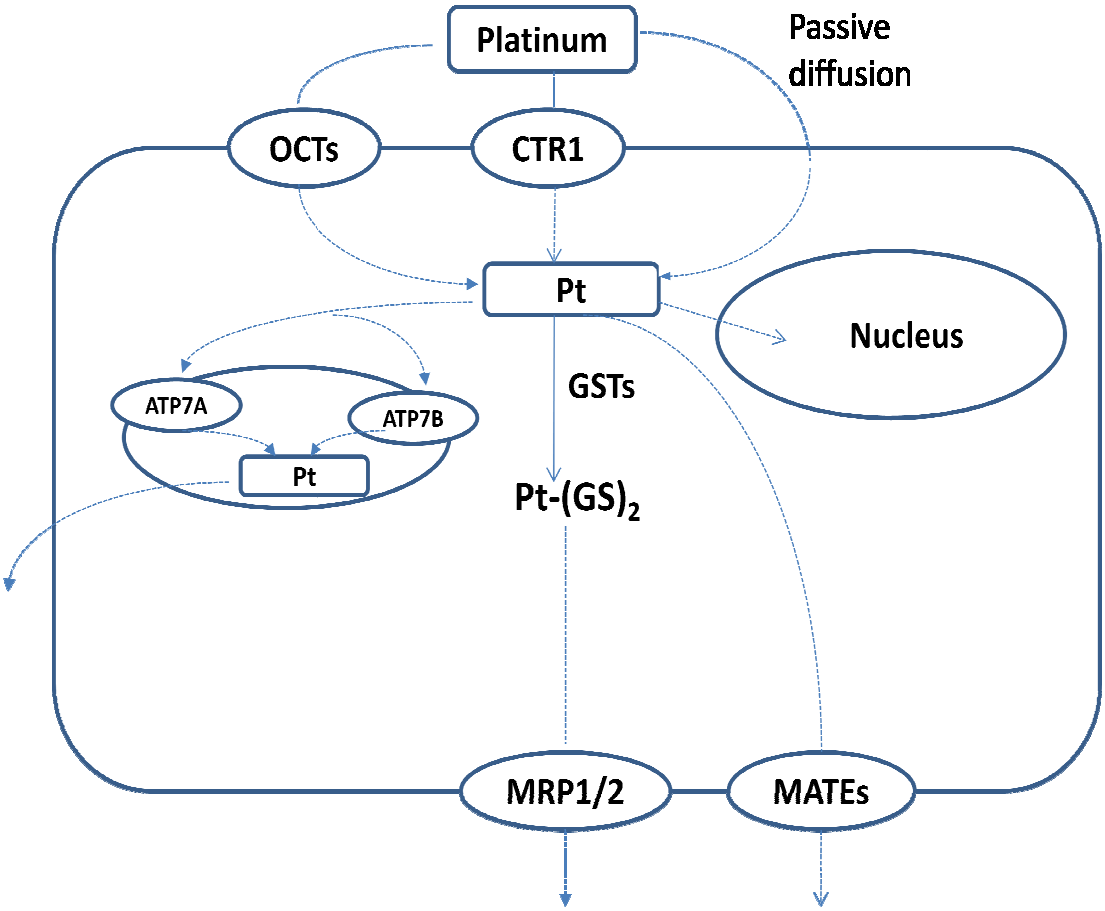

Figure 1.3. Representation of the candidate transporters involved in the transport of platinum containing drugs.

Platinum drugs, including cisplatin, carboplatin, and oxaliplatin have been used clinically for more than 30 years as part of the treatment of many types of cancers. Table 1.1 lists the major indications for these FDA-approved platinum drugs. However, these platinum drugs have also been used in other types of cancers, including head and neck, cervical, lung, and relapsed lymphoma. The cytotoxicity of platinum drugs arises primarily from covalent binding to DNA after aquation to form monoaqua and diaqua complexes [18, 19]. This chemistry initiates a series of biochemical cascades, eventually leading to cell death [18, 20]. Treatment with these agents is characterized by resistance, both acquired and intrinsic. In recent years, considerable information has been obtained about the mechanisms underlying tumor resistance to these agents [9]. Resistance can develop as a result of decreased influx or increased efflux of drug, although other mechanisms including increased cytoplasmic detoxification via elevated glutathione and/or metallothionein levels, increased DNA repair of platinum-DNA adducts, and increased cellular tolerance to platinum-DNA adducts may lead to resistance to platinum agents in combination with altered platinum transport or alone. In fact, a common observation, repeatedly reported over many years, in many tumor cells with acquired resistance to cisplatin is that of reduced platinum accumulation in comparison to the parental cells [21]. The intracellular concentration of unbound platinum agents is a balance of uptake processes into the cell, efflux processes out of the cell, binding to intracellular constituents and elimination mechanisms (Figure 1.3). Copper transporters have been shown to have a substantial role in the homeostasis of cisplatin, and are also thought to be key transporters in cisplatin resistance. Increasingly, other transporters have been reported to play a role in tumor resistance to platinum agents (Figure 1.3).

Table 1.1. Indications for FDA-approved platinum drugs

Platinum drugs	Indication	Approved use	Approval year
Cisplatin	First line treatment of metastatic testicular cancer	In established combination therapy with other approved chemotherapeutic agents, such as combination therapy with Platinol, Blenoxane and Velbam	1978
	First line treatment of metastatic ovarian tumors	In established combination therapy with other approved chemotherapeutic agents, such as combination therapy with Platinol and Adriamycin.	1978
	Secondary therapy of metastatic ovarian tumors	A single agent therapy	1978
	First line therapy of transitional cell bladder cancer	A single agent therapy	1993
Carboplatin	Secondary treatment of advanced ovarian carcinoma	A single agent therapy	1989
	First line treatment of advanced ovarian carcinoma	In established combination with other approved chemotherapeutic agents, such as combination therapy with cyclophosphamide	1991
Oxaliplatin	Adjuvant treatment of stage III colon cancer	In combination with infusional 5-FU/LV	2002
	First line treatment of advanced colorectal cancer	In combination with infusional 5-FU/LV	2004

Copper influx transporter 1

Copper influx transporter 1 (CTR1), encoded by SLC31A1, is an evolutionarily conserved copper influx transporter present in plants, yeast, and mammals, and is the main copper importer in mammalian cells. The human version, hCTR1, is a 190 amino acid protein with three transmembrane domains residing mainly in the plasma membrane. hCTR1 is expressed in all tissues and is a key player in the exquisite homeostatic regulation of intracellular copper levels to ensure that nutritional delivery of copper to enzymes, such as cytosolic Cu,Zn-superoxide dismutase and mitochondrial cytochrome oxidase, is maintained while surplus copper, which can cause toxicity, is avoided [22, 23]. Two recent studies in transgenic mice have demonstrated that CTR1 is essential for the survival of mammalian embryos [24, 25].

The role of CTR1 in mediating transport and sensitivity to the platinum drugs was first demonstrated in yeast and later demonstrated in mouse and human cells [26, 27]. Deletion of yeast CTR1 gene markedly reduces accumulation of cisplatin and increases resistance to cisplatin [26, 27]. Loss of CTR1 function in yeast also impairs uptake of several platinum analogs including carboplatin, oxaliplatin and picoplatin [27]. A study in mouse embryo fibroblasts lacking either one or both mCTR1 alleles demonstrated a progressive reduction in drug uptake and increase in drug resistance with loss of first one and then both mCTR1 alleles [26]. Holzer et al. also reported that accumulation of platinum in *Ctr1-/-* mouse embryo fibroblasts was only 35-36% of that in the *Ctr1+/+* cells, when exposed to cisplatin, carboplatin and oxaliplatin. The *Ctr1-/-* cells were 3.2-fold resistant to cisplatin, 2.0-fold resistant to carboplatin, 1.7-fold resistant to oxaliplatin [28]. Comparing the mRNA level of CTR1 in A2780cis-resistant ovarian and HeLa CK

cisplatin-resistant cell lines with their parental cells, resistant cells expressed lower levels of hCTR1than their sensitive counterparts. Accordingly, the resistant variants exhibited lower intracellular platinum concentrations, lower DNA platination and higher IC_{50} values than their respective parental cells [29]. hCTR1 gene expression in oxaliplatin-resistant HT29 colon cancer cells was found to be down-regulated in comparison to oxaliplatin sensitive counterparts [30]. In contrast, Song et al. showed that of five resistant small-cell lung cancer (SCLC) cell lines, only one (SR2) showed a substantial reduction in hCTR1 protein expression, along with a reduction in the accumulation of cisplatin, carboplatin and oxaliplatin [31]. Moreover, a correlation analysis in seven human colorectal cancer cell lines revealed that the cytotoxicity of cisplatin, carboplatin and oxaliplatin was not affected by the level of hCTR1 [32]. Collectively, these studies suggest that CTR1 contributes to platinum drug accumulation and the development of resistance, which may be a tumor specific phenomena.

Larson et al. showed that re-expression of CTR1 in the *Ctr1-/-* cells restored both cisplatin uptake and cytotoxicity. The growth of *Ctr1-/-* tumor xenografts, in which CTR1 levels were restored by infection with a lentivirus expressing wild-type CTR1, was reduced by a single maximum tolerated dose of cisplatin *in vivo*, whereas the *Ctr1-/-* xenografts failed to respond at all. The result suggests that CTR1 is a major determinant of responsiveness to cisplatin both *in vitro* and *in vivo* [33]. Involvement of human CTR1 in regulation of platinum drug uptake and cytotoxicity was further demonstrated by Song et al. who showed that cisplatin-resistant human cancer cells transfected with hCTR1 cDNA construct exhibited increased transport activities of cisplatin, carboplatin and oxaliplatin. Moreover, these transfected variants were sensitive to the toxicities of all

these platinum drugs [31]. Using transfected cell lines, BBR3464, a cationic trinuclear platinum drug, has also been shown to use hCTR1 to enter cells. Consistent with the increased cellular uptake, the cytotoxicity of cisplatin and BBR3464 was also enhanced in hCTR1 transfected A2780 cells, although the downstream effects are different for these two drugs [34].

However, there are some controversial reports in terms of the role of CTR1 in the cisplatin toxicity. Holzer et al. reported that the there was only a marginal increase in sensitivity to the cytotoxic effect of cisplatin, and no increase in the extent of cisplatin-DNA adduct formation, although the platinum accumulation in the ovarian carcinoma cell line A2780 with transfection of hCTR1 construct was found to be higher than the control A2780/empty vector cells after exposure to cisplatin [35]. These data suggest that the hCTR1-mediated cisplatin uptake routes the drug to other intracellular compartments from which they do not have ready access to their key cytotoxic targets. Another study showed that the overexpression of a functional CTR1 in a human cell line characterized by impaired cisplatin uptake did not restore cellular drug accumulation to the level of the parental cell line, and accordingly the cisplatin sensitivity was not restored as well [36]. Moreover, overexpression of hCTR1 in the HEK293 cell line did not result in increased sensitivity to cisplatin [37]. The reasons for these conflicting results are not clear, but since the mechanisms of cell killing by the platinum drugs are multi-factorial, it may not be surprising that exceptions exist.

Exposure of human ovarian carcinoma cells to cisplatin causes rapid degradation of hCTR1 in a concentration- and time-dependent manner. The effect was observed at

cisplatin concentrations within the range found in the plasma of patients being treated with cisplatin, and it occurred very quickly relative to the half-life of the drug [38]. Cisplatin-induced degradation of CTR1 has now been documented in most but not all types of cells [39]. The down regulation of CTR1 in *Ctr1*+/+ mouse embryo fibroblasts by cisplatin resulted in function change of CTR1 that was characterized by a reduced initial influx of cisplatin, carboplatin and oxaliplatin, and which subsequently rendered cells resistant to even high concentrations of cisplatin [33]. The rapid degradation produced by cisplatin provides an explanation for why the greatest effect of CTR1 on cisplatin transport is observed during the initial phase of cisplatin uptake [38]. A very recent study showed that levels of the hCtr1 protein at the plasma membrane of HEK293 cells were reduced when cells were exposed to elevated copper. This decrease in surface hCTR1 levels was associated with an increased rate of endocytosis and rapid degradation of the hCTR1 protein [40]. Both endocytosis and protein degradation are considered important to the amount of hCTR1 expressed in yeast and in the plasma membrane of mammalian cells. In addition, cisplatin was found to crosslink the N-terminal domain of hCTR1 at very high concentrations, suggesting that cisplatin itself regulate CTR1 transporter and, as a result, modulate cisplatin resistance [41].

Although CTR1 has been shown to be capable of transporting a number of platinum analogs, there are clear exceptions that suggest some structural discrimination is exercised by this transporter. Holzer et al. have shown that CTR1 regulates the cellular accumulation of cisplatin, carboplatin and oxaliplatin at concentrations attainable in humans. However, at 5-fold higher concentrations, oxaliplatin accumulation becomes CTR1-independent, while accumulation of cisplatin and carboplatin is still CTR1

dependent [28]. The results indicate that oxaliplatin is a substrate for some other cellular entry mechanism, a feature consistent with its different clinical spectrum of activity. Knockout of CTR1 in murine embryo cells has been found to increase the resistance to cisplatin and reduce cellular accumulation of cisplatin [28]. However, CTR1 knockout had no effect on sensitivity to the satraplatin active metabolite, JM118, and its uptake, indicating JM118 is not a CTR1 substrate [42]. Human ovarian carcinoma 2008 cells selected for cisplatin resistance accumulated less cisplatin and less JM118 reflecting a mechanism involving reduced accumulation. In contrast, the 2008 cells selected for JM118 resistance accumulated significantly more instead of lower platinum than the parental cells when exposed to JM118 or cisplatin indicating a detoxification process that involves intracellular sequestration [43]. In a recent study, hCTR1 has also failed to show any significant contribution to the cytotoxicity of picoplatin, a third-generation platinum agent [44].

Overall, the evidence is as follows: 1) absence of CTR1 expression in yeast, mouse, and mammalian cells results in reduced cisplatin accumulation; 2) over-expression of CTR1 in mammalian cells results in increased accumulation of platinum drugs; 3) cisplatin induces rapid degradation of hCTR1 in human cell lines supporting a role for CTR1 in the transport of platinum drugs. Given the huge body of literature concerning the role of CTR1 in the efficacy and toxicity of platinum agents, it is not surprising to see that there are some controversial observations. The difference in the interactions of CTR1 with different platinum analogs may indicate that there are other uptake mechanisms involved in addition to CTR1.

ATP7A and ATP7B

ATP7A and ATP7B are copper transporters that sequester copper from the cytoplasm into the trans-Golgi network for loading onto ceruloplasmin and other copper-requiring enzymes and subsequent export from the cell [45]. ATP7A is expressed in the majority of tissues except for the liver, while ATP7B expression is found mainly in the liver, but also in the kidney and placenta [45]. Mutations in these transporters have been related to the human genetic diseases of Cu metabolism, Menkes and Wilson's diseases, respectively.

The concept that copper efflux transporters might mediate cisplatin resistance was first introduced by Komatsu et al., who reported that overexpression of ATP7B by transfecting an ATP7B expression construct into the epidermoid carcinoma K-B-3-1 cell line resulted in the development of resistance to both cisplatin and copper with an enhanced efflux rate of cisplatin and reduced accumulation of cisplatin in the transfected cells [46]. In the same study, ATP7B was found to be overexpressed in cisplatin-resistant prostate carcinoma PC-5 cells but not in the parental PC-3 cells and the revertant PC-5R cells [46]. Nakayama et al. subsequently examined the relationship between mRNA expression level of ATP7B and sensitivity to cisplatin in nine human ovarian carcinoma cell lines and showed that cells with increased ATP7B expression were less sensitive to cisplatin [47]. Studies by Katano et al. extended these findings by showing that ATP7B-transfected 2008 cells not only reduced the whole cell and DNA content of platinum in cisplatin- and carboplatin-treated cells but also increased the rates of the primary and secondary phases of efflux for both of these platinum drugs [48]. ATP7B was shown to

be frequently overexpressed in several solid tumors, including gastric, breast, esophageal, hepatocellular, colorectal, uterine and oral squamous cell carcinomas [49-54]. Moreover, an association was also found between the level of ATP7B expression and presence of poorly or undifferentiated cells in tumors. Additionally, 82 primary ovarian carcinomas were profiled for expression of several known resistance genes including ATP7B, MDR1, MRP1, MRP2, LRP, and BCRP. With the exception of ATP7B, none were indicators for resistance of ovarian cancer to cisplatin [47]. On the other hand, ATP7B silencing in cisplatin-resistant cells resulted in 2.5-fold reduction of cisplatin IC_{50} values and increased DNA adduct formation. For *in vivo* therapy experiments, ATP7B siRNA was highly effective in reducing tumor growth in combination with cisplatin, causing 70-88% reduction in tumor weight compared with controls [55]. Also consistent with a role of ATP7B as an efflux transporter of the platinum drugs is the observation by confocal microscopy that an ECFP (enhanced cyan fluorescent protein)-tagged ATP7B (ATP7B-ECFP) colocalized with a fluorescein labeled cisplatin (F-cisplatin) and that both cisplatin and F-cisplatin caused trafficking of the ATP7B-ECFP containing vesicles toward the cell's surface [56]. The data published so far provide strong evidence that ATP7B mediates resistance to cisplatin by sequestering it into vesicles of the secretory pathway for export from the cell.

ATP7A is also likely to play a role in the transport of platinum-based antitumor agents. Human ovarian carcinoma cells transfected with an ATP7A expression construct confer resistance to cisplatin, carboplatin and oxaliplatin. Interestingly, overexpression leads to increased rather than decreased overall platinum drug accumulation, suggesting that the overexpressed transporters may alter intracellular platinum distribution to a non-

toxic compartment [57]. However, platinum drugs did not trigger ATP7A relocalization. Reports also showed that ATP7A is overexpressed in cisplatin-resistant ovarian carcinoma cell lines and the overexpression of ATP7A is causative for cisplatin resistant [58]. Patients whose ovarian tumors exhibited increased ATP7A expression after platinum-containing regimens were found to exhibit poorer actuarial survival than patients without increased ATP7A post-treatment [59]. Confocal microscopy demonstrated that ATP7A and F-cisplatin colocalized in the vesicular structures in human ovarian carcinoma 2008 cells [60]. These results suggest that the function of ATP7A is mainly in the sequestration of platinum drugs within the secretory vesicles.

The role of ATP7A/B is also platinum drug-type dependent and controversial; cells selected with JM118 did not show expression of either ATP7 gene [61]. Rabik et al. reported that overexpression of ATP7A or ATP7B in human Menkes' (Me32a) disease fibroblasts resulted in increased resistance to cisplatin, but not to carboplatin or oxaliplatin [37]. A correlation analysis also revealed that the level of ATP7A affects the cytotoxicity of cisplatin and oxaliplatin but not carboplatin [32]. Whereas Samimi et al. showed that transfection of ATP7A or ATP7B into Me32a fibroblasts conferred resistant not only to the cytotoxic effects of cisplatin, but also to carboplatin. Higher expression levels of both transporters conferred hypersensitivity rather than resistance to oxaliplatin [42]. In agreement with hypersensitivity to oxaliplatin in ATP7A/7B overexpression cells, oxaliplatin-resistant cells exhibited low instead of high basal expression levels of ATP7A and ATP7B compared to parental HT29 [30]. However, studies conducted by Martinez-Balibrea et al. and Thelie et al. showed that increased levels of ATP7B were associated with poor outcome in colorectal cancer patients receiving oxaliplatin-based

chemotherapy, and the suppression of ATP7B due to 5-FU treatment was accompanied by a significant sensitization to oxaliplatin [62, 63].

Given the involvement of ATP7A and ATP7B in cellular resistance to platinum drugs such as cisplatin, the polymorphisms of ATP7A and ATP7B may thus possibly affect the efficacy or toxicity of platinum drugs. Recently, Fukushima-Uesaka et al. sequenced the ATP7A and ATP7B genes of 203 Japanese subjects to survey novel variations of these genes and found that 38 and 61 genetic variations were detected in ATP7A and ATP7B, respectively [64]. However, the functional effects of these variants were not evaluated. If these variants alter function of the two transporters, the results would provide fundamental and useful information for genotyping the platinum drug transporters ATP7A and ATP7B in the Japanese and probably other populations.

Organic cation transporters

The polyspecific organic cation transporters (OCTs) belong to solute carrier family 22 (SLC22), which has three members: OCT1, OCT2 and OCT3 (SLC22A1-3). The OCTs mediate intracellular uptake of a broad range of structurally diverse organic cations with molecular weight generally less than 400 Da [65, 66]. Substrates of OCTs include endogenous compounds, such as choline, creatinine, and monoamine neurotransmitters; clinically used drugs, such as metformin, procainamide and pindolol; and a variety of xenobiotics, such as tetraethylammonium (TEA, model cation), N-methylquinine, and 1-methyl-4-phenylpyridinium (MPP^+) [65]. In humans, OCT1 is primarily expressed in the liver [66-68] and less so in the intestine[69], whereas OCT2 is predominantly expressed in the kidney [66, 68]. OCT3 has a more widespread tissue

distribution including placenta, prostate, heart, liver, and skeletal muscle [65]. Knockout mouse models have been generated for all three organic cation transporters including *Oct1-/-*, *Oct2-/-*, *Oct1/2-/-* and *Oct3-/-* mice. All these mice are viable and display no obvious phenotypical abnormalities, indicating that OCTs are not essential for normal physiological functioning in mice or there is a functional redundancy between the different OCTs.

The OCTs were first investigated as candidate uptake transporters of platinum compounds owing to their expression in tissues associated with cisplatin toxicities, and early observations that cisplatin inhibited the active uptake of TEA, a prototypical substrate for OCTs, in rat kidney slices [70]. Table 1.2 summarizes the studies reported to date on platinum substrate specificity for OCT1, OCT2 and OCT3. It has been observed that cisplatin induced nephrotoxicity occurs following cisplatin entry into the proximal tubule from the basolateral site, and that the toxicity is ameliorated in the presence of cimetidine, an OCT2 inhibitor, suggesting the involvement of basolateral drug transporters in the cisplatin uptake [71, 72]. Moreover, in epithelial cells derived from proximal tubules of opossum (OK cell line) basolateral-to-apical transport of cisplatin is higher than apical-to-basolateral transport [73]. Co-incubation of cisplatin with tetraethylammonium (TEA, a model substrate for organic cation transporters, OCT) significantly decreased accumulation and transport of cisplatin from the basolateral medium in OK cell line [73] and also in rabbit isolated proximal tubuli [73, 74]. Given the fact that OCT2 is expressed mainly in the proximal tubules of the kidney, which is the major site of cisplatin-induced renal injury, it has been assumed that OCT2 is one of the main transporters of cisplatin. Pan et al. reported that TEA uptake by NIH3T3 cells stably

Table 1.2. Observations on cisplatin, oxaliplatin, carboplatin and picoplatin substrate specificity for OCT1, OCT2 and OCT3

Cisplatin	**OCT1**	**OCT2**	**OCT3**
Pan et al. (1999) [75]	-	The uptake of TEA was inhibited by cisplatin in cells transfected with rOCT2	-
Briz et al. (2002) [76]	The uptake of cisplatin was not enhanced in oocytes overexpressing hOCT1	The uptake of cisplatin was not enhanced in oocytes overexpressing hOCT2	-
Yonezawa et al. (2005) [77]	-	The accumulation of cisplatin was increased in rOCT2-HEK cells; the cytotoxicity and the transport of cisplatin was inhibited by cimetidine and corticosterone in rOCT2-HEK cells	-
Ciarimboli et al. (2005) [78]	The uptake of 4-[4-(dimethyl-amino)styril]-methylpyridinium (ASP) was not inhibited by cisplatin in hOCT1-HEK cells; the uptake of ASP was not inhibited by cisplatin in human hepatocyte couplets	The uptake of ASP was inhibited by cisplatin in hOCT2-HEK cells; The uptake of cisplatin was increased in hOCT2-HEK cells; The uptake of ASP was inhibited by cisplatin in freshly isolated human proximal tubules from patients	-
Yonezawa et al. (2006) [79]	The cytotoxicity and accumulation of cisplatin was enhanced in hOCT1-HEK cells	The cytotoxicity and accumulation of cisplatin was enhanced in hOCT2-HEK cells; the uptake of cisplatin was inhibited by cimetidine in hOCT2-HEK cells	The cytotoxicity and accumulation of cisplatin was not enhanced in hOCT3-HEK cells
Zhang et al. (2006) [80]	The uptake of cisplatin was slightly increased, with no sensitivity change in hOCT1-MDCK cells	The uptake of cisplatin was slightly increased along with slight increase in cisplatin sensitivity in hOCT2-HEK cells	

Table 1.2. Observations on cisplatin, oxaliplatin, carboplatin and picoplatin substrate specificity for OCT1, OCT2 and OCT3 (continued)

Cisplatin	**OCT1**	**OCT2**	**OCT3**
Yokoo et al. (2007) [81]	The uptake of cisplatin was not affected in rOCT1-HEK cells	The uptake of cisplatin was increased in rOCT2-HEK cells	The accumulation of cisplatin was not affected in rOCT3-HEK cells
Kitada et al. (2008) [32]	No correlation between the cytotoxicity of oxaliplatin and the level of hOCT2 mRNA was found	No correlation between the cytotoxicity of oxaliplatin and the level of hOCT2 mRNA was found	No correlation between the cytotoxicity of oxaliplatin and the level of hOCT3 mRNA was found
Yokoo et al. (2008) [82]	-	-	The accumulation of cisplatin was independent of hOCT3 expression
Filipski et al. (2008) [83]	-	The accumulation of cisplatin was increased in hOCT2-HEK cells; the uptake of TEA was greatly inhibited by cisplatin in hOCT2-HEK cells	-
Burger et al. (2010) [84]	-	The uptake of cisplatin was slightly increased along with a small increase in cisplatin sensitivity in hOCT2-HEK cells	-
Carboplatin	**OCT1**	**OCT2**	**OCT3**
Ciarimboli et al. (2005) [78]	-	The uptake of ASP was not inhibited by carboplatin in hOCT2-HEK cells	-
Yonezawa et al. (2006) [79]	The cytotoxicity and accumulation of carboplatin was not enhanced in hOCT1-HEK cells	The cytotoxicity and accumulation of carboplatin was not enhanced in hOCT2-HEK cells	The cytotoxicity and accumulation of carboplatin was not enhanced in hOCT3-HEK cells
Zhang et al. (2006) [80]	The uptake of carboplatin was slightly increased with no sensitivity change in hOCT1-MDCK cells	The uptake of carboplatin was slightly increased with no sensitivity change in hOCT2-HEK cells	The uptake and sensitivity of carboplatin was not affected in hOCT3-HEK cells

Table 1.2. Observations on cisplatin, oxaliplatin, carboplatin and picoplatin substrate specificity for OCT1, OCT2 and OCT3 (continued)

Carboplatin	**OCT1**	**OCT2**	**OCT3**
Yokoo et al. (2007) [81]	The uptake of carboplatin was not affected in rOCT1-HEK cells	The uptake of carboplatin was not affected in rOCT2-HEK cells	The uptake of carboplatin was not affected in rOCT3-HEK cells
Kitada et al. (2008) [32]	No correlation between the cytotoxicity of oxaliplatin and the level of hOCT2 mRNA was found	No correlation between the cytotoxicity of oxaliplatin and the level of hOCT2 mRNA was found	No correlation between the cytotoxicity of oxaliplatin and the level of hOCT3 mRNA was found
Burger et al. (2010) [84]	-	The uptake of carboplatin was not affected in hOCT2-HEK cells	-
Oxaliplatin	**OCT1**	**OCT2**	**OCT3**
Ciarimboli et al. (2005) [78]	-	The uptake of ASP was not inhibited by oxaliplatin in hOCT2-HEK cells	-
Yonezawa et al. (2006) [79]	The cytotoxicity and accumulation of oxaliplatin was not enhanced in hOCT1-HEK cells	The cytotoxicity and accumulation of oxaliplatin was enhanced in hOCT2-HEK cells	The cytotoxicity and accumulation of oxaliplatin was enhanced in hOCT3-HEK cells
Zhang et al. (2006) [80]	The uptake of oxaliplatin was dramatically increased along with increased sensitivity in hOCT1-MDCK cells	The uptake of oxaliplatin was dramatically increased along with increased sensitivity in hOCT2-HEK cells	The uptake and sensitivity of oxaliplatin was not affected in hOCT3-HEK cells
Yokoo et al. (2007) [81]	The uptake of oxaliplatin was not affected in rOCT1-HEK cells	The uptake of oxaliplatin was increased in rOCT2-HEK cells	The uptake of oxaliplatin was increased in rOCT3-HEK cells
Lovejoy et al. (2008) [85]	The uptake of oxaliplatin was increased along with increased cytotoxicity in hOCT1-MDCK cells	The uptake of oxaliplatin was increased along with increased cytotoxicity in hOCT2-HEK cells	-

Table 1.2. Observations on cisplatin, oxaliplatin, carboplatin and picoplatin substrate specificity for OCT1, OCT2 and OCT3 (continued)

Oxaliplatin	**OCT1**	**OCT2**	**OCT3**
Kitada et al. (2008) [32]	The cytotoxicity of oxaliplatin was affected by the level of hOCT1 mRNA	No correlation between the cytotoxicity of oxaliplatin and the level of hOCT2 mRNA was found	No correlation between the cytotoxicity of oxaliplatin and the level of hOCT3 mRNA was found
Yokoo et al. (2008) [82]	-	-	The cytotoxicity and accumulation of oxaliplatin was enhanced in hOCT3 transfected SW480 cells; The cytotoxicity and accumulation of oxaliplatin was correlated with hOCT3 expression
Burger et al. (2010) [84]	-	The uptake of oxaliplatin was dramatically increased along with a large increase in oxaliplatin sensitivity in hOCT2-HEK cells	-
Picoplatin	**OCT1**	**OCT2**	**OCT3**
More et al. (2010) [44]	The cytotoxicity and accumulation of picoplatin were enhanced in hOCT1-HEK cells	The cytotoxicity and accumulation of picoplatin were enhanced in hOCT2-HEK cells	The accumulation but not cytotoxicity of picoplatin was enhanced in hOCT3-HEK cells

transfected with rat (r) organic cation transporter 2 was competitively inhibited by cisplatin [75]. Moreover, rOCT2 has been found to facilitate the transport of cisplatin in HEK-rOCT2 cells and was responsible for cisplatin-induced nephrotoxicity in rats [77, 81, 86]. Yokoo et al. further compared the renal function and renal accumulation of platinum after the administration of four platinum agents including cisplatin, carboplatin, nedaplatin and oxaliplatin in rats [81]. Among these four drugs, only cisplatin induced nephrotoxicity after its intraperitoneal administration and the renal accumulation of cisplatin was much greater than that of the other drugs. The nephrotoxicity of cisplatin was remarkably reduced by the concomitant administration of imatinib, a cationic anticancer agent [87].

The interaction of cisplatin with human OCTs has been investigated, and the results are discordant. In oocytes expressing hOCT1, or hOCT2, the amount of cisplatin taken up was not higher than that observed in oocytes injected with buffer, indicating that cisplatin is not a substrate of these transporters [76]. Whereas Ciarimboli et al. reported a significant interaction of cisplatin with hOCT2 in both hOCT2-HEK cells and freshly isolated human proximal tubules, and cisplatin induced apoptosis was completely suppressed by concomitant incubation with the hOCT2 substrate cimetidine [78]. Cisplatin was not found to interact with hOCT1 in hOCT1-HEK cells and in freshly isolated human hepatocyte couplets in the same study [78]. In a different study, both hOCT1 and hOCT2 were found to enhance the cytotoxicity and accumulation of cisplatin and the uptake of cisplatin was inhibited by cimetidine [79]. Interestingly, Zhang et al. observed that hOCT1 only slightly enhanced the uptake of cisplatin, but the cytotoxicity was not affected by the hOCT1 overexpression [80]. More recent studies

confirmed that cisplatin was substrate of hOCT2 [80, 81, 83, 84]. However, the specificity of cisplatin for hOCT2 varies a lot, which may be attributable to the differences in transfection efficiencies or expression levels of hOCT2 in HEK cells. In all studies summarized in Table 1.2, no interaction of cisplatin with OCT3 has been reported.

The interaction of OCTs with oxaliplatin was first investigated by Ciarimboli et al., who reported that the less nephrotoxic derivate oxaliplatin did not inhibit the uptake of 4-[4-(dimethyl-amino)styril]-methylpyridinium (ASP), a fluorescent cation in stably transfected HEK293 cells [78]. However, when the platinum uptake and cytotoxicity of oxaliplatin was compared between hOCT2-HEK cells and MOCK cells, hOCT2 indeed enhanced the platinum uptake and sensitized the cells to the cytotoxicity of oxaliplatin while hOCT1 and hOCT3 overexpression did not affect the platinum accumulation, and the cytotoxicity of oxaliplatin was not enhanced in the cells transfected with either hOCT1 or hOCT3 accordingly [79, 84]. A further study showed that oxaliplatin was responsible for significant toxicity both in hOCT1 and hOCT2 expressing cells [80]. A more recent study found that hOCT3 was significantly involved in the oxaliplatin-induced cytotoxicity and accumulation of platinum in colorectal cancer [82]. Oxaliplatin uptake is enhanced by all rOCTs, including rOCT1, rOCT2 and rOCT3 [81]. In an attempt to identify the factors affecting sensitivity to platinum agents in human colorectal tumor cell lines, hOCT1 mRNA level was found to associate with the cytotoxicity of oxaliplatin but not cisplatin [32]. It is clear from all studies summarized in Table 1.2 that carboplatin was not considered as a good substrate of human and rat OCTs [32, 78-81, 84]. More et al. were the first to determine the influence of hOCTs and their genetic variants on cellular uptake of picoplatin and on the individual components of the ensuing

cytotoxicity such as DNA adduct formation, which were found to be significantly enhanced by the expression of the OCTs [44]. Expression of OCT1 and OCT2, but not OCT3, significantly enhanced picoplatin cytotoxicity, which was reduced in the presence of an OCT inhibitor. Common genetic variants with altered function in platinum uptake and DNA adduct formation were also identified for both OCT1 and OCT2.

Multidrug and toxin extrusion family

Mammalian multidrug and toxin extrusion (MATE) family transporters i.e. human (h)MATE1, hMATE2, mouse (m)MATE1 and mMATE2 were first cloned and characterized by Moriyama and his colleagues [88]. Subsequently, Inui and his colleagues identified hMATE2-K, hMATE2-B and rat (r)MATE1 [89, 90]. The MATE family was assigned as the SLC47 family (SLC47A1: MATE1, SLC47A2: MATE2 and MATE2-K) by HUGO Gene Nomenclature Committee in 2007.

hMATE1 is primarily expressed in the kidney, and is also expressed in the adrenal gland, liver, testis and skeletal muscle [88, 89], and has been shown to mediate the cellular uptake of structurally diverse small-molecular-weight organic cations such as tetraethylammonium (TEA), *N*-methylpyridinium, metformin and paraquat [91, 92]. hMATE2-K is specifically expressed in the kidney and interacts with various organic cations with a substrate specificity overlapping that of hMATE1 [89, 91]. The location in the kidney and the overlapping specificities suggest that hMATE1 and hMATE2-K may function somewhat redundantly in the kidney by mediating tubular transport of cationic organic molecules across the apical membrane. mMATE1 is predominantly found in the kidney and liver and is localized to the renal brush-border membrane and bile canaliculi

[88], while rMATE1 was expressed abundantly in the kidney and placenta, slightly in the spleen, but not expressed in the liver [90]. Rodent MATE2 is predominantly expressed in the testis. In addition, based on the genomic database, it was found that there are no rodent isoforms corresponding to hMATE2-K [93]. In general, substrate specificity of hMATE1 and hMATE2-K is similar. However, species differences regarding substrate specificity have not been reported in the MATE family among human, mouse, rat and rabbit.

Upon the identification and characterization of MATE family, Inui and his colleagues examined the role of hMATE1 and hMATE2-K in the cellular accumulation and cytotoxicity of platinum agents using HEK293 cells transiently transfected with the transporter cDNA. The results showed that the accumulation of oxaliplatin was markedly enhanced by hMATE2-K, and significantly but weakly by hMATE1 [79, 81]. On the other hand, there was no significant stimulation of the accumulation of platinum in the cells transfected with hMATE1 and hMATE2-K after treatment with cisplatin and carboplatin [81]. These results may explain the relationship between the renal accumulation and nephrotoxicity of platinum drugs: (1) cisplatin is taken up into the proximal tubule cells via OCT2 but not extruded from these cell via MATE2-K, which leads to significantly higher accumulation and subsequent nephrotoxicity; (2) OCT2 and MATE2-K work in concert to regulate the renal accumulation of oxaliplatin, therefore, its cellular accumulation is lower, consistent with its lack of associated nephrotoxicity. In more recent studies , two singleton variants of MATE1, G64D and V480M, were found to produce a complete loss of function for oxaliplatin uptake, whereas the polymorphic variant hMATE1-C497S (allele frequency = 2.4% in African American) increased

oxaliplatin uptake in comparison to hMATE1 reference [94]. These data suggest that genetic variants in hMATE1 may alter the disposition of oxaliplatin and ultimately affect its clinical efficacy.

Multidrug resistance-associated transporters

In the cytoplasm, platinum agents become aquated, which then enables them to react with thiol-containing molecules, including glutathione (GSH) and metallothionein. Many platinum-resistant cell lines express increased levels of glutathione [95], and once the platinum drug is chelated by glutathione, the glutathione-platinum complex is effluxed from the cell in an ATP-dependent fashion by a group of transporters termed the GS-X pumps [96]. It has been reported that MRP1 and MRP2 function as GS-X export pumps to confer platinum drug resistance [97, 98].

Ishikawa et al. demonstrated that a 200kDa protein, now known as MRP1, was over-expressed in cisplatin-resistant human promyelocytic leukemia HL-60 (HL-60/R-CP) cells, in which GSH was substantially elevated. Conversely, other reports have suggested that MRP1 is not the major pump responsible for cisplatin resistance. These studies have involved the use of a cervical cancer cell line, HeLa [99], a non-small-cell-lung cancer (NSCLC) cell line (SW-1573) [100] or pairs of cisplatin-sensitive and acquired resistant sublines [101]. Hamaguchi et al. found no relationship between MRP1 mRNA expression level and resistance to cisplatin by examining a panel of seven human ovarian cancer cell lines that exhibit a wide range of primary resistance to cisplatin [102]. Ikuta et al. also found no relationship in NSCLC cell lines between MRP1 expression levels and cisplatin cytotoxicity and accumulation [103]. Furthermore, Sharp et al. reported that

overexpression of MRP1 was not detected in a panel of human ovarian carcinoma cell lines and their variants with acquired cisplatin resistance. MRP1 transfection into an intrinsically cisplatin-resistant cell line SKOV3, previously shown to have elevated GSH levels, neither conferred cross-resistance to cisplatin, satraplatin and picoplatin, nor decreased cisplatin accumulation [104]. A number of investigations found no clinical correlation between MRP1 mRNA expression levels and clinical outcome of platinum agents as well [105-108].

Another MRP that has been studied as a candidate for platinum resistance is the canalicular Multispecific Organic Anion Transporter (cMOAT), also called MRP2. A number of cisplatin-resistant carcinoma cells exhibit an overexpression of MRP2 at the mRNA and protein level [109], and the resistant cells also showed a decreased formation of platinum-DNA adducts [110]. Cisplatin has also been shown to induce MRP2 expression in both rat primary hepatocytes and human cell lines (HepG2 and MCF-7), as demonstrated in Northern and Western Blots [111, 112]. Human MRP2 overexpressed in HEK-293 cells enhanced the resistance to cisplatin (10-fold) compared to MOCK cells, suggesting that MRP2 confers resistance to cytotoxic drugs [98]. Furthermore, introduction of anti-MRP2 hammerhead ribozymes, MRP2 antisense-expressing construct or short hairpin RNA (shRNA) into cell cultures increased both sensitivity to and accumulation of cisplatin, along with intracellular glutathione levels [113-116]. However, MRP2 is not required for cisplatin resistance as some resistant lines do not contain detectable levels of MRP2 (e.g. PXN94/tetR), whereas the KCP-4(+) line even lost its MRP2 when it became highly resistant [109].

While MRP expression could contribute to cisplatin resistance in some tissue types by exporting the platinum-GSH complex, it does not appear to be a global mechanism by which resistance to cisplatin occurs.

Future Directions

During the past decade significant progress has been made in elucidating the role of drug transporters in tumor resistance to platinum drugs. However, it is obvious that much more work is needed to clearly understand how transporters mediate drug sensitivity and resistance to anti-cancer platinum analogs. Further, studies that focus on strategies to enhance the efficacy and reduce the toxicity of anti-cancer platinum drugs by modulating transporter activity are clearly needed. For example, a recent study demonstrated that administration of a copper chelator greatly enhanced cisplatin efficacy by reducing copper levels in the vicinity of the tumor, thereby allowing cisplatin to enter the tumor cells via CTR1 unimpeded by copper [117]. This strategy may be exploited in clinical studies to enhance cisplatin sensitivity via modulation of its uptake.

Recent studies have linked genetic variants in membrane transporters in the solute carrier superfamily (SLC) with altered drug disposition and response [118-120]. In particular, such studies have taken a genotype to phenotype approach, focusing on variants that exhibited altered function in cellular assays. For example, Shu et al. [118, 119] demonstrated that genetic variants that exhibited altered function in cellular assays, affected the disposition and pharmacologic effects of metformin in healthy volunteers. Similarly, Urban et al. [120] also reported that a common variant of the novel organic cation transporter, OCTN1, which exhibited reduced uptake of gabapentin, in cellular

assays was associated with a reduced renal clearance of gabapentin in healthy volunteers. These studies provide strong evidence that genetic variants in uptake transporters may have important clinical effects. To shed more light on the role of genetic variants in OCTs in modifying the disposition and response to platinum drugs, extensive functional and clinical studies of genetic variants of OCTs are needed for each platinum drug.

Summary of Dissertation Chapters.

Membrane transporters act as gatekeepers to mediate the uptake and efflux of endogenous compounds, environmental toxins, chemical carcinogens, and clinically used drugs in all tissues in the human body, thereby influencing total body homeostasis and drug disposition, and ultimately the efficacy and safety of drugs. In platinum-resistant cells, the reduced platinum accumulation is the most common observation. Therefore, by targeting influx transporters overexpressed in tumors, the concentrations of platinum compounds in tumors can be selectively increased and the corresponding efficacy can be enhanced. On the other hand, off-target toxicities may be reduced due to lower platinum levels in tissues. The major goal of this dissertation was to examine the role of organic cation transporters in the systemic, tissue and tumor levels of platinum compounds and in the modulation of toxicity and anti-cancer efficacy. The underlying hypothesis was that organic cation transporters can be used as drug delivery targets for platinum-based anticancer chemotherapy.

Chapter 2. Role of organic cation transporter 1, Oct1, in the pharmacokinetics and tissue distribution of pyroplatin in mice

Cellular entry represents the first step in the mechanism of action of platinum anticancer agents. Pyroplatin (CDPCP) is distinct from currently used anti-cancer platinum drugs in that it only forms monofunctional, rather than bifunctional, lesions with DNA. It has been shown to be an excellent substrate for organic cation transporters (OCTs). The goal of studies in this chapter was to test the hypothesis that by controlling intracellular uptake, OCT1 is a key determinant of the disposition of pyroplatin. Specifically, we compared the intracellular uptake and DNA adduct formation of pyroplatin in primary hepatocytes derived from both *Oct1-/-* and wild-type mice *in vitro*. Furthermore, the effects of Oct1 on pharmacokinetics and tissue accumulation of pyroplatin were also examined by comparing the pharmacokinetics and tissue accumulation of pyroplatin between *Oct1-/-* and wild-type mice *in vivo*. Our study showed that Oct1 facilitated the intracellular accumulation and DNA adduct formation of pyroplatin in primary mouse hepatocytes *in vitro*. Pyroplatin had favorable pharmacokinetic properties. However, Oct1 enhanced hepatic and intestinal accumulation of pyroplatin *in vivo* and Oct1 deletion resulted in decreased clearance and volume distribution, which led to increased systemic exposure in *Oct1-/-* mice. The results of our study suggest that Oct1 plays a role in the elimination and tissue distribution of pyroplatin. This study set the stage for further toxicity and efficacy studies described in subsequent chapters.

Chapter 3. Effect of Oct1 on the toxicity profile of pyroplatin in mice

In this chapter, we characterize the toxicity profile of pyroplatin and the role of OCT1 in the hepatic, intestinal and renal toxicity, where OCT1 is abundantly expressed. In general, pyroplatin appears to possess a favorable toxicity profile. Oct1 deletion

resulted in enhanced body weight loss, renal toxicity and hematological effects of pyroplatin. However, the hepatic toxicity of pyroplatin was less in *Oct1-/-*mice in comparison to *Oct1+/+* mice. The level of hepatic toxicity was mild and reversible. The higher systemic plasma concentrations of pyroplatin and differences in tissue accumulation explained the toxicity profile differences between the *Oct1-/-* and *Oct1* wild-type mice. Our study supported the concept that by targeting drug influx transporters, off-target toxicities can be greatly spared. The study also suggests that genetic variants in drug transporters will not only modulate pharmacokinetics but also toxicity.

Chapter 4. Role of Oct1 in the antitumor effect of pyroplatin in mice

Studies in the literature and our unpublished data indicate that OCT1 is abundantly expressed in hepatocellular carcinoma, suggesting that pyroplatin may be useful in the treatment of HCC. The goal of the studies in this chapter was to test the hypothesis that Oct1 mediates the antitumor effect of pyroplatin in HCC. Firstly, we assessed the role of Oct1 in tumor responsiveness of pyroplatin *in vivo* to establish the link between OCT1 expression and antitumor efficacy of pyroplatin using a xenograft model of stably transfected HEK-OCT1 cell lines. Further, we investigated the effect of pyroplatin in hepatocellular carcinoma (HCC) and the role of Oct1 on pyroplatin response in *Oct1+/+* and *Oct1-/-* mice bearing HCC, which was induced by hydrodynamic transfection of oncogenes. We demonstrated that OCT1 facilitated pyroplatin accumulation in tumor xenografts and the increased pyroplatin levels appeared to reduce the rate of tumor growth, though not statistically significant. As confirmed in this chapter, Oct1 expression was not altered during hepatocarcinogenesis, which

validated the feasibility of the HCC mouse model in different Oct1 backgrounds to assess the role of Oct1 in the anti-HCC activity of pyroplatin. We also observed that in *Oct1*+/+ mice pyroplatin accumulated in HCC to greater levels than in Oct1-/- mice. However, increased pyroplatin levels in Oct1 wildtype mice did not prolong survival time of mice bearing HCC. In addition, the interaction of pyroplatin with glutathione was minimal compared with other platinum compounds and did not explain the lack of efficacy of pyroplatin in our mouse models of HCC. The most likely reason for the ineffectiveness of pyroplatin is due to its weak intrinsic antitumor activity. Collectively, our studies demonstrated that OCT1 can control pyroplatin concentrations in tumor tissues; however, more efficacious platinum drugs targeted to OCT1 may be needed in the treatment of HCC.

Chapter 5. Role of Oct1 and Oct2 in the disposition of oxaliplatin in mice

Oxaliplatin, approved in 2002 for the treatment of colorectal cancer in combination with 5-FU/LV, exhibits a different pattern of sensitivity to that of cisplatin. Moreover, compared with cisplatin, oxaliplatin shows a more favorable toxicity profile. Recently, the differences in the mechanism(s) controlling cellular uptake and efflux of these platinum compounds have gained attention and are now considered to be one of the major mechanisms of contributing to their disparate activities. In this chapter, we investigated the role of Oct1 and Oct2 at physiological expression levels in the disposition of oxaliplatin using genetically engineered mouse models and the role of Oct1 in the hepatic toxicity of oxaliplatin. In primary hepatocytes isolated from *Oct1-/-* and *Oct1* wildtype mice, Oct1 deletion in *Oct1-/-* mice slightly but significantly decreased the intracellular accumulation of oxaliplatin compared with *Oct1* wildtype mice.

Pharmacokinetics studies in *Oct1-/-* and *Oct1/2-/-* mice showed that Oct1 and Oct2 have slight effects on the disposition of oxaliplatin; Oct1 deletion mainly affected the distribution phase of oxaliplatin, whereas Oct1 and Oct2 double deletion mainly affected the terminal elimination phase of oxaliplatin. Either Oct1 deletion or Oct1/2 double deletion had no significant effect on normalized tissue accumulation of oxaliplatin. Although Oct1 enhanced the hepatic accumulation after multiple dosing, the increase hepatic platinum levels did not result in obvious liver toxicity.

References

1. Ayrton, A. and Morgan, P., *Role of transport proteins in drug discovery and development: A pharmaceutical perspective.* Xenobiotica, 2008. **38**(7-8): p. 676-708.

2. Ayrton, A. and Morgan, P., *Role of transport proteins in drug absorption, distribution and excretion.* Xenobiotica, 2001. **31**(8-9): p. 469-497.

3. Shitara, Y., Horie, T., and Sugiyama, Y., *Transporters as a determinant of drug clearance and tissue distribution.* European Journal of Pharmaceutical Sciences, 2006. **27**(5): p. 425-446.

4. http://www.cancer.org/docroot/PRO/content/PRO_1_1_Cancer_Statistics_2009_Presentation.asp.

5. Wong, E. and Giandomenico, C.M., *Current status of platinum-based antitumor drugs.* Chemical Reviews, 1999. **99**(9): p. 2451-2466.

6. Bosl, G.J., Bajorin, D.F., and Sheinfeld, J., *Cancer of the testis*, in *Cancer: Principles and practice of oncology*, Devita, V.T., Hellman, S, Rosenberg S.A Editor. 2000, Lippincott, Williams and Wilkins. p. 1491.

7. Rabik, C.A. and Dolan, M.E., *Molecular mechanisms of resistance and toxicity associated with platinating agents.* Cancer Treatment Reviews, 2007. **33**(1): p. 9-23.

8. Harrap, K.R., *Preclinical studies identifying carboplatin as a viable cisplatin alternative.* Cancer Treatment Reviews, 1985. **12**: p. 21-33.

9. Kelland, L., *The resurgence of platinum-based cancer chemotherapy.* Nature Reviews Cancer, 2007. **7**(8): p. 573-584.

10. Wagstaff, A.J., Ward, A., Benfield, P., and Heel, R.C., *Carboplatin: A preliminary review of its pharmacodynamic and pharmacokinetic properties and therapeutic efficacy in the treatment of cancer.* Drugs, 1989. **37**(2): p. 162-190.

11. Ibrahim, A., Hirschfeld, S., Cohen, M.H., Griebel, D.J., Williams, G.A., and Pazdur, R., *FDA drug approval summaries: Oxaliplatin.* Oncologist, 2004. **9**(1): p. 8-12.

12. Fernandez, F.G., Ritter, J., Goodwin, J.W., Linehan, D.C., Hawkins, W.G., and Strasberg, S.M., *Effect of steatohepatitis associated with irinotecan or oxaliplatin pretreatment on resectability of hepatic colorectal metastases.* Journal of the American College of Surgeons, 2005. **200**(6): p. 845-853.

13. Rubbia-Brandt, L., Audard, V., Sartoretti, P., Roth, A.D., Brezault, C., Le Charpentier, M., Dousset, B., Morel, P., Soubrane, O., Chaussade, S., Mentha, G., and Terris, B., *Severe hepatic sinusoidal obstruction associated with oxaliplatin-*

based chemotherapy in patients with metastatic colorectal cancer. Annals of Oncology, 2004. **15**(3): p. 460-466.

14. Kelland, L., *Broadening the clinical use of platinum drug-based chemotherapy with new analogues: Satraplatin and picoplatin.* Expert Opinion on Investigational Drugs, 2007. **16**(7): p. 1009-1021.

15. http://www.poniard.com/clinical/sclc.html.

16. Bhargava, A. and Vaishampayan, U.N., *Satraplatin: Leading the new generation of oral platinum agents.* Expert Opinion on Investigational Drugs, 2009. **18**(11): p. 1787-1797.

17. Armstrong, A.J. and George, D.J., *Satraplatin in the treatment of hormone-refractory metastatic prostate cancer.* Therapeutics and Clinical Risk Management, 2007. **3**(5): p. 7.

18. Pinto, A.L. and Lippard, S.J., *Binding of the antitumor drug cis-diamminedichloroplatinum(II) (cisplatin) to DNA.* Biochimica Et Biophysica Acta, 1984. **780**(3): p. 167-180.

19. Zamble, D.B. and Lippard, S.J., *Cisplatin and DNA-repair in cancer-chemotherapy.* Trends in Biochemical Sciences, 1995. **20**(10): p. 435-439.

20. Wang, D. and Lippard, S.J., *Cellular processing of platinum anticancer drugs.* Nature Reviews Drug Discovery, 2005. **4**(4): p. 307-320.

21. Gately, D.P. and Howell, S.B., *Cellular accumulation of the anticancer agent cisplatin - a review.* British Journal of Cancer, 1993. **67**(6): p. 1171-1176.

22. Moller, L.B., Petersen, C., Lund, C., and Horn, N., *Characterization of the hCTR1 gene: Genomic organization, functional expression, and identification of a highly homologous processed gene.* Gene, 2000. **257**(1): p. 13-22.

23. Hall, M.D., Okabe, M., Shen, D.W., Liang, X.J., and Gottesman, M.M., *The role of cellular accumulation in determining sensitivity to platinum-based chemotherapy.* Annual Review of Pharmacology and Toxicology, 2008. **48**: p. 495-535.

24. Lee, J., Prohaska, J.R., and Thiele, D.J., *Essential role for mammalian copper transporter CTR1 in copper homeostasis and embryonic development.* Proceedings of the National Academy of Sciences of the United States of America, 2001. **98**(12): p. 6842-6847.

25. Kuo, Y.-M., Zhou, B., Cosco, D., and Gitschier, J., *The copper transporter CTR1 provides an essential function in mammalian embryonic development.* Proceedings of the National Academy of Sciences of the United States of America, 2001. **98**(12): p. 6836-6841.

26. Ishida, S., Lee, J., Thiele, D.J., and Herskowitz, I., *Uptake of the anticancer drug cisplatin mediated by the copper transporter Ctr1 in yeast and mammals.* Proceedings of the National Academy of Sciences of the United States of America, 2002. **99**: p. 14298-14302.

27. Lin, X., Okuda, T., Holzer, A., and Howell, S.B., *The copper transporter CTR1 regulates cisplatin uptake in saccharomyces cerevisiae.* Molecular Pharmacology, 2002. **62**(5): p. 1154-1159.

28. Holzer, A.K., Manorek, G.H., and Howell, S.B., *Contribution of the major copper influx transporter ctr1 to the cellular accumulation of cisplatin, carboplatin, and oxaliplatin.* Molecular Pharmacology, 2006. **70**(4): p. 1390-1394.

29. Zisowsky, J., Koegel, S., Leyers, S., Devarakonda, K., Kassack, M.U., Osmak, M., and Jaehde, U., *Relevance of drug uptake and efflux for cisplatin sensitivity of tumor cells.* Biochemical Pharmacology, 2007. **73**(2): p. 298-307.

30. Plasencia, C., Martinez-Balibrea, E., Martinez-Cardus, A., Quinn, D.I., Abad, A., and Neamati, N., *Expression analysis of genes involved in oxaliplatin response and development of oxaliplatin-resistant ht29 colon cancer cells.* International Journal of Oncology, 2006. **29**(1): p. 225-235.

31. Song, I.-S., Savaraj, N., Siddik, Z.H., Liu, P., Wei, Y., Wu, C.J., and Kuo, M.T., *Role of human copper transporter Ctr1 in the transport of platinum-based antitumor agents in cisplatin-sensitive and cisplatin-resistant cells.* Molecular Cancer Therapeutics, 2004. **3**(12): p. 1543-1549.

32. Kitada, N., Takara, K., Minegaki, T., Itoh, C., Tsujimoto, M., Sakaeda, T., and Yokoyama, T., *Factors affecting sensitivity to antitumor platinum derivatives of human colorectal tumor cell lines.* Cancer Chemotherapy and Pharmacology, 2008. **62**(4): p. 577-584.

33. Larson, C.A., Blair, B.G., Safaei, R., and Howell, S.B., *The role of the mammalian copper transporter 1 in the cellular accumulation of platinum-based drugs.* Molecular Pharmacology, 2009. **75**(2): p. 324-330.

34. Kabolizadeh, P., Ryan, J., and Farrell, N., *Differences in the cellular response and signaling pathways of cisplatin and BBR3464 ([{trans-PtCl(NH3)(2)}(2)mu-(trans-Pt(NH3)(2)(H2N(Ch2)(6)-NH2)(2))](4+)) influenced by copper homeostasis.* Biochemical Pharmacology, 2007. **73**(9): p. 1270-1279.

35. Holzer, A.K., Samimi, G., Katano, K., Naerdemann, W., Lin, X.J., Safaei, R., and Howell, S.B., *The copper influx transporter human copper transport protein 1 regulates the uptake of cisplatin in human ovarian carcinoma cells.* Molecular Pharmacology, 2004. **66**(4): p. 817-823.

36. Beretta, G.L., Gatti, L., Tinelli, S., Corna, E., Colangelo, D., Zunino, F., and Perego, P., *Cellular pharmacology of cisplatin in relation to the expression of human copper transporter ctr1 in different pairs of cisplatin-sensitive and -resistant cells.* Biochemical Pharmacology, 2004. **68**(2): p. 283-291.

37. Rabik, C.A., Maryon, E.B., Kasza, K., Shafer, J.T., Bartnik, C.M., and Dolan, M.E., *Role of copper transporters in resistance to platinating agents.* Cancer Chemotherapy and Pharmacology, 2009. **64**(1): p. 133-142.

38. Holzer, A.K., Katano, K., Klomp, L.W.J., and Howell, S.B., *Cisplatin rapidly down-regulates its own influx transporter hCTR1 in cultured human ovarian carcinoma cells.* Clinical Cancer Research, 2004. **10**(19): p. 6744-6749.

39. Howell, S.B., Safaei, R., Larson, C.A., and Sailor, M.J., *Copper transporters and the cellular pharmacology of the platinum-containing cancer drugs.* Molecular Pharmacology, 2010. **77**(6): p. 887-894.

40. Petris, M.J., Smith, K., Lee, J., and Thiele, D.J., *Copper-stimulated endocytosis and degradation of the human copper transporter, hCTR1.* The Journal of Biological Chemistry, 2003. **278**(11): p. 9639-9646.

41. Guo, Y., Smith, K., Lee, J., Thiele, D.J., and Petris, M.J., *Identification of methionine-rich clusters that regulate copper-stimulated endocytosis of the human CTR1 copper transporter.* Journal of Biological Chemistry, 2004. **279**(17): p. 17428-17433.

42. Samimi, G. and Howell, S.B., *Modulation of the cellular pharmacology of JM118, the major metabolite of satraplatin, by copper influx and efflux transporters.* Cancer Chemotherapy and Pharmacology, 2006. **57**(6): p. 781-788.

43. Samimi, G., Kishimoto, S., Manorek, G., Breaux, J.K., and Howell, S.B., *Novel mechanisms of platinum drug resistance identified in cells selected for resistance to JM118 the active metabolite of satraplatin.* Cancer Chemotherapy and Pharmacology, 2007. **59**(3): p. 301-312.

44. More, S.S., Li, S., Yee, S.W., Chen, L., Xu, Z., Jablons, D.M., and Giacomini, K.M., *Organic cation transporters modulate the uptake and cytotoxicity of picoplatin, a third-generation platinum analogue.* Molecular Cancer Therapeutics, 2010. **9**(4): p. 1058-1069.

45. La Fontaine, S. and Mercer, J.F.B., *Trafficking of the copper-ATPases, ATP7A and ATP7B: Role in copper homeostasis.* Archives of Biochemistry and Biophysics, 2007. **463**(2): p. 149-167.

46. Komatsu, M., Sumizawa, T., Mutoh, M., Chen, Z.S., Terada, K., Furukawa, T., Yang, X.L., Gao, H., Miura, N., Sugiyama, T., and Akiyama, S., *Copper-transporting P-type adenosine triphosphatase (ATP7B) is associated with cisplatin resistance.* Cancer Research, 2000. **60**(5): p. 1312-1316.

47. Nakayama, K., Miyazaki, K., Kanzaki, A., Fukumoto, M., and Takebayashi, Y., *Expression and cisplatin sensitivity of copper-transporting P-type adenosine triphosphatase (ATP7B) in human solid carcinoma cell lines.* Oncology Reports, 2001. **8**(6): p. 1285-1287.

48. Katano, K., Safaei, R., Samimi, G., Holzer, A., Rochdi, M., and Howell, S.B., *The copper export pump ATP7B modulates the cellular pharmacology of carboplatin in ovarian carcinoma cells.* Molecular Pharmacology, 2003. **64**(2): p. 466-473.

49. Ohbu, M., Ogawa, K., Konno, S., Kanzaki, A., Terada, K., Sugiyama, T., and Takebayashi, Y., *Copper-transporting P-type adenosine triphosphatase (ATP7B) is expressed in human gastric carcinoma.* Cancer Letters, 2003. **189**(1): p. 33-38.

50. Atsuko, K., Masakazu, T., Nouri, N., Hitoshi, M., Masahiro, O., Kentaro, N., Hiroko, B., Kenji, O., Masato, M., Shiro, M., Kunihiko, T., Toshihiro, S., Manabu, F., and Yuji, T., *Copper-transporting P-type adenosine triphosphatase (ATP7B)*

is expressed in human breast carcinoma. Japanese Journal of Cancer Research : Gann, 2002. **93**(1): p. 70-77.

51. Higashimoto, M., Kanzaki, A., Shimakawa, T., Konno, S., Naritaka, Y., Nitta, Y., Mori, S., Shirata, S., Yoshida, A., Terada, K., Sugiyama, T., Ogawa, K., and Takebayashi, Y., *Expression of copper-transporting P-type adenosine triphosphatase in human esophageal carcinoma.* International Journal of Molecular Medicine, 2003. **11**(3): p. 337-341.

52. Nakayama, K., Kanzaki, A., Terada, K., Mutoh, M., Ogawa, K., Sugiyama, T., Takenoshita, S., Itoh, K., Yaegashi, N., Miyazaki, K., Neamati, N., and Takebayashi, Y., *Prognostic value of the Cu-transporting ATPase in ovarian carcinoma patients receiving cisplatin-based chemotherapy.* Clinical Cancer Research, 2004. **10**(8): p. 2804-2811.

53. Sugeno, H., Takebayashi, Y., Higashimoto, M., Ogura, Y., Shibukawa, G., Kanzaki, A., Terada, K., Sugiyama, T., Watanabe, K., Katoh, R., Nitta, Y., Fukushima, T., Koyama, Y., Inoue, N., Sekikawa, K., Ogawa, K., Sato, Y., and Takenoshita, S., *Expression of copper-transporting P-type adenosine triphosphatase(ATP7B) in human hepatocellular carcinoma.* Anticancer Research, 2004. **24**(2C): p. 1045-1048.

54. Aida, T., Takebayashi, Y., Shimizu, T., Okamura, C., Higasimoto, M., Kanzaki, A., Nakayama, K., Terada, K., Sugiyama, T., Miyazaki, K., Ito, K., Takenoshita, S., and Yaegashi, N., *Expression of copper-transporting P-type adenosine*

triphosphatase (ATP7B) as a prognostic factor in human endometrial carcinoma. Gynecologic Oncology, 2005. **97**(1): p. 41-45.

55. Mangala, L.S., Zuzel, V., Schmandt, R., Leshane, E.S., Halder, J.B., Armaiz-Pena, G.N., Spannuth, W.A., Tanaka, T., Shahzad, M.M.K., Lin, Y.G., Nick, A.M., Danes, C.G., Lee, J.-W., Jennings, N.B., Vivas-Mejia, P.E., Wolf, J.K., Coleman, R.L., Siddik, Z.H., Lopez-Berestein, G., Lutsenko, S., and Sood, A.K., *Therapeutic targeting of ATP7B in ovarian carcinoma.* Clinical Cancer Research, 2009. **15**(11): p. 3770-3780.

56. Katano, K., Safaei, R., Samimi, G., Holzer, A., Tomioka, M., Goodman, M., and Howell, S.B., *Confocal microscopic analysis of the interaction between cisplatin and the copper transporter ATP7B in human ovarian carcinoma cells.* Clinical Cancer Research, 2004. **10**(13): p. 4578-4588.

57. Samimi, G., Safaei, R., Katano, K., Holzer, A.K., Rochdi, M., Tomioka, M., Goodman, M., and Howell, S.B., *Increased expression of the copper efflux transporter ATP7A mediates resistance to cisplatin, carboplatin, and oxaliplatin in ovarian cancer cells.* Clinical Cancer Research, 2004. **10**(14): p. 4661-4669.

58. Katano, K., *Acquisition of resistance to cisplatin is accompanied by changes in the cellular pharmacology of copper.* Cancer Research, 2002. **62**: p. 6559-6565.

59. Samimi, G., Varki, N.M., Wilczynski, S., Safaei, R., Alberts, D.S., and Howell, S.B., *Increase in expression of the copper transporter ATP7A during platinum*

drug-based treatment is associated with poor survival in ovarian cancer patients. Clinical Cancer Research, 2003. **9**(16): p. 5853-5859.

60. Safaei, R., Katano, K., Larson, B.J., Samimi, G., Holzer, A.K., Naerdemann, W., Tomioka, M., Goodman, M., and Howell, S.B., *Intracellular localization and trafficking of fluorescein-labeled cisplatin in human ovarian carcinoma cells.* Clinical Cancer Research, 2005. **11**(2): p. 756-767.

61. Helleman, J., Jansen, M., Span, P.N., van Staveren, I.L., Massuger, L., Meijer-van Gelder, M.E., Sweep, F., Ewing, P.C., Van der Burg, M.E.L., Stoter, G., Nooter, K., and Berns, E., *Molecular profiling of platinum resistant ovarian cancer* International Journal of Cancer, 2006. **119**(3): p. 726-726.

62. Theile, D., Grebhardt, S., Haefeli, W.E., and Weiss, J., *Involvement of drug transporters in the synergistic action of FOLFOX combination chemotherapy.* Biochemical Pharmacology, 2009. **78**(11): p. 1366-1373.

63. Eva, M.-B., Anna, M.-C., Eva, M., Alba, G., Jose Luis, M., Enrique, A., Carmen, P., Nouri, N., and Albert, A., *Increased levels of copper efflux transporter ATP7B are associated with poor outcome in colorectal cancer patients receiving oxaliplatin-based chemotherapy.* International Journal of Cancer, 2009. **124**(12): p. 2905-2910.

64. Fukushima-Uesaka, H., Saito, Y., Maekawa, K., Kurose, K., Sugiyama, E., Katori, N., Kaniwa, N., Hasegawa, R., Hamaguchi, T., Eguchi-Nakajima, T., Kato, K., Yamada, Y., Shimada, Y., Yoshida, T., Yamamoto, N., Nokihara, H., Kunitoh, H.,

Ohe, Y., Tamura, T., Ura, T., Saito, M., Muro, K., Doi, T., Fuse, N., Yoshino, T., Ohtsu, A., Saijo, N., Matsumura, Y., Okuda, H., and Sawada, J., *Genetic polymorphisms of copper- and platinum drug-efflux transporters ATP7A and ATP7B in Japanese cancer patients.* Drug Metabolism and Pharmacokinetics, 2009. **24**(6): p. 565-574.

65. Jonker, J.W. and Schinkel, A.H., *Pharmacological and physiological functions of the polyspecific organic cation transporters: OCT1, 2, and 3 (SLC22A1-3).* Journal of Pharmacology and Experimental Therapeutics, 2004. **308**(1): p. 2-9.

66. Wright, S.H., *Role of organic cation transporters in the renal handling of therapeutic agents and xenobiotics.* Toxicology and Applied Pharmacology, 2005. **204**(3): p. 309-319.

67. Zhang, L., Dresser, M.J., Gray, A.T., Yost, S.C., Terashita, S., and Giacomini, K.M., *Cloning and functional expression of a human liver organic cation transporter.* Molecular Pharmacology, 1997. **51**(6): p. 913-921.

68. Gorboulev, V., Ulzheimer, J.C., Akhoundova, A., UlzheimerTeuber, I., Karbach, U., Quester, S., Baumann, C., Lang, F., Busch, A.E., and Koepsell, H., *Cloning and characterization of two human polyspecific organic cation transporters.* DNA and Cell Biology, 1997. **16**(7): p. 871-881.

69. Muller, J., Lips, K.S., Metzner, L., Neubert, R.H.H., Koepsell, H., and Brandsch, M., *Drug specificity and intestinal membrane localization of human organic*

cation transporters (OCT). Biochemical Pharmacology, 2005. **70**(12): p. 1851-1860.

70. Nelson, J.A., Santos, G., and Herbert, B.H., *Mechanisms for the renal secretion of cisplatin.* Cancer Treatment Reports, 1984. **68**(6): p. 849-853.

71. Ludwig, T., Riethmuller, C., Gekle, M., Schwerdt, G., and Oberleithner, H., *Nephrotoxicity of platinum complexes is related to basolateral organic cation transport.* Kidney International, 2004. **66**(1): p. 196-202.

72. Okuda, M., Tsuda, K., Masaki, K., Hashimoto, Y., and Inui, K., *Cisplatin-induced toxicity in LLC-PK1 kidney epithelial cells: Role of basolateral membrane transport.* Toxicology Letters, 1999. **106**(2-3): p. 229-235.

73. Endo, T., Kimura, O., and Sakata, M., *Carrier-mediated uptake of cisplatin by the OK renal epithelial cell line.* Toxicology, 2000. **146**(2-3): p. 187-195.

74. Kolb, R.J., Ghazi, A.M., and Barfuss, D.W., *Inhibition of basolateral transport and cellular accumulation of cDDP and N-acetyl-L-cysteine-cDDP by TEA and PAH in the renal proximal tubule.* Cancer Chemotherapy and Pharmacology, 2003. **51**(2): p. 132-138.

75. Pan, B.F., Sweet, D.H., Pritchard, J.B., Chen, R., and Nelson, J.A., *A transfected cell model for the renal toxin transporter, rOct2.* Toxicological Sciences, 1999. **47**(2): p. 181-186.

76. Briz, O., Serrano, M.A., Rebollo, N., Hagenbuch, B., Meier, P.J., Koepsell, H., and Marin, J.J.G., *Carriers involved in targeting the cytostatic bile acid-cisplatin derivativescis-diammine-chloro-cholylglycinate-platinum(II) andcis-diammine-bisursodeoxycholate-platinum(II) toward liver cells.* Molecular Pharmacology, 2002. **61**(4): p. 853-860.

77. Yonezawa, A., Masuda, S., Nishihara, K., Yano, I., Katsura, T., and Inui, K., *Association between tubular toxicity of cisplatin and expression of organic cation transporter rOct2 (Slc22a2) in the rat.* Biochemical Pharmacology, 2005. **70**(12): p. 1823-1831.

78. Ciarimboli, G., Ludwig, T., Lang, D.F., Pavenstadt, H., Koepsell, H., Piechota, H.J., Haier, J., Jaehde, U., Zisowsky, J., and Schlatter, E., *Cisplatin nephrotoxicity is critically mediated via the human organic cation transporter 2.* American Journal of Pathology, 2005. **167**(6): p. 1477-1484.

79. Yonezawa, A., Masuda, S., Yokoo, S., Katsura, T., and Inui, K., *Cisplatin and oxaliplatin, but not carboplatin and nedaplatin, are substrates for human organic cation transporters (SLC22A1-3 and multidrug and toxin extrusion family).* Journal of Pharmacology and Experimental Therapeutics, 2006. **319**(2): p. 879-886.

80. Zhang, S.Z., Lovejoy, K.S., Shima, J.E., Lagpacan, L.L., Shu, Y., Lapuk, A., Chen, Y., Komori, T., Gray, J.W., Chen, X., Lippard, S.J., and Giacomini, K.M.,

Organic cation transporters are determinants of oxaliplatin cytotoxicity. Cancer Research, 2006. **66**(17): p. 8847-8857.

81. Yokoo, S., Yonezawa, A., Masuda, S., Fukatsu, A., Katsura, T., and Inui, K.-I., *Differential contribution of organic cation transporters, OCT2 and MATE1, in platinum agent-induced nephrotoxicity.* Biochemical Pharmacology, 2007. **74**(3): p. 477-487.

82. Yokoo, S., Masuda, S., Yonezawa, A., Terada, T., Katsura, T., and Inui, K.I., *Significance of organic cation transporter 3 (SLC22A3) expression for the cytotoxic effect of oxaliplatin in colorectal cancer.* Drug Metabolism and Disposition, 2008. **36**(11): p. 2299-2306.

83. Filipski, K.K., Loos, W.J., Verweij, J., and Sparreboom, A., *Interaction of cisplatin with the human organic cation transporter 2.* Clinical Cancer Research, 2008. **14**(12): p. 3875-3880.

84. Burger, H., Zoumaro-Djayoon, A., Boersma, A.W.M., Helleman, J., Berns, E., Mathijssen, R.H.J., Loos, W.J., and Wiemer, E.A.C., *Differential transport of platinum compounds by the human organic cation transporter hOCT2 (hSLC22A2).* British Journal of Pharmacology. **159**(4): p. 898-908.

85. Lovejoy, K.S., Todd, R.C., Zhang, S.Z., McCormick, M.S., D'Aquino, J.A., Reardon, J.T., Sancar, A., Giacomini, K.M., and Lippard, S.J., *Cis-diammine(pyridine)chloroplatinum(II), a monofunctional platinum(II) antitumor agent: Uptake, structure, function, and prospects.* Proceedings of the National

Academy of Sciences of the United States of America, 2008. **105**(26): p. 8902-8907.

86. Yonezawa, A., Masuda, S., Nishihara, K., Ikuko, Y., Katsura, T., and Inui, K., *Organic cation transporter Oct2 (Slc22a2) as a determinant of the cisplatin-induced nephrotoxicity in the rat.* Yakugaku Zasshi-Journal of the Pharmaceutical Society of Japan, 2005. **125**: p. 46-47.

87. Tanihara, Y., Masuda, S., Katsura, T., and Inui, K.-i., *Protective effect of concomitant administration of imatinib on cisplatin-induced nephrotoxicity focusing on renal organic cation transporter Oct2.* Biochemical Pharmacology, 2009. **78**(9): p. 1263-1271.

88. Otsuka, M., Matsumoto, T., Morimoto, R., Arioka, S., Omote, H., and Moriyama, Y., *A human transporter protein that mediates the final excretion step for toxic organic cations.* Proceedings of the National Academy of Sciences of the United States of America, 2005. **102**(50): p. 17923-17928.

89. Masuda, S., Terada, T., Yonezawa, A., Tanihara, Y., Kishimoto, K., Katsura, T., Ogawa, O., and Inui, K.-i., *Identification and functional characterization of a new human kidney-specific H+/organic cation antiporter, kidney-specific multidrug and toxin extrusion 2.* Journal of the American Society of Nephrology, 2006. **17**(8): p. 2127-2135.

90. Terada, T., Masuda, S., Asaka, J.-i., Tsuda, M., Katsura, T., and Inui, K.-i., *Molecular cloning, functional characterization and tissue distribution of rat*

H+/organic cation antiporter mate1. Pharmaceutical Research, 2006. **23**(8): p. 1696-1701.

91. Tanihara, Y., Masuda, S., Sato, T., Katsura, T., Ogawa, O., and Inui, K.-i., *Substrate specificity of MATE1 and MATE2-K, human multidrug and toxin extrusions/H(+) organic cation antiporters.* Biochemical Pharmacology, 2007. **74**(2): p. 359-371.

92. Chen, Y., Zhang, S.Z., Sorani, M., and Giacomini, K.M., *Transport of paraquat by human organic cation transporters and multidrug and toxic compound extrusion family.* Journal of Pharmacology and Experimental Therapeutics, 2007. **322**(2): p. 695-700.

93. Hiasa, M., Matsumoto, T., Komatsu, T., Omote, H., and Moriyama, Y., *Functional characterization of testis-specific rodent multidrug and toxic compound extrusion 2, a class III mate-type polyspecific H+/organic cation exporter.* American Journal of Physiology. Cell physiology, 2007. **293**(5): p. C1437-1444.

94. Chen, Y., Teranishi, K., Li, S., Yee, S.W., Hesselson, S., Stryke, D., Johns, S.J., Ferrin, T.E., Kwok, P., and Giacomini, K.M., *Genetic variants in multidrug and toxic compound extrusion-1, hMATE1, alter transport function.* Pharmacogenomics Journal, 2009. **9**(2): p. 127-136.

95. Godwin, A.K., Meister, A., Odwyer, P.J., Huang, C.S., Hamilton, T.C., and Anderson, M.E., *High-resistance to cisplatin in human ovarian-cancer cell-lines*

is associated with marked increase of glutathione synthesis. Proceedings of the National Academy of Sciences of the United States of America, 1992. **89**(7): p. 3070-3074.

96. Ishikawa, T. and Aliosman, F., *Glutathione-associated cis-diamminedichloroplatinum(II) metabolism and ATP-dependent efflux from leukemia-cells - molecular characterization of glutathione-platinum complex and its biological significance.* Journal of Biological Chemistry, 1993. **268**(27): p. 20116-20125.

97. Ishikawa, T., Wright, C.D., and Ishizuka, H., *GS-X pump is functionally overexpressed in cis-diamminedichloroplatinum(II)-resistant human leukemia HL-60 cells and down-regulated by cell-differentiation.* Journal of Biological Chemistry, 1994. **269**(46): p. 29085-29093.

98. Cui, Y., *Drug resistance and ATP-dependent conjugate transport mediated by the apical multidrug resistance protein, MRP2, permanently expressed in human and canine cells.* Molecular Pharmacology, 1999. **55**: p. 929-937.

99. Cole, S.P.C., Sparks, K.E., Fraser, K., Loe, D.W., Grant, C.E., Wilson, G.M., and Deeley, R.G., *Pharmacological characterization of multidrug-resistant MRP-transfected human tumor-cells.* Cancer Research, 1994. **54**(22): p. 5902-5910.

100. Zaman, G.J.R., Flens, M.J., Vanleusden, M.R., Dehaas, M., Mulder, H.S., Lankelma, J., Pinedo, H.M., Scheper, R.J., Baas, F., Broxterman, H.J., and Borst, P., *The human multidrug resistance-associated protein MRP is a plasma-*

membrane drug-efflux pump. Proceedings of the National Academy of Sciences of the United States of America, 1994. **91**(19): p. 8822-8826.

101. Devries, E.G.E., Muller, M., Meijer, C., Jansen, P.L.M., and Mulder, N.H., *Role of the glutathione s-conjugate pump in cisplatin resistance.* Journal of the National Cancer Institute, 1995. **87**(7): p. 537-538.

102. Hamaguchi, K., Godwin, A.K., Yakushiji, M., Odwyer, P.J., Ozols, R.F., and Hamilton, T.C., *Cross-resistance to diverse drugs is associated with primary cisplatin resistance in ovarian-cancer cell-lines.* Cancer Research, 1993. **53**(21): p. 5225-5232.

103. Ikuta, K., Takemura, K., Sasaki, K., Kihara, M., Nishimura, M., Ueda, N., Naito, S., Lee, E., Shimizu, E., and Yamauchi, A., *Expression of multidrug resistance proteins and accumulation of cisplatin in human non-small cell lung cancer cells.* Biological & Pharmaceutical Bulletin, 2005. **28**(4): p. 707-712.

104. Sharp, S.Y., Smith, V., Hobbs, S., and Kelland, L.R., *Lack of a role for MRP1 in platinum drug resistance in human ovarian cancer cell lines.* British Journal of Cancer, 1998. **78**(2): p. 175-180.

105. de Cremoux, P., Jourdan-Da-Silva, N., Couturier, J., Tran-Perennou, C., Schleiermacher, G., Fehlbaum, P., Doz, F., Mosseri, V., Delattre, O., Klijanienko, J., Vielh, P., and Michon, J., *Role of chemotherapy resistance genes in outcome of neuroblastoma.* Pediatric Blood & Cancer, 2007. **48**(3): p. 311-317.

106. Nicholson, D.L., Purser, S.M., and Maier, R.H., *Differential cytotoxicity of trace metals in cisplatin-sensitive and -resistant human ovarian cancer cells.* Biometals, 1998. **11**(3): p. 259-263.

107. Suzuki, T., Nishio, K., and Tanabe, S., *The MRP family and anticancer drug metabolism.* Current Drug Metabolism, 2001. **2**(4): p. 367-377.

108. Kim, Y.H., Ishii, G., Goto, K., Ota, S., Kubota, K., Murata, Y., Mishima, M., Saijo, N., Nishiwaki, Y., and Ochiai, A., *Expression of breast cancer resistance protein is associated with a poor clinical outcome in patients with small-cell lung cancer.* Lung Cancer, 2009. **65**(1): p. 105-111.

109. Borst, P., Kool, M., and Evers, R., *Do cMOAT (MRP2), other MRP homologues, and LRP play a role in MDR?* Seminars in Cancer Biology, 1997. **8**(3): p. 205-213.

110. Liedert, B., Materna, V., Schadendorf, D., Thomale, J., and Lage, H., *Overexpression of cMOAT (MRP2/ABCC2) is associated with decreased formation of platinum-DNA adducts and decreased G2-arrest in melanoma cells resistant to cisplatin.* The Journal of Investigative Dermatology, 2003. **121**(1): p. 172-176.

111. Schrenk, D., Baus, P.R., Ermel, N., Klein, C., Vorderstemann, B., and Kauffmann, H.M., *Up-regulation of transporters of the MRP family by drugs and toxins.* Toxicology Letters, 2001. **120**(1-3): p. 51-57.

112. Kauffmann, H.M., Keppler, D., Kartenbeck, J., and Schrenk, D., *Induction of cMRP/cMOAT gene expression by cisplatin, 2-acetylaminofluorene, or cycloheximide in rat hepatocytes.* Hepatology, 1997. **26**(4): p. 980-985.

113. Verena, M., Bernd, L., Jürgen, T., and Hermann, L., *Protection of platinum-DNA adduct formation and reversal of cisplatin resistance by anti-MRP2 hammerhead ribozymes in human cancer cells.* International Journal of Cancer, 2005. **115**(3): p. 393-402.

114. Koike, K., Kawabe, T., Tanaka, T., Toh, S., Uchiumi, T., Wada, M., Akiyama, S., Ono, M., and Kuwano, M., *A canalicular multispecific organic anion transporter (cMOAT) antisense cDNA enhances drug sensitivity in human hepatic cancer cells.* Cancer Research, 1997. **57**(24): p. 5475-5479.

115. Ma, J.J., Chen, B.L., and Xin, X.Y., *Inhibition of multi-drug resistance of ovarian carcinoma by small interfering RNA targeting to MRP2 gene.* Archives of Gynecology and Obstetrics, 2009. **279**(2): p. 149-157.

116. Folmer, Y., Schneider, M., Blum, H.E., and Hafkemeyer, P., *Reversal of drug resistance of hepatocellular carcinoma cells by adenoviral delivery of anti-ABCC2 antisense constructs.* Cancer Gene Therapy, 2007. **14**(11): p. 875-884.

117. Marques, M., and Sweet-Cordero, A., *New insights into tumor suppressors.* Genome Biology, 2008. **9**(9): p. 320.1-320.3.

118. Shu, Y., Brown, C., Castro, R.A., Shi, R.J., Lin, E.T., Owen, R.P., Sheardown, S.A., Yue, L., Burchard, E.G., Brett, C.M., and Giacomini, K.M., *Effect of genetic variation in the organic cation transporter 1, OCT1, on metformin pharmacokinetics.* Clinical Pharmacology & Therapeutics, 2008. **83**(2): p. 273-280.

119. Shu, Y., Sheardown, S.A., Brown, C., Owen, R.P., Zhang, S.Z., Castro, R.A., Ianculescu, A.G., Yue, L., Lo, J.C., Burchard, E.G., Brett, C.M., and Giacomini, K.M., *Effect of genetic variation in the organic cation transporter 1 (OCT1) on metformin action.* Journal of Clinical Investigation, 2007. **117**(5): p. 1422-1431.

120. Urban, T.J., Brown, C., Castro, R.A., Shah, N., Mercer, R., Huang, Y., Brett, C.M., Burchard, E.G., and Giacomini, K.M., *Effects of genetic variation in the novel organic cation transporter, OCTN1, on the renal clearance of gabapentin.* Clinical Pharmacology & Therapeutics, 2008. **83**(3): p. 416-421.

CHAPTER 2

ROLE OF ORGANIC CATION TRANSPORTER 1, OCT1, IN THE PHARMACOKINETICS OF PYROPLATIN

Introduction

Membrane transporters are major determinants of drug absorption, disposition, toxicity and response. For many years the focus of pharmacologic studies of membrane transporters was on efflux pumps primarily in the ATP Binding Cassette (ABC) superfamily, many of which have been found to be major determinants of drug absorption, distribution and sensitivity [1]. However more recent pharmacologic studies have focused on influx transporters, which also appear to play important roles in drug disposition and response [2-4].

Recently, organic cation transporter 1 (OCT1), encoded by *SLC22A1*, has been shown to affect the pharmacokinetics and pharmacodynamics of metformin in both humans and rodents [5, 6]. In humans, OCT1 is primarily expressed in the liver, with much lower levels in other tissues, including intestine and skeletal muscle [7-9]. In rodents, OCT1 is expressed in equal abundance in the liver, kidney, and small intestine [10, 11]. In general the human OCT1 mediates intracellular uptake of a broad range of structurally diverse monovalent organic cations with molecular weights of less than 400 Daltons [12, 13]. Substrates of OCT1 include endogenous compounds, such as choline, creatinine, and monoamine neurotransmitters; clinically used drugs, such as metformin, oxaliplatin and cimetidine; and a variety of xenobiotics, such as tetraethylammonium

(TEA, model cation), N-methylquinine, and 1-methyl-4-phenylpyridinium (MPP^+) [12]. *In vivo*, *Oct1-/-* mice display impaired liver uptake and intestinal excretion of a subset of organic cations, such as TEA, MPP^+, and metformin [5, 14], suggesting that the transporter Oct1 is important for the uptake of certain xenobiotics and drugs into various tissues including the liver in the animal model.

Platinum based chemotherapies have been widely used to treat solid tumors since the introduction in clinical use of cisplatin in the 1970's [15]. Although cisplatin is effective against several solid tumors, its clinical use is limited because of its toxic effects as well as the intrinsic and acquired resistance of some tumors to this drug [16]. To overcome limitations related to toxicities, carboplatin was developed [17]. Carboplatin is equally effective as cisplatin, but with a more acceptable side-effect profile [18]. More recent efforts to overcome tumor resistance to cisplatin have resulted in not only the approval of oxaliplatin but also the clinical development of picoplatin and satraplatin [19].

Pyroplatin, also known as cis-diammine(pyridine)chloroplatinum(II), belongs to a different series of platinum analogues from cisplatin. In particular, it is a cationic triamine complex that possesses desirable physical properties, such as high stability and solubility in aqueous media. Although pyroplatin violates some of the classical structure-activity relationships, its anticancer activity was established in murine tumor models 20 years ago [20]. However, pyroplatin has never been tested in humans, probably because this compound only forms monofunctional complexes with DNA and due to its polarity, the drug was thought to have unfavorable pharmacokinetic properties [21]. Recently, we showed that pyroplatin is an excellent substrate of OCT1 [21]. When overexpressed in

transfected cells, OCT1 substantially increased the cellular uptake and cytotoxicity of pyroplatin indicating that OCT1 facilitates intracellular accumulation of pyroplatin, thereby sensitizing the cells to pyroplatin cytotoxicity. These *in vitro* studies suggest that OCT1 may be a major determinant of the pharmacokinetics of pyroplatin and that this polar drug may have more favorable pharmacokinetic properties than was previously thought.

In this study, we determined the pharmacokinetic properties of pyroplatin in mice, and tested the hypothesis that Oct1 contributes to the pharmacokinetics of pyroplatin using *Oct1-/-* mice. Specifically, we examined the role of Oct1 in the intracellular accumulation and DNA adduct formation of pyroplatin in primary hepatocytes derived from both *Oct1-/-* and wild-type mice. Furthermore, the effects of Oct1 on the pharmacokinetics and tissue accumulation of pyroplatin were also examined in *Oct1-/-* and wild-type mice. The results of our study suggest that pyroplatin has favorable pharmacokinetic properties and that Oct1 plays a role in the elimination and tissue distribution of the drug. Our study sets the stage for further toxicity and efficacy studies.

Materials and Methods

Synthesis of pyroplatin *cis*-[Pt(NH$_3$)$_2$(Pyr)Cl]NO$_3$. Pyroplatin was synthesized by a method adapted from that of Hollis et.al [20]. Briefly, to a solution of cisplatin (900 mg, 3 mmol) in 15 mL of anhydrous DMF was added $AgNO_3$ (485 mg, 2.85 mmol) at room temperature and the mixture was stirred for 24 h. The resulting precipitate of AgCl was removed by filtration before the addition of pyridine (242 µL, 3 mmol) to the filtrate. After the solution was stirred for an additional day, the DMF was removed under vacuum,

and the remaining oil was triturated with CH_2Cl_2 (100 mL), followed by trituration with diethyl ether (50 mL). The resulting solid was filtered and then recrystallized from hot methanol to obtain product *cis*-[$Pt(NH_3)_2(Pyr)Cl](NO_3$) as a light yellow solid (yield 720 mg, 1.77 mmol, 59%). ^{1}H NMR (400 MHz, D_2O) δ 8.90 (m, 1H, Ar), 8.45 (m, 2H, Ar), 7.31 (m, 2H, Ar), 4.72, 4.26 (bs, 3H, N*H*$_3$); ESI-MS 343.1 $[M]^+$; Elemental Analysis: Found (%) C, 15.12; H, 2.50; N, 13.62. Calculate for $C_5H_{11}ClN_4O_3Pt$ (%): C, 14.80; H, 2.73; N, 13.81.

Primary mouse hepatocytes. Primary hepatocytes were isolated from *Oct1+/+* and *Oct1-/-* mice by the UCSF Liver Center using the standard collagenase method [22]. The cells were seeded onto collagen-coated 6-well plates (Becton Dickenson, Bedford, MA) at a density of 0.8 x 10^6 cells/well in William's E medium supplemented with 100 units/ml penicillin, 100 µg/ml streptomycin, 10% fetal bovine serum (FBS), 0.1 µM dexamethasone, 2 mM L-glutamine, 1X ITS (100X Insulin-Transferrin-Selenium from Invitrogen). After attachment (2-3 hours), the cells were maintained in fresh medium for another 16 -24 hours followed by drug treatment as described below.

Intracellular accumulation of pyroplatin in primary hepatocytes. The intracellular accumulation of platinum was determined after 1 hour exposure to pyroplatin as described previously [23] with some modifications. Briefly, the primary hepatocytes on collagen-coated 6-well plates (0.8 x 10^5 cells/well) were washed with PBS once and then were incubated in the serum-free culture medium containing pyroplatin with or without an OCT1 inhibitor at 37°C in 5% CO_2 for 1 hour unless specified. After incubation, cells were washed three times with ice-cold PBS. The cells

were dissolved in 300 µl of 70% nitric acid at 65°C for at least 2.5 hours. Distilled water containing 10 ppb of iridium (Sigma) and 0.1% Triton X-100 was added to the samples to dilute nitric acid to 7%. The platinum content was measured by inductively coupled plasma mass spectrometry (ICP-MS) in the Analytical Facility at the University of California at Santa Cruz (Santa Cruz, CA). Cell lysates from a set of identical cultures were used for BCA protein assay. Cellular platinum accumulation was normalized to the protein content.

Platinum-DNA adduct formation in primary hepatocytes. The platinum content associated with genomic DNA in primary hepatocytes was determined as described previously [23] with some modifications. Briefly, the primary hepatocytes on collagen-coated 6-well plates (0.8×10^5 cells/well) were washed with PBS once and then were incubated in the serum-free culture medium containing pyroplatin with or without an OCT1 inhibitor at 37°C in 5% CO_2 for 1 hour unless specified. After incubation, cells were washed three times with ice-cold PBS. Genomic DNA was isolated from the cells using Wizard Genomic DNA Purification kit (Promega, Madison, WI) according to the manufacturer's protocol. The DNA-bound platinum was determined by ICP-MS. The DNA content from the same DNA preparation was measured by absorption spectroscopy at 260 nm. Platinum-DNA adduct level was normalized to total DNA content.

RNA Isolation. Total RNA from primary hepatocytes was isolated using an RNeasy Mini kit (Qiagen, Valencia, CA) according to the manufacturer's protocols. Total RNA from tissues was extracted using Trizol (Invitrogen). During the RNA purification

procedure, DNase I was treated to digest residual genomic DNA. RNA was quantified spectrophotometrically at 260 nm. Extracted RNA was stored at -80^{o}C until use.

Quantitative real-time PCR. 5 µg of total RNA from each sample was reverse transcribed into cDNA using a superscript first-strand cDNA synthesis kit (Invitrogen, Carlsbad, Calif., USA) according to the manufacturer's protocol. Quantitative real-time PCR was carried out in a 96-well plate in a total volume of 10 µl reaction solution that includes a cDNA equivalent of 2 µg total RNA, specific probe and Taqman Universal Master Mix (Applied Biosystems, Foster City, CA). Reactions were run on an ABI Prism 7700, and the thermal cycling conditions were 95 ^{o}C for 20 seconds followed by 40 cycles of 95 ^{o}C for 3 seconds and 60 ^{o}C for 30 seconds. The amplification of glyceraldehydes-3-phosphate dehydrogenase (GAPDH) mRNA was used as an internal control.

Animals. *Oct1*+/+ and *Oct1*-/- mice in FVB background were housed in a virus-free, temperature-controlled facility on a 12-h light–dark cycle. They were allowed standard mouse food and water *ad libitum*. *Oct1*-/- mice were generated as described elsewhere [14]. The experiments on mice were approved by the Institutional Animal Care and Use Committee of University of California at San Francisco.

Pyroplatin tissue accumulation in mice: Eight weeks old *Oct1*+/+ and *Oct1*-/- mice were given 8 mg/kg of pyroplatin in PBS via tail vein injection. The animals weighed 25.7 ± 2.4 g and 23.2 ± 1.2 g for *Oct1*+/+ and *Oct1*-/- mice, respectively, at the time of treatment. The animals were sacrificed 1 hour after pyroplatin treatment. Blood samples were collected by heart puncture and transferred into heparinized BD vacutainer

blood collection tubes. Blood was centrifuged for 30 min at 1000 x g and the plasma was decanted and frozen at -80^{o}C until analysis. Tissues (liver, kidney, heart, brain, ileum, intestine, muscle) were collected as quickly as possible and snap frozen in liquid nitrogen. Plasma and tissue were dissolved in 70% nitric acid in 10 volumes of plasma and in 10 volumes of tissue weight, respectively, and incubated at 65°C for at least 2.5 hours. Distilled water containing 10 ppb of iridium (Sigma) and 0.1% Triton X-100 was added to the samples to dilute nitric acid to 7%. 5 µl of plasma and about 10-30 mg of tissue were used for total platinum measurement by ICP-MS.

Pyroplatin pharmacokinetics in mice: Eight weeks old male *Oct1*+/+ and *Oct1*-/- mice were given 8 mg/kg of pyroplatin in PBS via tail vein injection and placed in metabolic cages for 24 hrs. The animals weighed 30.2 ± 1.7 g and 29.6 ± 0.4 g for *Oct1*+/+ and *Oct1*-/- mice, respectively at the time of treatment. Blood samples (20 µl) were collected at 15, 30 min, 1, 2, 3, 4, 8, 10, 24, 48 hr after pyroplatin treatment by tail vein bleeding into heparinized micro-hematocrit capillary tubes (Fisher, Pittsburg, PA). Blood was centrifuged for 5 min using a Microhematocrit Centrifuge (Thermo Fisher Scientific Inc. Waltham, MA) and the plasma was decanted and frozen at -80^{o}C until analysis. Urine was collected from tubes attached to the cages. Tissues (liver, kidney, intestine, muscle) were collected as quickly as possible at the last time point and snap frozen in liquid nitrogen. Plasma, urine and tissue were dissolved in 70% nitric acid in 10 volumes of plasma, urine and in 10 volumes of tissue weight, respectively, and incubated at 65°C for at least 2.5 hours. Distilled water containing 10 ppb of iridium (Sigma) and 0.1% Triton X-100 was added to the samples to dilute nitric acid to 7%. 5 ul of plasma, urine and about 10-30 mg of tissue powders were used for total platinum measurement by

ICP-MS. The pharmacokinetics parameters were obtained by two compartmental analysis using WinNonlin 4.0 (Pharsight Corporation, Mountain view, CA).

Statistical analysis. Unless specified, data are expressed as mean ± standard deviation (SD). Data were analyzed statistically using the unpaired Student's t test. Multiple comparisons were performed with Dunnett's two-tailed test after one-way ANOVA. A P value of less than 0.05 was considered statistically significant.

Results

Oct1 facilitated the rate of intracellular accumulation and DNA adduct formation of pyroplatin in primary mouse hepatocytes *in vitro*. To examine the role of Oct1 in the disposition of pyroplatin to the liver, we compared the intracellular accumulation rate and DNA adduct formation rate of pyroplatin in hepatocytes derived from *Oct1* wild-type mice with that in hepatocytes derived from *Oct1-/-* mice. The studies showed that the hepatocellular accumulation rate of pyroplatin (10 μM) after 1 hr exposure in hepatocytes from *Oct1* wild-type mice [251.2 ± 94.6 pmol/mg protein/hr] was 2.9-fold of that in hepatocytes from *Oct1 -/-* mice [87.8 ± 7.6 pmol/mg protein/hr] ($p < 0.01$; Figure 2.1A). Coincubation of pyroplatin with disopyramide (150 μM), an OCT1 inhibitor, resulted in a 4.5-fold decrease in the rate of platinum accumulation in hepatocytes from *Oct1* wild-type mice [control versus disopyramide treated, 251.2 ± 94.6 pmol/mg protein/hr versus 55.9 ± 1.4 pmol/mg protein/hr] ($p < 0.01$) with no effect in hepatocytes from *Oct1-/-* mice [control versus disopyramide treated, 87.8 ± 7.6 pmol/mg protein/hr versus 95.8 ± 17.6 pmol/mg protein/hr] ($p > 0.05$; Figure 2.1A).

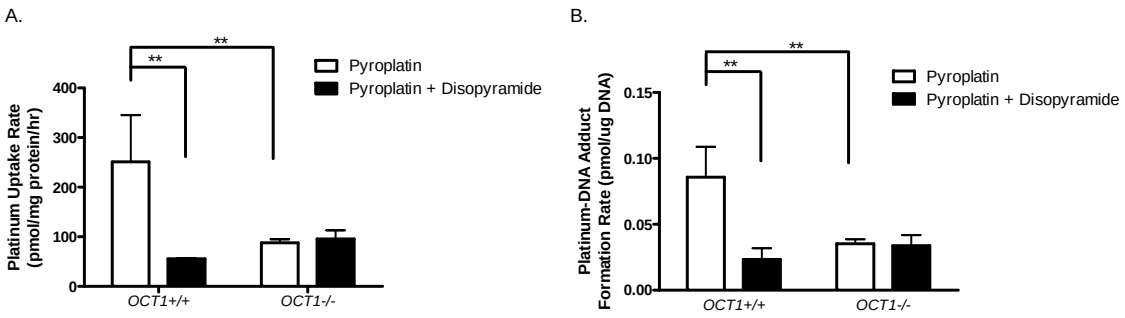

Figure 2.1. Effects of Oct1 on the rate of intracellular accumulation and DNA adduct formation of pyroplatin in primary mouse hepatocytes. Intracellular platinum accumulation rates (A) and platinum-DNA adduct formation (B) in hepatocytes from *Oct1* wild-type and *Oct1-/-* mice after 1 hour exposure to 10 µM pyroplatin in the presence (black bars) absence (white bars) of an Oct1 inhibitor, disopyramide (150 µM) were determined as described in Materials and Methods. Briefly, freshly isolated hepatocytes from *Oct1* wild-type and *Oct1-/-* mice were incubated in the serum-free culture medium containing 10 µM pyroplatin at 37^{o}C and 5% CO_2 for 1 hour following overnight incubation. Total platinum concentration inside the cells and DNA-bound platinum were determined using ICP-MS. Total platinum concentration was normalized to protein content, and DNA-bound platinum was normalized to DNA content. Data are presented as the mean ± SD (n=3) and from a representative experiment. ** $P < 0.01$.

To determine whether the pyroplatin taken up by hepatocytes via Oct1 was available for reaction with DNA, the molecular target of platinum-based drugs, we also measured platinum-DNA adduct formation after 1 hour of exposure to pyroplatin with or without the OCT1 inhibitor, disopyramide (Figure 2.1B). The platinum-DNA adduct level after one hour exposure to pyroplatin in hepatocytes from *Oct1* wild-type mice [0.086 ± 0.023 pmol/µg DNA] was 2.4-fold greater than that in hepatocytes from *Oct1-/-* mice [0.035 ± 0.003 pmol/µg DNA] ($p < 0.01$; Figure 2.1B). Co-incubation of pyroplatin with disopyramide (150 µM) significantly decreased (3.7-fold; $p< 0.01$) platinum-DNA adduct formation in hepatocytes from *Oct1* wild-type mice [control versus disopyramide treated, 0.086 ± 0.023 pmol/µg DNA versus 0.023 ± 0.008 pmol/µg DNA] ($p < 0.01$) with no effect in hepatocytes from *Oct1-/-* mice [control versus disopyramide treated, 0.035 ± 0.003 pmol/µg DNA versus 0.034 ± 0.008 pmol/µg DNA] ($p > 0.05$; Figure 2.1B). Collectively, data shown in Figure 2.1 suggest that Oct1 mediates the uptake and binding to DNA of pyroplatin in mouse hepatocytes.

Oct1 enhanced the hepatic and intestinal accumulation of pyroplatin *in vivo*.

To extend the *in vitro* cellular studies, we examined the role of Oct1 in the accumulation of pyroplatin in various tissues after dosing of pyroplatin (8 mg/kg) to *Oct1* wild-type and *Oct1-/-* mice (Figure 2.2). Total levels of platinum in the plasma were significantly higher (1.3-fold) in *Oct1-/-* mice than in *Oct1* wild-type mice (Figure 2.2A, $p < 0.001$). Comparing the absolute platinum level in various tissues (Table 2.1), we observed that the platinum accumulation levels in liver (Figure 2.2B) and intestine (Figure 2.2C) were significantly higher in *Oct1* wild-type mice than in *Oct1-/-* mice ($p < 0.01$). However, the platinum accumulation levels in kidney (Figure 2.2D), heart (Figure 2.2E) and muscle

(Figure 2.2F) in *Oct1* wild-type mice were significantly lower than that in *Oct1-/-* mice ($p < 0.05$). No platinum accumulation difference was measured in brain (Figure 2.2G) between *Oct1* wild-type and *Oct1-/-* mice. When the absolute platinum level in the various tissues was normalized to the corresponding plasma concentration (Figure 2.3), we observed that platinum levels in the muscle and kidney were no longer significantly different between *Oct1* wild-type and *Oct1-/-* mice (Figure 2.3C, Figure 2.3E; $p > 0.05$), while the normalization to plasma concentration had no effect on the platinum accumulation level in the heart (Figure 2.3D, $p < 0.01$). Normalization to plasma concentrations exaggerated the difference of platinum accumulation levels in liver (Figure 2.3A) and intestine (Figure 2.3B) between *Oct1* wild-type and *Oct1-/-* mice, the differences in liver and intestine were 2.7-fold and 3.9-fold, respectively. Comparing the platinum accumulation in different tissues, we also observed that the highest platinum accumulation levels were found in liver and intestine; brain had the lowest levels in both *Oct1* wild-type and *Oct1-/-* mice (Table 2.1). Taken together, this study suggests that the expression of Oct1 in liver and intestine contributes to the enhanced accumulation of pyroplatin in these organs.

Oct1 affected the pharmacokinetics of pyroplatin in mice. The time-course of platinum in plasma following a single i.v. dose of pyroplatin (8 mg/kg) to *Oct1* wild-type and *Oct1-/-* mice is shown in Figure 2.4. Similar to the pharmacokinetics of AMD473 (picoplatin), a third generation platinum agent, which has been evaluated in Phase-III clinical trials for treatment of non-small cell lung cancer (NSCLC) [24], the concentration versus time course of total platinum followed a two-compartment model in both *Oct1* wild-type and *Oct1-/-* mice. The mean plasma concentrations of pyroplatin in

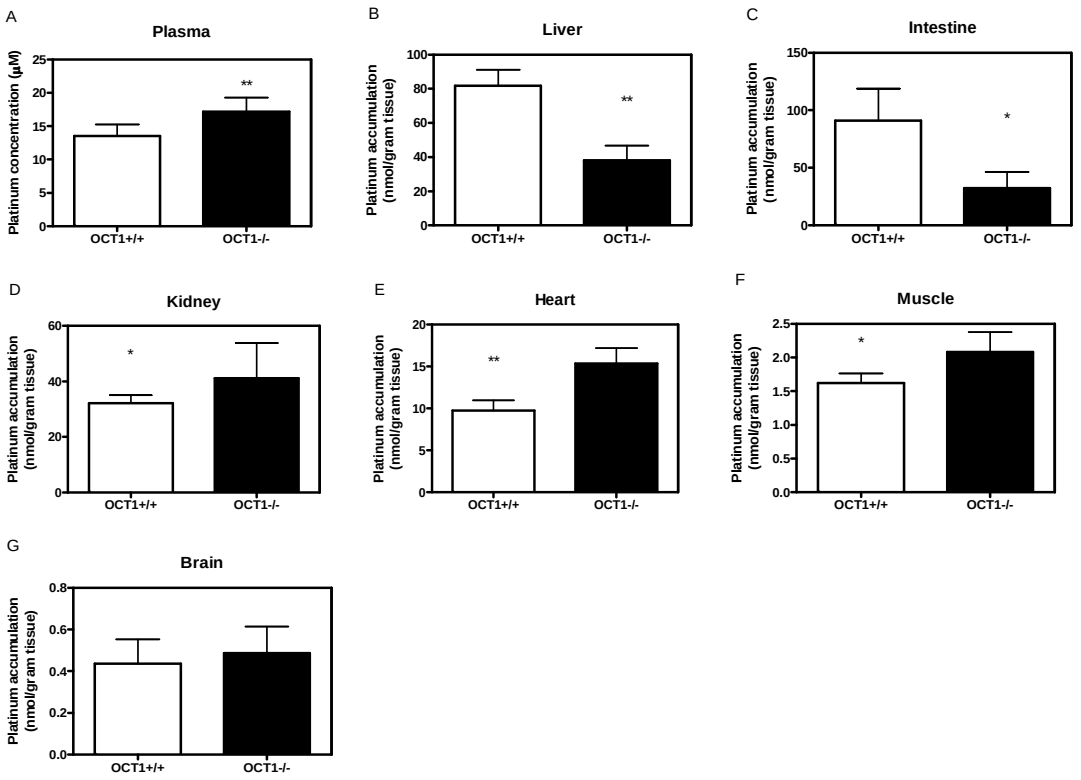

Figure 2.2. Effect of Oct1 on tissue accumulation of pyroplatin (absolute platinum levels) in various organs one hour after dosing. Absolute platinum accumulation levels in plasma (A), liver (B), intestine (C), kidney (D), heart (E), muscle (F) and brain (G) were measured one hour post dosing in *Oct1* wild-type and *Oct1-/-* mice. Briefly, the mice were given 8 mg/kg of pyroplatin in PBS via tail vein. Plasma, liver, intestine, kidney, heart, muscle and brain were harvested one hour post dosing. The platinum levels in plasma and various organs were determined using ICP-MS. Data are presented as the mean ± SD ($n \geq 5$). * $P < 0.05$; ** $P < 0.001$.

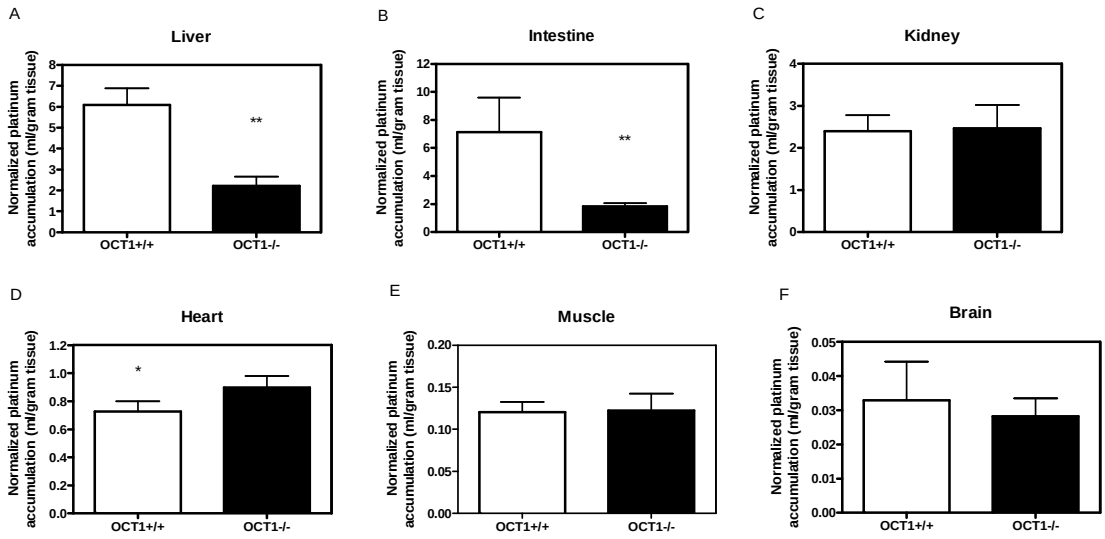

Figure 2.3. Effects of Oct1 on tissue accumulation of pyroplatin (normalized to plasma platinum levels) in various organs one hour after dosing. Normalized platinum accumulation levels in liver (A), intestine (B), kidney (C), heart (D), muscle (E) and brain (F) were measured one hour post dosing in *Oct1* wild-type and *Oct1-/-* mice. Briefly, the mice were given 8 mg/kg of pyroplatin in PBS via tail vein, and plasma, liver, intestine, kidney, heart, muscle and brain were harvested one hour after dosing. The platinum levels in plasma and various organs were determined using ICP-MS. The platinum levels in various organs were normalized to the plasma concentration of platinum. Data are presented as the mean ± SD ($n \geq 5$). * $P < 0.05$; ** $P < 0.001$.

Table 2.1 Pyroplatin accumulation in various tissues one hour post dosing. *Oct1+/+* (n=5) and *Oct1-/-* (n=7) mice were given a single dose of pyroplatin (8 mg/kg) by tail vein injection; blood and various tissues (liver, kidney, intestine, heart, muscle and brain) were harvested one hour post dosing. Total platinum in plasma and tissues was determined by ICP-MS. Normalized platinum levels in various tissues were obtained by dividing the total platinum levels by plasma concentration. Data are expressed as the mean ± SD. * $p < 0.05$; ** $p < 0.001$

		Liver		Kidney		Intestine	
	Plasma (uM)	Absolute (pmol/g tissue)	Normalized (ml/g tissue)	Absolute (pmol/g tissue)	Normalized (ml/g tissue)	Absolute (pmol/g tissue)	Normalized (ml/g tissue)
OCT1 WT	13.5 ± 1.7	81.8 ± 9.3	6.09 ± 0.79	32.1 ± 2.9	2.40 ± 0.37	90.9 ± 28.0	7.13 ± 2.47
OCT1 KO	17.2 ± 2.1	38.2 ± 8.5	2.23 ± 0.44	44.3 ± 11.5	2.47 ± 0.55	32.3 ± 14.2	1.84 ± 0.57
OCT1 WT/KO	0.8**	2.1**	2.7**	0.7*	1.0	2.8*	3.9**

	Muscle		Heart		Brain	
	Absolute (pmol/g tissue)	Normalized (ml/g tissue)	Absolute (pmol/g tissue)	Normalized (ml/g tissue)	Absolute (pmol/g tissue)	Normalized (ml/g tissue)
OCT1 WT	1.62 ± 0.14	0.121 ± 0.0112	9.77 ± 1.20	0.725 ± 0.075	0.436 ± 0.116	0.0328 ± 0.0114
OCT1 KO	2.08 ± 0.29	0.122 ± 0.020	15.4 ± 1.8	0.898 ± 0.081	0.487 ± 0.128	0.0282 ± 0.0052
OCT1 WT/KO	0.8*	1.0	0.6**	0.8*	0.9	1.2

Oct1-/- mice were significantly higher than that in *Oct1* wild-type mice at all time pointes (Figure 2.4). The mean pharmacokinetics parameters are shown in Table 2.2. Comparing the pharmacokinetics parameters of pyroplatin in *Oct1* wild-type mice with that in *Oct1-/-* mice, we observed that the platinum exposure over 48 hrs (AUC_{0-48}) in *Oct1-/-*mice [434 ± 29 μM*hr] was 1.69 fold of that in *Oct1* wild-type mice [257 ±7 μM*hr] ($p < 0.01$). The volume of distribution of pyroplatin in *Oct1* wild-type mice was 1.77 fold of that in *Oct1-/-* mice [3.37 ± 0.20 L/kg versus 1.90 ± 0.16 L/kg] ($p < 0.01$). Moreover, a significantly greater clearance was observed in *Oct1* wild-type mice in comparison to *Oct1-/-* mice [0.649 ± 0.081 ml/min*kg versus 0.444 ± 0.039 ml/min*kg] ($p < 0.05$), although renal clearance showed no difference between *Oct1+/+* mice and *Oct1-/-* mice. The renal clearance contributes to about 50% of the total clearance of platinum from plasma in both *Oct1+/+* and *Oct1-/-* mice. There was no difference in the distribution $t_{1/2}$ and terminal $t_{1/2}$ between *Oct1* wild-type and *Oct1-/-* mice.

Platinum accumulation in various tissues was also measured at the end of study, i.e. 48 hours after dosing. Similar to the data obtained at 1-hr, total platinum concentration in *Oct1-/-* mice was significantly higher than that in *Oct1+/+* mice (Figure 2.5A, $p < 0.001$). The absolute platinum accumulation levels in liver (Figure 2.5B, $p < 0.05$) and intestine (Figure 2.5C, $p < 0.001$) were significantly higher in *Oct1* wild-type mice than that in *Oct1-/-* mice; the platinum accumulation levels in kidney (Figure 2.5D), and muscle (Figure 2.5E) in *Oct1* wild-type mice were significantly lower than that in *Oct1-/-* mice ($p< 0.05$). The fold difference of platinum levels between *Oct1+/+* and *Oct1-/-* mice in liver and intestine increased to 2.98-fold and 4.10-fold from 1.93-fold and 2.65-fold after normalization to plasma concentration at 48 hr (Figure 2.6A, Figure 2.6B),

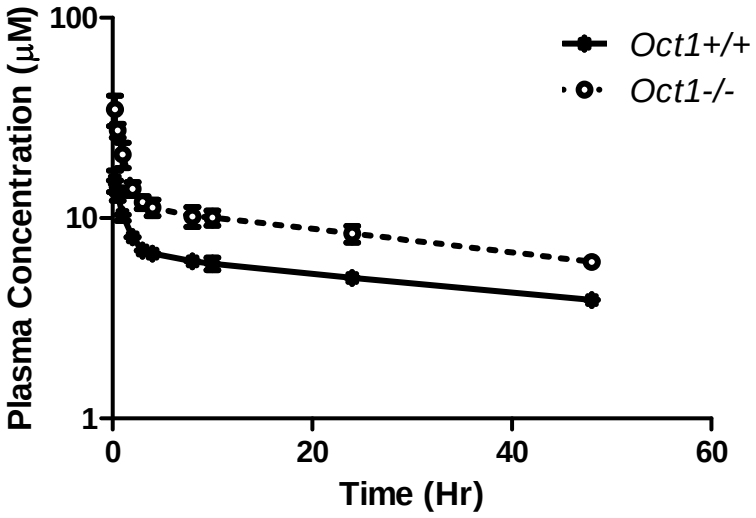

Figure 2.4. Effect of Oct1 on the total platinum concentrations in plasma after intravenous dosing of pyroplatin in mice. The mice (n = 3 per group) were treated with pyroplatin (8 mg/kg) by tail vein injection. Blood samples (20 µl) were collected at 15 and 30 min, and at 1, 2, 3, 4, 8, 10, 24, and 48 hr after pyroplatin treatment. Platinum levels in plasma were determined by ICP-MS. Data are presented as the mean ± SD (n =3).

Table 2.2. Plasma platinum pharmacokinetic parameters following a single intravenous dose of pyroplatin (8 mg/kg) in *Oct1*+/+ and *Oct1*-/- mice (3 per group). Blood samples for pharmacokinetic analysis were drawn up to 48 hours. The pharmacokinetic parameters were obtained by two compartmental analysis using WinNonlin 4.0.

	Oct1+/+	*Oct1*-/-	*Oct1*-/-/	
	Mean ± SD	Mean ± SD	*Oct1*+/+	P value
AUC_{0-48} (uM*hr)	257 ± 7	434 ± 29	1.69	0.009
AUC_{inf} (uM*hr)	604 ± 71	878 ± 74.	1.45	0.009
CL (ml/min*kg)	0.649 ± 0.081	0.444 ± 0.039	0.68	0.017
CL_R(ml/min*kg)	0.320 ± 0.246	0.221 ± 0.177	0.69	0.603
V_{SS} (L/kg)	3.37 ± 0.20	1.90 ± 0.16	0.56	0.0006
C_{max} (uM)	17.9 ± 2.2	43.1 ± 7.7	2.41	0.005
$T_{1/2,\alpha}$ (hr)	0.639 ± 0.032	0.494 ± 0.137	0.77	0.37
$T_{1/2,\beta}$ (hr)	66.6 ± 9.8	48.3 ± 6.8	0.73	0.20

Note: $T_{1/2,\alpha}$: distribution half life; $T_{1/2,\beta}$: terminal half life; C_{max}: maximal plasma concentration; AUC_{inf}: area under the curve of plasma concentration from time 0 to infinity; V_{SS}: volume of distribution at steady state; CL: clearance; CL_R: renal clearance.

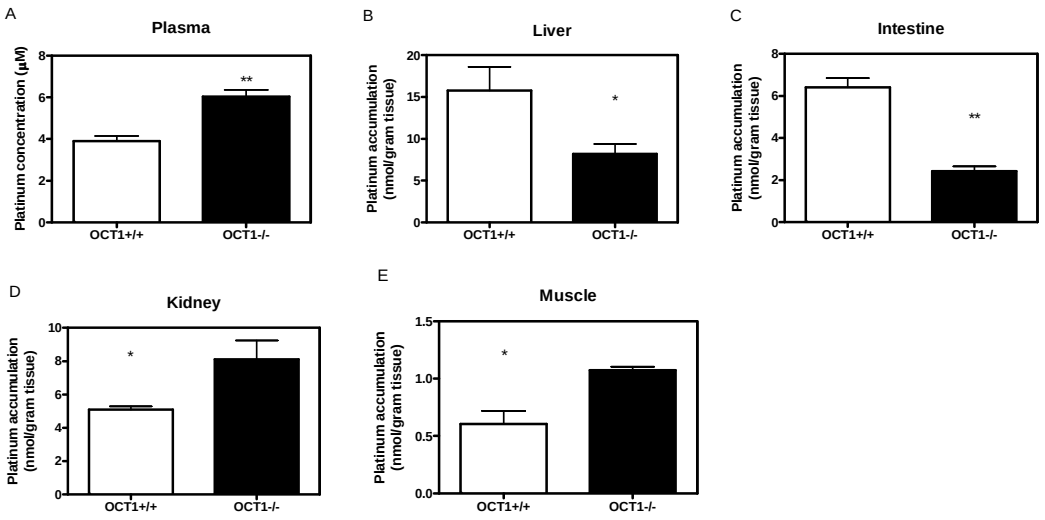

Figure 2.5. Effects of Oct1 on tissue accumulation of pyroplatin (absolute platinum levels) in various organs 48 hours after dosing. Absolute platinum accumulation levels in plasma (A), liver (B), intestine (C), kidney (D), and muscle (E) were measured 48 hours after dosing in *Oct1* wild-type and *Oct1-/-* mice. Briefly, the mice were given 8 mg/kg of pyroplatin in PBS via tail vein, and plasma, liver, intestine, kidney, and muscle were harvested at the end of pharmacokinetic study (48 hours post dosing). The platinum levels in plasma and various organs were determined using ICP-MS. Data are presented as the mean ± SD (n = 3). * $P < 0.05$; ** $P < 0.001$.

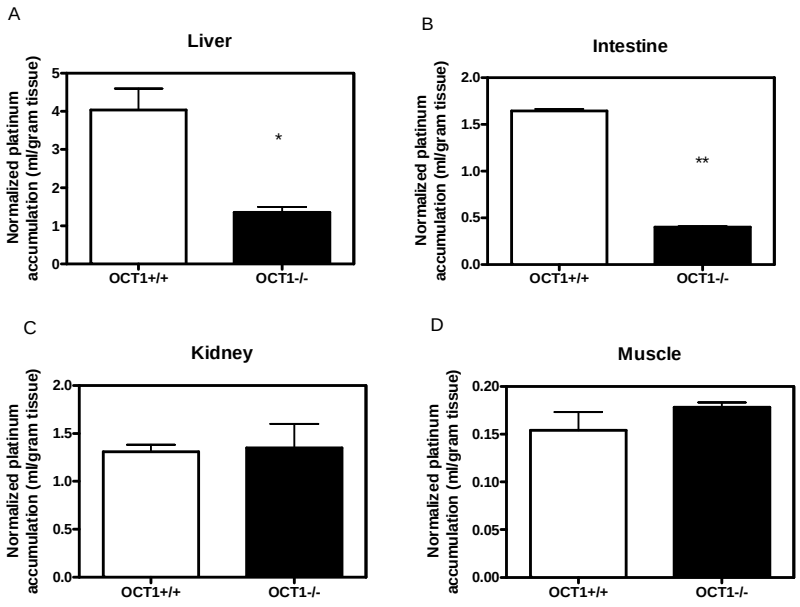

Figure 2.6. Effects of Oct1 on tissue accumulation of pyroplatin (normalized to plasma platinum levels) in various organs 48 hours after dosing. Normalized platinum accumulation levels in liver (A), intestine (B), kidney (C), and muscle (D) were determined 48 hours post after dosing in wild-type and *Oct1-/-* mice. Briefly, the mice were given 8 mg/kg of pyroplatin in PBS via tail vein, and plasma, liver, intestine, kidney, and muscle were harvested at the end of pharmacokinetic study (48 hours post dosing). The platinum levels in plasma and various organs were determined using ICP-MS. The platinum levels in various organs were normalized to the plasma concentration of platinum. Data are presented as the mean ± SD (n = 3). * $P < 0.05$; ** $P < 0.001$.

respectively. Again, liver had the highest platinum levels, whereas muscle had the lowest platinum levels. Comparing the tissue accumulation data at 48 hr with the data at 1 hr, the platinum levels in plasma and various tissues were dramatically decreased.

***Oct1* deletion resulted in enhanced expression of Oct2 and Oct3 in various tissues.** To determine the effects of Oct1 deletion on expression of different drug transporters, total RNA was extracted from liver, kidney, intestine and muscle. mRNA levels of Oct2, Oct3, Ent1, Mate1 and Ctr1 were determined by quantitative RT-PCR. The expression levels of Oct2 in liver, kidney, and intestine were increased by 2.6, 1.8 and 2.5 -fold in *Oct1*-/- mice compared with *Oct1*+/+ mice (Figure 2.7). Comparing the expression level of Oct2 and Oct3 in liver in *Oct1*+/+ mice, we observed that the expression level of Oct3 in liver was 24 fold higher than that of Oct2 (Figure 2.7 and Figure 2.8). The expression of Oct3 in liver in *Oct1*-/- mice was 5.7-fold of that in *Oct1*+/+ mice (Figure 2.8, $p < 0.001$). There was no change in the expression levels of Ent1, Mate1 and Ctr1in liver between *Oct1*+/+ mice and *Oct1*-/- mice.

Discussion

Though shown to be a potent anti-tumor platinum compound, pyroplatin was never tested clinically. One reason for this was that because of its positive charge, the drug was predicted to have poor pharmacokinetic characteristics. In particular, it was questioned whether pyroplatin would cross biological membranes to any extent and would be available for elimination or accessible to tissues that harbor tumors.

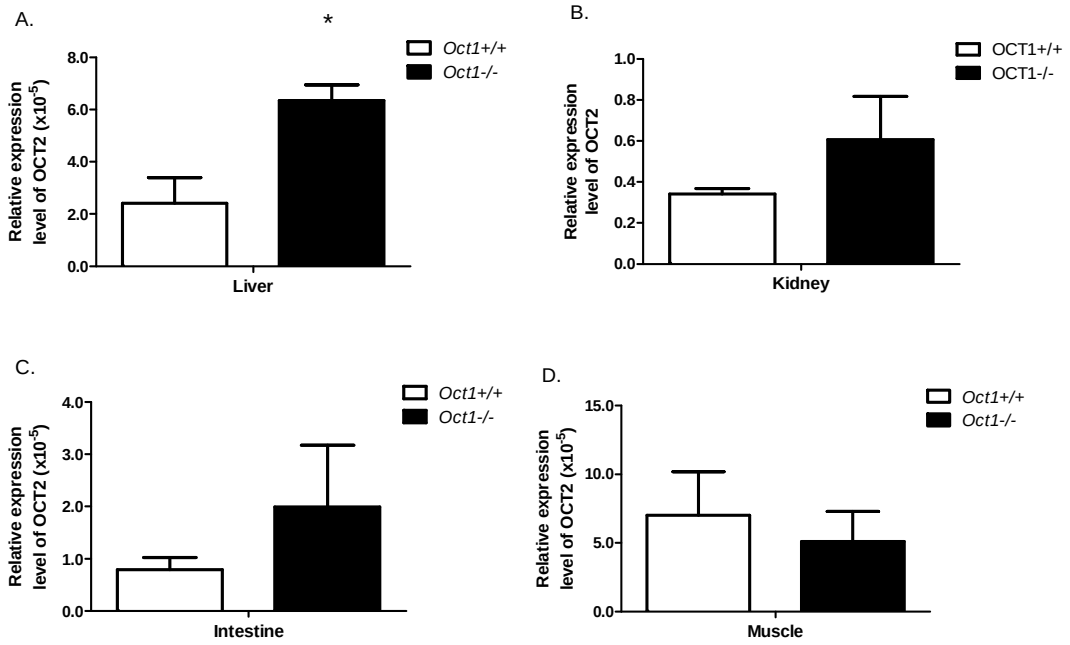

Figure 2.7. Effects of Oct1 deletion on the expression of Oct2 in various tissues in mice. Liver (A), kidney (B), intestine (C) and muscle (D) were harvested from age-matched *Oct1*+/+ and *Oct1*-/- mice. Total RNA was extracted from these tissues and reverse-transcribed. The synthesized cDNA was subject to qRT-PCR using an Oct2 probe. The amplification of glyceraldehyde-3-phosphate dehydrogenase (GAPDH) mRNA was used as an internal control. Data are presented as the mean ± SD (n = 3). * $P < 0.05$ compared with *Oct1*+/+ mice.

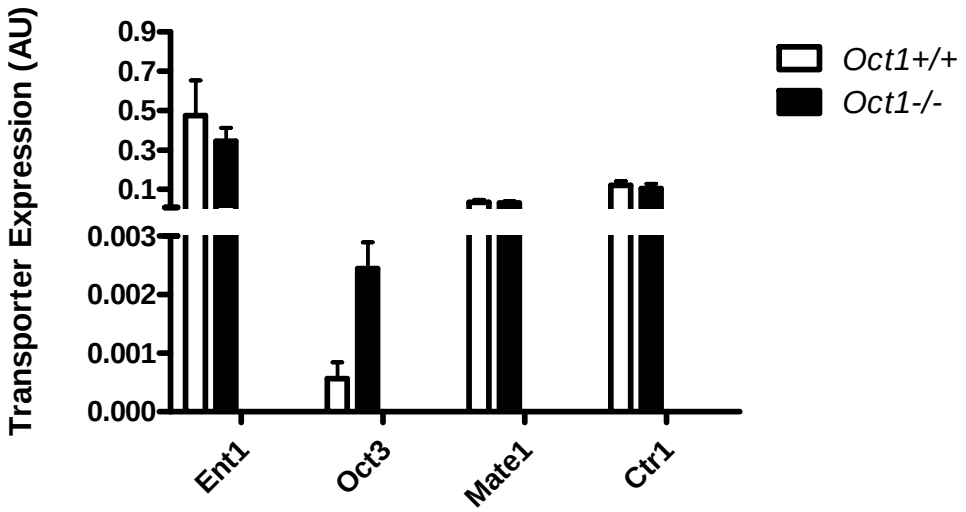

Figure 2.8. Effects of Oct1 deletion on the expression level of various drug transporters in mouse liver. Total RNA was extracted from liver and reverse-transcribed. The synthesized cDNA was subject to qRT-PCR using Ent1, Oct3, Mate1 and Ctr1 probes. The amplification of glyceraldehydes-3-phosphate dehydrogenase (GAPDH) mRNA was used as an internal control. Data are presented as the mean ± SD (n = 3). * $P < 0.001$ compared with *Oct1*+/+ mice.

In recent studies, OCT1 was shown to play a role in the cellular uptake and consequent cytotoxicity of pyroplatin in cell lines over-expressing OCT1[21]. Accordingly, we hypothesized that OCT1 mediates the uptake of pyroplatin *in vivo* in various tissues, particularly the intestine and liver, and that OCT1-mediated transmembrane flux may result in a favorable pharmacokinetic profile for pyroplatin. To test our hypothesis, we performed a comprehensive pharmacokinetic analysis using genetically modified *Oct1-/-* mice in this study. The results suggest that deletion of Oct1 not only decreased the rate of cellular platinum accumulation but also reduced the level of platinum-DNA adduct formation in hepatocytes after pyroplatin exposure (Figure 2.1). These results are in agreement with those in cells transfected with human OCT1 [21], although the fold-difference in platinum levels between hepatocytes harvested from *Oct1+/+* versus *Oct1-/-* mice was much less than that between HEK293 cells overexpressing human OCT1 and control cells [21]. Species differences in the interaction of pyroplatin with human OCT1 versus mouse Oct1 were not observed (unpublished data). However, unpublished data from this laboratory demonstrate that the expression level of Oct1 in mouse liver is considerably higher than in primary hepatocytes cultured from mouse liver, suggesting that the isolation and culture procedures likely resulted in a reduced expression level of the Oct1 protein and therefore a reduction in the observed effect of Oct1 in the hepatocytes.

The significantly higher hepatic accumulation of pyroplatin in *Oct1+/+* mice was consistent with the abundance of Oct1 in liver. It is noteworthy that the intestinal accumulation of pyroplatin in *Oct1+/+* was significantly higher than that in *Oct1-/-* mice, consistent with expression levels of the transporter in the rodent intestine [10, 11].

Normalization of tissue platinum levels to plasma concentrations of pyroplatin excluded the effects of different plasma exposure on the uptake of pyroplatin into the various tissues. Although there is strong Oct1 expression in the kidney of mice [12], it was notable that no differences were observed in normalized levels of platinum in the kidneys of *Oct1*+/+ versus *Oct1*-/- mice. This may be explained by a compensating role of Oct2, which is primarily expressed in kidney. Expression levels of Oct2 were increased in the kidney of *Oct1*-/- mice (Figure 2.7B). Previously pyroplatin was shown to be a substrate of OCT2 [21]. It is notable that enhanced expression of Oct2 and Oct3 in the liver of *Oct1*-/- mice may have resulted in a reduction in the observed effect of Oct1 on pyroplatin uptake in the liver. Because of the high accumulation of pyroplatin in intestine and liver, we examined the toxicity of the drug. Liver enzymes at 10 mg/kg iv were not elevated, nor were there any observed changes in the liver weight or gross macroscopic examination, suggesting that pyroplatin at 10 mg/kg is safe in terms of liver toxicity.

The pharmacokinetics of pyroplatin were consistent with the pharmacokinetics observed previously for oxaliplatin and picoplatin suggesting that the drug has a pharmacokinetic profile similar to clinically used anti-cancer platinum agents. [24, 25] The plasma platinum concentration *versus* time curve showed a classical bi-exponential decay with long elimination half-lives (66.6 hr in *Oct1*+/+ mice versus 48.3 hr in *Oct1*-/- mice, $p>0.05$) after i.v. administration. This long terminal half-life corresponds to the protein elimination half-life as covalent binding occurs and is similar to that seen for other anti-cancer platinum analogs. The short initial half-lives of platinum (0.639 hr in

Oct1+/+ mice versus 0.494 hr in *Oct1*-/- mice) reflect the rapid clearance of pyroplatin into tissues and removal from the systemic circulation.

Deletion of Oct1 resulted in a reduction in the clearance and volume of distribution of pyroplatin, which may be explained by the differences in the distribution of pyroplatin to the tissues with high Oct1 expression, in particular, liver and intestine. The higher plasma platinum concentrations and AUC in *Oct1*-/- mice in comparison to *Oct1*+/+ mice can be attributed to the lower clearance and volume of distribution in *Oct1*-/- mice. Since the renal clearance of pyroplatin was similar between *Oct1*+/+ and *Oct1*-/- mice, the lower total clearance of pyroplatin in the *Oct1*-/- mice is likely due to a reduction in the uptake and subsequent covalent binding of pyroplatin in the liver and intestine, organs that accumulate high levels of platinum. It is also likely that the biliary excretion of pyroplatin was reduced in the *Oct1*-/- mice. A reduction in the biliary excretion of the model organic cation, tetraethylammonium (TEA), in *Oct1*-/- mice compared to mice has been reported [14]. OCT1 is also strongly expressed in intestine and localized on the basolateral membrane of the intestine [7, 10, 11]; therefore, intestinal clearance of pyroplatin may be reduced in *Oct1*-/- mice as well. A significantly reduced distribution of metformin, a good substrate of OCT1, has been reported previously in *Oct1*-/- mice [5, 26] and in humans with reduced function polymorphisms of OCT1 [6].

Though other transporters may affect the disposition of pyroplatin, this study clearly demonstrates that Oct1 plays a significant role in the pharmacokinetics of the drug. Our results also demonstrate that pyroplatin exhibits excellent pharmacokinetic properties, comparable to other clinically used platinum analogs, and suggest the need for further

pre-clinical evaluation including detailed efficacy and toxicity studies. Further, this study provides another example of a drug distinct from metformin for which Oct1 may play a profound role in its pharmacokinetics [6].

References

1. Lin, J.H. and Yamazaki, M., *Clinical relevance of P-glycoprotein in drug therapy.* Drug Metabolism Reviews, 2003. **35**(4): p. 417-454.

2. Maeda, K., Ieiri, I., Yasuda, K., Fujino, A., Fujiwara, H., Otsubo, K., Hirano, M., Watanabe, T., Kitamura, Y., Kusuhara, H., and Sugiyama, Y., *Effects of organic anion transporting polypeptide 1B1 haplotype on pharmacokinetics of pravastatin, valsartan, and temocapril.* Clinical Pharmacology and Therapeutics, 2006. **79**(5): p. 427-439.

3. Hirano, M., Maeda, K., Shitara, Y., and Sugiyama, Y., *Drug-drug interaction between pitavastatin and various drugs via OATP1B1.* Drug Metabolism and Disposition, 2006. **34**(7): p. 1229-1236.

4. Chung, J.-Y., Cho, J.-Y., Yu, K.-S., Kim, J.-R., Oh, D.-S., Jung, H.-R., Lim, K.-S., Moon, K.-H., Shin, S.-G., and Jang, I.-J., *Effect of OATP1B1 (SLCO1B1) variant alleles on the pharmacokinetics of pitavastatin in healthy volunteers.* Clinical Pharmacology and Therapeutics, 2005. **78**(4): p. 342-350.

5. Shu, Y., Sheardown, S.A., Brown, C., Owen, R.P., Zhang, S.Z., Castro, R.A., Ianculescu, A.G., Yue, L., Lo, J.C., Burchard, E.G., Brett, C.M., and Giacomini, K.M., *Effect of genetic variation in the organic cation transporter 1 (OCT1) on metformin action.* Journal of Clinical Investigation, 2007. **117**(5): p. 1422-1431.

6. Shu, Y., Brown, C., Castro, R.A., Shi, R.J., Lin, E.T., Owen, R.P., Sheardown, S.A., Yue, L., Burchard, E.G., Brett, C.M., and Giacomini, K.M., *Effect of genetic*

variation in the organic cation transporter 1, OCT1, on metformin pharmacokinetics. Clinical Pharmacology & Therapeutics, 2008. **83**(2): p. 273-280.

7. Zhang, L., Dresser, M.J., Gray, A.T., Yost, S.C., Terashita, S., and Giacomini, K.M., *Cloning and functional expression of a human liver organic cation transporter.* Molecular Pharmacology, 1997. **51**(6): p. 913-921.

8. Gorboulev, V., Ulzheimer, J.C., Akhoundova, A., UlzheimerTeuber, I., Karbach, U., Quester, S., Baumann, C., Lang, F., Busch, A.E., and Koepsell, H., *Cloning and characterization of two human polyspecific organic cation transporters.* DNA and Cell Biology, 1997. **16**(7): p. 871-881.

9. Su, A.I., Wiltshire, T., Batalov, S., Lapp, H., Ching, K.A., Block, D., Zhang, J., Soden, R., Hayakawa, M., Kreiman, G., Cooke, M.P., Walker, J.R., and Hogenesch, J.B., *A gene atlas of the mouse and human protein-encoding transcriptomes.* Proceedings of the National Academy of Sciences of the United States of America, 2004. **101**(16): p. 6062-6067.

10. Gruendemann, D., Gorboulev, V., Gambaryan, S., Veyhl, M., and Koepsell, H., *Drug excretion mediated by a new prototype of polyspecific transporter.* Nature (London), 1994. **372**(6506): p. 549-552.

11. Schweifer, N. and Barlow, D.P., *The lx1 gene maps to mouse chromosome 17 and codes for a protein that is homologous to glucose and polyspecific transmembrane transporters.* Mammalian Genome, 1996. **7**(10): p. 735-740.

12. Jonker, J.W. and Schinkel, A.H., *Pharmacological and physiological functions of the polyspecific organic cation transporters: OCT1, 2, and 3 (SLC22A1-3).* Journal of Pharmacology and Experimental Therapeutics, 2004. **308**(1): p. 2-9.

13. Wright, S.H., *Role of organic cation transporters in the renal handling of therapeutic agents and xenobiotics.* Toxicology and Applied Pharmacology, 2005. **204**(3): p. 309-319.

14. Jonker, J.W., Wagenaar, E., Mol, C., Buitelaar, M., Koepsell, H., Smit, J.W., and Schinkel, A.H., *Reduced hepatic uptake and intestinal excretion of organic cations in mice with a targeted disruption of the organic cation transporter 1 (Oct1 [Slc22a1]) gene.* Molecular and Cellular Biology, 2001. **21**(16): p. 5471-5477.

15. Wong, E. and Giandomenico, C.M., *Current status of platinum-based antitumor drugs.* Chemical Reviews, 1999. **99**(9): p. 2451-2466.

16. Weiss, R.B. and Christian, M.C., *New cisplatin analogs in development - a review.* Drugs, 1993. **46**(3): p. 360-377.

17. Harrap, K.R., *Preclinical studies identifying carboplatin as a viable cisplatin alternative.* Cancer Treatment Reviews, 1985. **12**: p. 21-33.

18. Aabo, K., Adams, M., Adnitt, P., Alberts, D.S., Athanazziou, A., Barley, V., Bell, D.R., Bianchi, U., Bolis, G., Brady, M.F., Brodovsky, H.S., Bruckner, H., Buyse, M., Canetta, R., Chylak, V., Cohen, C.J., Colombo, N., Conte, P.F., Crowther, D.,

Edmonson, J.H., Gennatas, C., Gilbey, E., Gore, M., Guthrie, D., Kaye, S.B., Laing, A.H., Landoni, F., Leonard, R.C., Lewis, C., Liu, P.Y., Mangioni, C., Marsoni, S., Meerpohl, H., Omura, G.A., Parmar, M.K.B., Pater, J., Pecorelli, S., Presti, M., Sauerbrei, W., Skarlos, D.V., Smalley, R.V., Solomon, H.J., Stewart, L.A., Sturgeon, J.F.G., Tattersall, M.H.N., Wharton, J.T., Huinink, W.W.T., Tomirotti, M., Torri, W., Trope, C., Turbow, M.M., Vermorken, J.B., Webb, M.J., Wilbur, D.W., Williams, C.J., Wiltshaw, E., Yeap, B.Y., and Advanced Ovarian Canc Trialists, G., *Chemotherapy in advanced ovarian cancer: Four systematic meta-analyses of individual patient data from 39 randomized trials.* British Journal of Cancer, 1998. **78**(11): p. 1479-1487.

19. Kelland, L., *The resurgence of platinum-based cancer chemotherapy.* Nature Reviews Cancer, 2007. **7**(8): p. 573-584.

20. Hollis, L.S., Amundsen, A.R., and Stern, E.W., *Chemical and biological properties of a new series of cis-diammineplatinum(II) antitumor agents containing 3 nitrogen donors - cis-[Pt(NH3)2(N-donor)Cl]+*. Journal of Medicinal Chemistry, 1989. **32**(1): p. 128-136.

21. Lovejoy, K.S., Todd, R.C., Zhang, S.Z., McCormick, M.S., D'Aquino, J.A., Reardon, J.T., Sancar, A., Giacomini, K.M., and Lippard, S.J., *Cis-diammine(pyridine)chloroplatinum(II), a monofunctional platinum(II) antitumor agent: Uptake, structure, function, and prospects.* Proceedings of the National Academy of Sciences of the United States of America, 2008. **105**(26): p. 8902-8907.

22. Moldeus, P., Hogberg, J., and Orrenius, S., *Isolation and use of liver cells.* Fleischer, Sidney and Lester Packer (Ed.). Methods in Enzymology, Vol. Lii. Biomembranes. Part C: Biological Oxidations Microsomal, Cytochrome P-450, and Other Hemoprotein Systems. Xxii+595p. Illus. Academic Press, Inc.: New York, N.Y., USA; London, England. Isbn 0-12-181952-3, 1978: p. 60-71.

23. Zhang, S.Z., Lovejoy, K.S., Shima, J.E., Lagpacan, L.L., Shu, Y., Lapuk, A., Chen, Y., Komori, T., Gray, J.W., Chen, X., Lippard, S.J., and Giacomini, K.M., *Organic cation transporters are determinants of oxaliplatin cytotoxicity.* Cancer Research, 2006. **66**(17): p. 8847-8857.

24. Raynaud, F.I., Boxall, F.E., Goddard, P.M., Valenti, M., Jones, M., Murrer, B.A., Abrams, M., and Kelland, L.R., *Cis-aminedichloro(2-methylpyridine)platinum(II) (AMD473), a novel sterically hindered platinum complex: In vivo activity, toxicology, and pharmacokinetics in mice.* Clinical Cancer Research, 1997. **3**(11): p. 2063-2074.

25. Luo, F.R., Wyrick, S.D., and Chaney, S.G., *Pharmacokinetics and biotransformations of oxaliplatin in comparison with ormaplatin following a single bolus intravenous injection in rats.* Cancer Chemotherapy and Pharmacology, 1999. **44**(1): p. 19-28.

26. Wang, D.S., Jonker, J.W., Kato, Y., Kusuhara, H., Schinkel, A.H., and Sugiyama, Y., *Involvement of organic cation transporter 1 in hepatic and intestinal*

distribution of metformin. Journal of Pharmacology and Experimental Therapeutics, 2002. **302**(2): p. 510-515.

CHAPTER 3

EFFECT OF OCT1 ON THE TOXICITY PROFILE OF PYROPLATIN IN MICE

1. Introduction

The platinum coordination complex cisplatin, cis-diaminedichloroplatinum(II) has a central role in cancer chemotherapy, especially for testicular cancer, for which the overall cure rate exceeds 90%, and is nearly 100% for early stage disease [1]. However, the drug possesses significant limitations because of its toxicity to normal tissues. In particular, the drug exhibits nephrotoxicity, peripheral neurotoxicity and ototoxicity [2]. These limitations have driven intensive synthetic efforts to discover new platinum-based drugs with reduced toxicity profiles and also activity against resistant disease. These efforts resulted in the development of carboplatin and its introduction into clinical care in the mid-1980s [3, 4]. Carboplatin rarely results in nephrotoxicity and peripheral neuropathy, with its major toxicity being myelosuppression principally thrombocytopenia [5]. Efforts to improve on tumor resistance have resulted in the approval of oxaliplatin in the Europe in 1999 and in the United States in 2002 [4]. Oxaliplatin shows no inheritant cross resistance with both cisplatin and carboplatin, and a very favorable toxicity profile. It is essentially devoid of nephrotoxicity, is less toxic to the gastrointestinal tract and less myelotoxic. The most common toxicity associated with oxaliplatin treatment is peripheral neuropathy, which ranges from acute and transient to a cumulative neuropathy. Oxaliplatin is generally free of ototoxicity and nephrotoxicity, with only moderate isolated cases of neutropenia and thrombocytopenia [6].

Plasma membrane transporters regulate the toxicological effect of drugs by controlling systemic drug concentrations and concentrations in normal tissues. For example, cisplatin nephrotoxicity is mediated by its accumulation in tubular epithelial cells. In studies of cisplatin, carboplatin, nedaplatin and oxaliplatin nephrotoxicity in rats, only cisplatin induced nephrotoxicity at 2 days of dosing and the renal accumulation of cisplatin was much greater than that of the other drugs. Organic cation transporter 2 (OCT2) is the most abundant organic cation transporter expressed in the basolateral membrane of the proximal tubule and mediates the accumulation of various cationic drugs including cisplatin into proximal tubular epithelial cells from the blood [7]. OCT2 has been found to mediate cisplatin-induced nephrotoxicity in rats [8, 9]. The transporter may also play a role in cisplatin-induced ototoxicity since its expression level has been found to correlate well with cochlear localization of platinum-DNA adducts following cisplatin administration [10]. Recently, we and others demonstrated that oxaliplatin is a substrate of OCT1, OCT2 and OCT3 and that these transporters may play a role in its anti-tumor efficacy and its toxicity to normal tissues. For example, OCT1 is primarily expressed in the liver and localized to the sinusoidal membrane and has been indicated in the transport of oxaliplatin across cell membrane [11]. Therefore, it is possible that OCT1 contributes to the hepatotoxicity of oxaliplatin.

Pyroplatin, which is in a new series of platinum analogues, has been found to be a substrate of OCT1 and OCT2. That is, overexpression of OCT1 and OCT2 facilitates the uptake of pyroplatin and sensitizes the cells to pyroplatin cytotoxicity [12]. However, its toxicity profile and role of OCTs in its toxicities have not been investigated. The goal of this study was to elucidate the toxicity profile of pyroplatin and determine the role of

OCT1 in the *in vivo* toxicity of pyroplatin using an Oct1 knockout mouse model. In addition, the interaction of pyroplatin with other transporters, i.e., OCT3, MATE1, and MATE2K was also examined in cell lines over-expressing these transporters.

2. Materials and Methods

2.1. Synthesis of Pyroplatin *cis*-[Pt(NH$_3$)$_2$(Pyr)Cl]NO$_3$. Pyroplatin was synthesized as previously described (refer to chapter 2).

2.2. Animals. *Oct1*-/- mice were generated as described elsewhere [13]. The animals used in all experiments were in FVB background and were age-matched *Oct1-/-* and *Oct1*+/+ (wildtype) mice between 8-10 weeks of age. All animals were housed in a virus-free, temperature-controlled facility on a 12-h light–dark cycle. They were allowed standard mouse food and water *ad libitum*. All experiments on mice were approved by the Institutional Animal Care and Use Committee of University of California at San Francisco.

2.3. Toxicology studies. All toxicity studies were performed under strict control. The animals were checked several times on the dosing day and sacrificed at the onset of moribundity. Body weight was monitored three times per week. All surviving animals were sacrificed 24 hours after the last treatment.

2.3.1. Dose-range finding toxicity study. Eight weeks old *Oct1*+/+ mice were randomized into 6 groups and were given 0, 10, 30, 90, 120, and 150 mg/kg of pyroplatin in saline via tail vein injection once weekly for a total three weeks (n = 4 animals per group). On the day of sacrifice, the animals were first bled from the tail vein for the

evaluation of hematological toxicity. Following the tail vein bleeding, the animals were anesthetized with isoflurane, and blood (500 – 1000 µl) was collected by heart puncture and centrifuged for 30 min at 1000 X g at 4^{o}C. The serum was decanted and frozen at -80^{o}C until analysis. Tissues (liver, kidney, intestine, and muscle) were collected and divided into two halves, one half of the tissues was fixed in 4% paraformaldehyde for histopathology examination, the other half of the tissues was snap frozen in liquid nitrogen.

2.3.2. Definitive toxicity study. Eight weeks old *Oct1-/-* and *Oct1+/+* mice were randomized and treated with saline or pyroplatin via tail vein injection once weekly for a total three weeks (at least 9 animals per group). Blood and tissues were collected and treated as described above.

2.3.3. Hematological evaluation. The whole blood (50 - 100 µl) was placed in K2EDTA coated tubes, and complete blood count (CBC) test were conducted within 6 hours by Mouse Pathology Core of UCSF Helen Diller Family Comprehensive Cancer Center.

2.3.4. Clinical chemistry evaluation. Alanine transaminase (ALT), aspartate transaminase (AST), alkaline phosphatase (ALP), total protein, albumin, glucose, blood urea nitrogen (BUN), creatinine and electrolytes in serum were measured by the Clinical Laboratory of the San Francisco General Hospital.

2.3.5. Histopathological examination. The tissues (liver, intestine and kidney) fixed in 4% paraformaldehyde were embedded in paraffin, cut into thin sections and

mounted on glass slides. The tissue sections were stained with hematoxylin and eosin for microscopic examination.

2.3.6. Plasma and tissue platinum measurement. Plasma and tissue samples were dissolved in 70% nitric acid and incubated at 65°C for at least 2.5 hours. Distilled water containing 10 ppb of iridium (Sigma) and 0.1% Triton X-100 was added to the samples to dilute nitric acid to 7%. 5 µl of plasma and about 10-30 mg of tissue powders were used for total platinum measurement by ICP-MS.

2.3.7. Isolation of total RNA and quantitative real-time polymerase chain reaction (qRT-PCR) analysis. Total RNA from kidney was extracted using Trizol (Invitrogen). During the RNA purification procedure, DNase I was treated to digest residual genomic DNA. RNA was quantified spectrophotometrically at 260 nm. Extracted RNA was stored at -80^{o}C until use.

Total RNA from each sample was reverse transcribed into cDNA using a superscript first-strand cDNA synthesis kit (Invitrogen, Carlsbad, Calif., USA) according to the manufacturer's protocol. Quantitative RT-PCR was carried out in a 96-well plate in a total volume of 10 µl reaction solution which includes a cDNA equivalent of 2 µg total RNA, specific probe and Taqman Universal Master Mix (Applied Biosystems, Foster City, CA). Reactions were run on an ABI Prism 7700, and the thermal cycling conditions were 95 ^{o}C for 20 seconds followed by 40 cycles of 95 ^{o}C for 3 seconds and 60 ^{o}C for 30 seconds. The amplification of glyceraldehydes-3-phosphate dehydrogenase (GAPDH) mRNA was used as an internal control.

2.4. Cell lines and transfection. Human embryonic kidney (HEK) 293 cells used in the present study were from the American Type Culture Collection (Manassas, VA). HEK293 cells stably transfected with pcDNA5/FRT vector containing the full length reference human MATE1 cDNA (HEK-hMATE1) and the empty vector (HEK-MOCK) were established previously in our laboratory [14, 15]. The stably transfected HEK-hOCT3 and HEK-MATE2K cell lines were established by transfection of pcDNA5/FRT vector containing the full-length hMATE1 and hMATE2K into HEK293 Flp-In cells (Invitrogen) using Lipofectamine 2000 (Invitrogen). Forty-eight hours after transfection, 75 µg/ml hygromycin B was added to the medium, and stable clones were selected.

2.5. Cell culture. The culture medium for stably transfected cells is DMEM H21 medium supplemented with 10% FBS, 100 units/ml penicillin and 100 µg/ml streptomycin and 60 µg/ml hygromycin B. All cell lines were grown at 37 °C in a humidified atmosphere with 5% CO_2.

2.6. Cellular accumulation of platinum. The cellular accumulation of platinum was determined as described previously [15] with some modifications. Briefly, the cells were incubated in uptake buffer* containing 10 µM pyroplatin with or without a specific inhibitor at 37°C in 5% CO_2 for 1 hour. After incubation, cells were washed with ice-cold PBS three times. Then the cells were dissolved in 100 µl of 70% nitric acid at 65°C for at least 2.5 hours. Distilled water containing 10 ppb of iridium (Sigma) and 0.1% Triton X-100 was added to the samples to dilute nitric acid to 7%. The platinum content was measured by inductively coupled plasma mass spectrometry (ICP-MS) in the Analytical Facility at the University of California at Santa Cruz (Santa Cruz, CA). Cell lysates from

a set of identical cultures were used for BCA protein assay. Cellular platinum accumulation was normalized to the protein content.

* Uptake buffer for HEK293 and HEK-hOCT3 was PBS; uptake buffer for HEK-hMATE1 and HEK-hMATE2K was buffer containing 125 mM NaCl, 4.8 mM KCl, 5.6 mM D-glucose, 1.2 mM $CaCl_2$, 1.2 mM KH_2PO_4, 1.2 mM $MgSO_4$ and 25 mM Tricine (pH 8.0).

2.7. Platinum-DNA adduct formation. The platinum content associated with genomic DNA was determined as described previously [15] with some modifications. Briefly, the cells were washed with PBS once and then were incubated in the uptake buffer containing pyroplatin with or without an OCT3 inhibitor, corticosterone at 37°C in 5% CO_2 for 1 hour unless specified. After incubation, cells were washed three times with ice-cold PBS. Genomic DNA was isolated from the cells using Wizard Genomic DNA Purification kit (Promega, Madison, WI) according to the manufacturer's protocol. The DNA-bound platinum was determined by ICP-MS. The DNA content from the same DNA preparation was measured by absorption spectroscopy at 260 nm. Platinum-DNA adduct level was normalized to total DNA content.

2.8. Statistical analysis. Unless specified, data are expressed as mean ± standard deviation (SD). Data were analyzed statistically using the unpaired Student's t test. Multiple comparisons were performed with Dunnett's two-tailed test after one-way ANOVA. A P value of less than 0.05 was considered statistically significant.

3. Results

3.1. Dose-range finding toxicity study. To determine the dose to use in the toxicity study, a dose-range finding toxicity study was conducted in *Oct1+/+* mice with the highest dose of 150 mg/kg. All animals in the 150 mg/kg group died before the second dose. The animals in the lower dose groups survived until the end of the study. The body weight change was comparable between saline control and the 10 mg/kg group; the body weight in the 120 mg/kg group had the most dramatic decrease compared to other treatment groups. At 8 days, significant differences in body weight were observed in the 30 mg/kg, 90 mg/kg and 120 mg/kg groups in comparison with the control group. However, these differences were not apparent starting at 13 days (Figure 3.1). The plasma platinum concentration increased proportionally with increasing dose of pyroplatin (Figure 3.2).

Pyroplatin resulted in a dose-dependent increase in the liver to body weight ratio; the ratio was significantly greater at dose of 90 mg/kg and 120 mg/kg compared with saline control group ($p < 0.005$; Figure 3.3). Liver function tests, LFT, were used to detect liver damage. Albumin and total protein were significantly decreased at 90 mg/kg and 120 mg/kg compared with the saline control group ($p < 0.01$; Figure 3.4A). Pyroplatin at a dose of 30 mg/kg and above resulted in a significant increase in ALT activity compared with saline control group (Figure 3.4B; $p < 0.01$). ALT activity in the 120 mg/kg group was about three times that of the control group, indicating that there was a likelihood of hepatocyte damage at 120 mg/kg. The activities of AST and ALKP were not affected by pyroplatin at the tested doses (data not shown). Fasting glucose levels were not affected up to the dose of 30 mg/kg, and were then significantly increased at 90 mg/kg and 120 mg/kg ($p < 0.01$; Figure 3.4C).

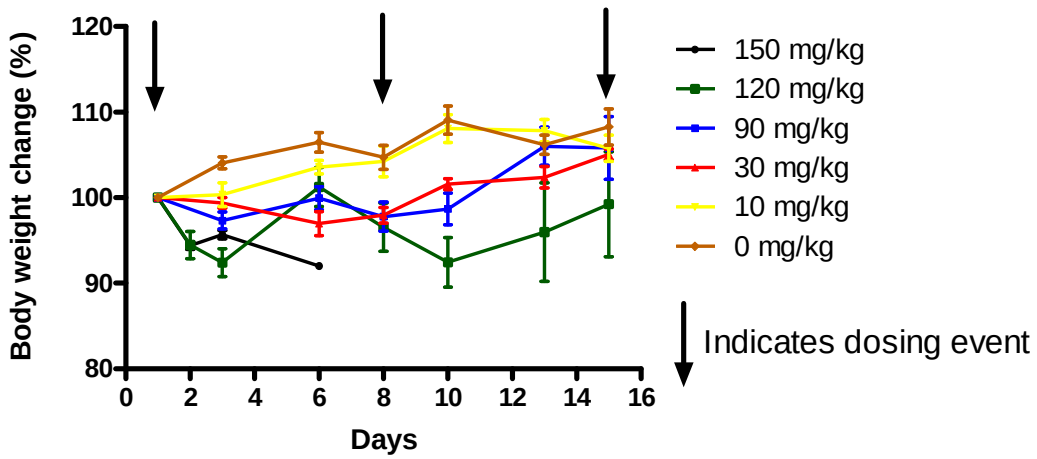

Figure 3.1. Dose-dependent body weight change after pyroplatin treatment in dose-range finding toxicity study. *Oct1*+/+ mice were treated with 0, 10, 30, 90, 120, and 150 mg/kg of pyroplatin in saline via tail vein injection once weekly for a total three weeks (n = 4 animals per group). Body weight was monitored three times per week. The mice were fasted for at least 16 hours before sacrifice. Data are presented as the mean ± SD.

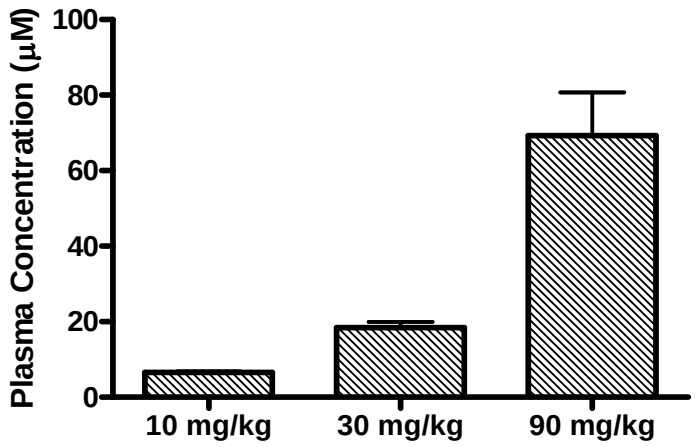

Figure 3.2. Dose proportional increase in plasma platinum concentration in dose-range finding toxicity study. *Oct1*+/+ mice were treated with 0, 10, 30, 90, 120 and 150 mg/kg of pyroplatin in saline via tail vein injection once weekly for a total three weeks (n = 4 animals per group). The mice were fasted for at least 16 hours before sacrifice. Blood was collected 24 hrs after the last dose. Plasma platinum concentration was determined by ICP-MS. No sample was collected due to early death at 150 mg/kg group. The platinum level was not measured for 120 mg/kg group. Data are presented as the mean ± SD.

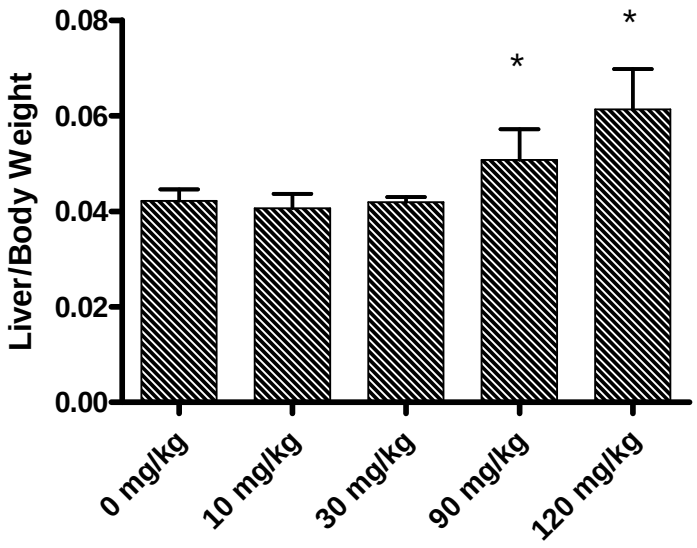

Figure 3.3. Dose-dependent hepatomegaly in dose-range finding toxicity study. *Oct1*+/+ mice were treated with 0, 10, 30, 90, 120, and 150 mg/kg of pyroplatin in saline via tail vein injection once weekly for a total three weeks (n = 4 animals per group). The mice were fasted for at least 16 hours before sacrifice. Liver was collected 24 hrs after the last dose, liver weight was measured. Liver to body weight ratio was compared among groups. No sample was collected due to early death at 150 mg/kg group. Data are presented as the mean ± SD. * $p < 0.05$ compared with saline control group.

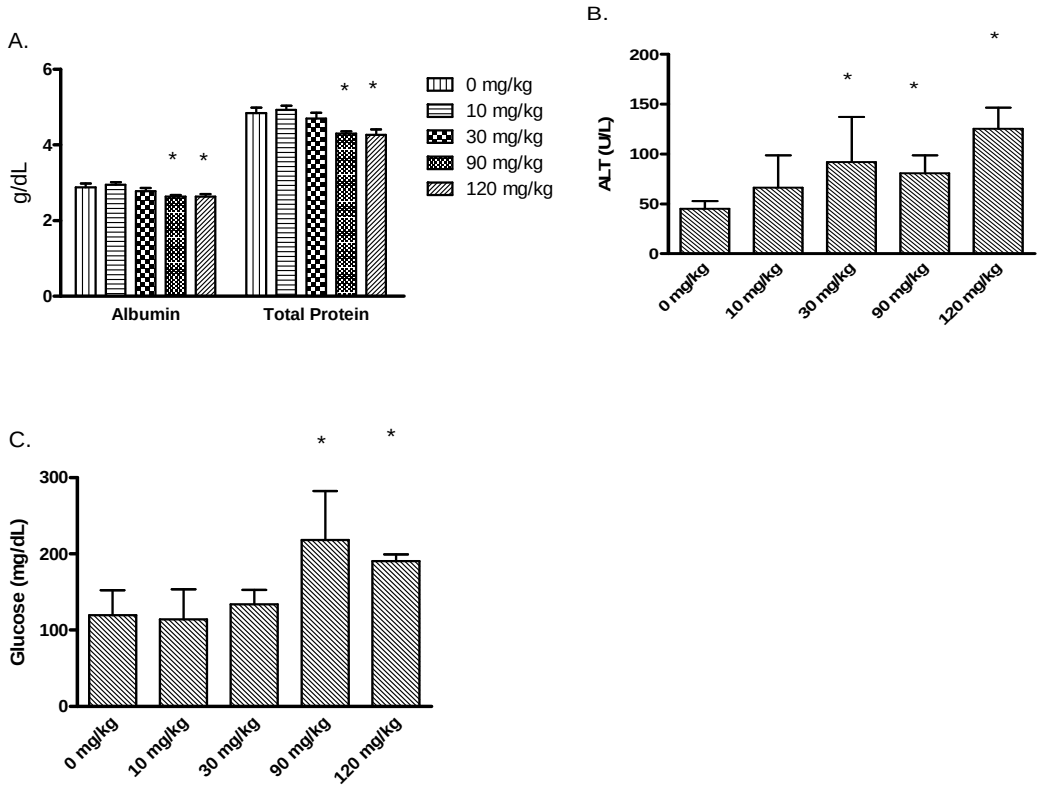

Figure 3.4. Liver function tests in dose-range finding toxicity study. *Oct1*+/+ mice were treated with 0, 10, 30, 90, 120, and 150 mg/kg of pyroplatin in saline via tail vein injection once weekly for a total three weeks (n = 4 animals per group). The mice were fasted for at least 16 hours before sacrifice. Blood was collected 24 hrs after the last dose; albumin, total protein (A) and the activity of alanine aminotransferase (ALT) (B) and glucose level (C) in serum were measured. No sample was collected due to early death at 150 mg/kg group. Data are represented as the mean ± SD. * $p < 0.01$ compared with saline control group.

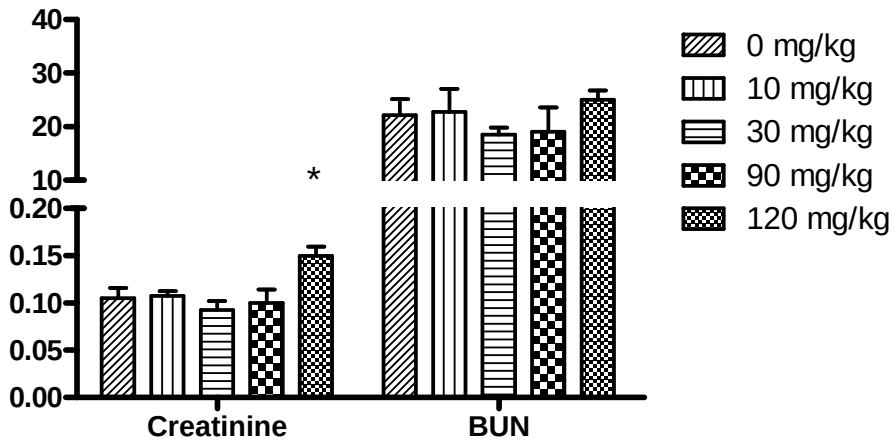

Figure 3.5. Renal function test in dose-range finding toxicity study. *Oct1*+/+ mice were treated with 0, 10, 30, 90, 120, and 150 mg/kg of pyroplatin in saline via tail vein injection once weekly for a total three weeks (n = 4 animals per group). The mice were fasted for at least 16 hours before sacrifice. Blood was collected 24 hrs after the last dose; Creatinine and blood urea nitrogen (BUN) in serum were measured. No sample was collected due to early death at 150 mg/kg group. Data are presented as the mean ± SD. * $p < 0.05$ compared with saline control group.

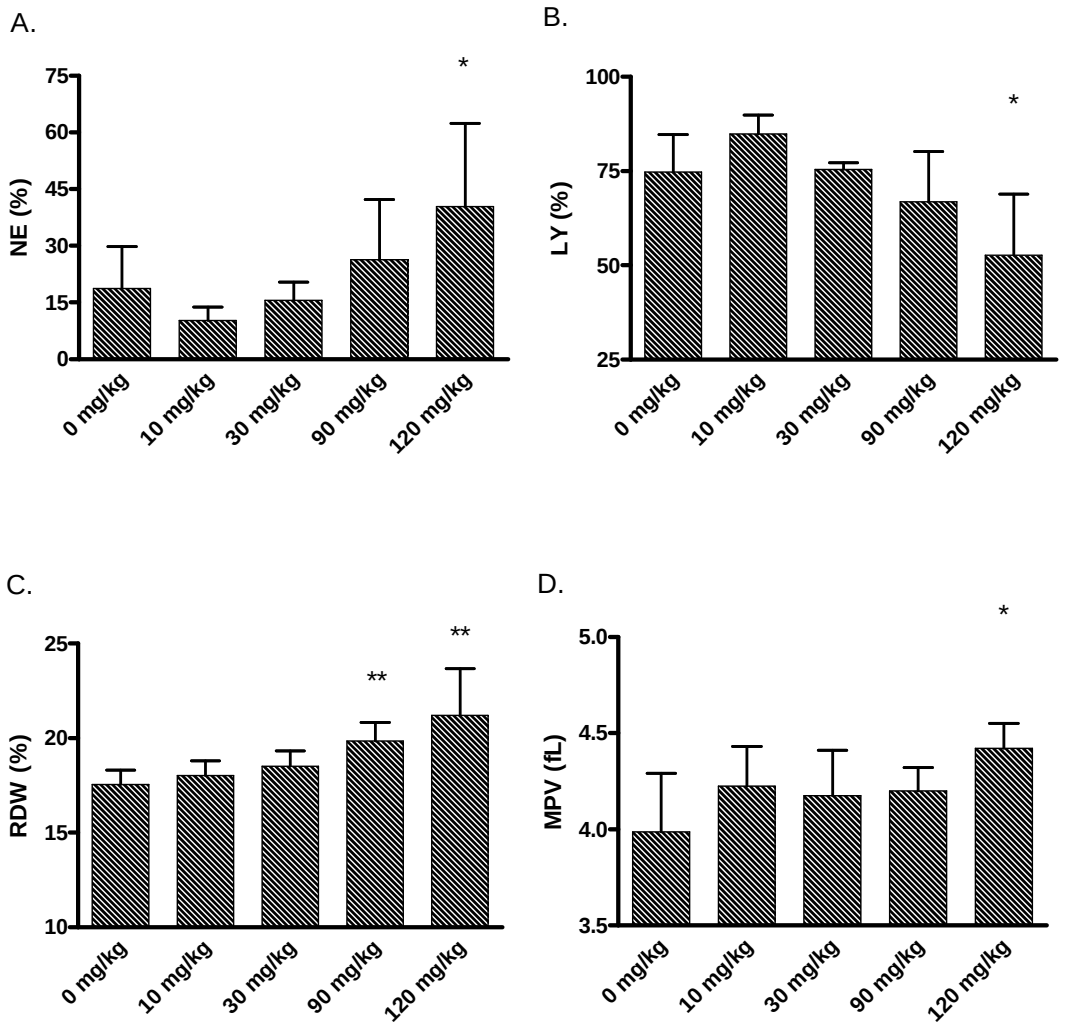

Figure 3.6. Hematological effects of pyroplatin in dose-range finding toxicity study. *Oct1*+/+ mice were treated with 0, 10, 30, 90, 120, and 150 mg/kg of pyroplatin in saline via tail vein injection once weekly for a total three weeks (n = 4 animals per group). The mice were fasted for at least 16 hours before sacrifice. Blood was collected via tail vein bleeding 24 hrs after the last dose; CBC was measured within 24 hr after collection. No sample was collected due to early death at 150 mg/kg group. Data are presented as the mean ± SD. * $p < 0.05$ compared with saline control group; ** $p < 0.005$ compared with saline control group.

Pyroplatin treatment at 120 mg/kg, but not at lower doses, resulted in a significant increase in creatinine levels compared with the control group ($p < 0.05$; Figure 3.5); however, blood urea nitrogen (BUN) level was not affected at all tested doses suggesting that the drug does not produce substantial nephrotoxicity.

The hematological toxicity of pyroplatin was revealed by significantly increased red blood cell distribution width (RDW), beginning at doses of 90 mg/kg ($p < 0.005$, Figure 3.6C). Elevated neutrophil levels (%), decreased lymphocyte levels (%) and elevated mean platelet volume (MPV) were observed at dose of 120 mg/kg ($p < 0.05$; Figure 3.6.A., B., and D).

3.2. Definitive toxicity study. Based on the results of the dose-range finding toxicity study indicating that pyroplatin at 90 mg/kg and above resulted in significant changes in body weight reduction, liver to body weight ratio, liver function and hematology, we selected doses between 90 mg/kg to 120 mg/kg for use in evaluating the role of Oct1 in pyroplatin toxicity. The role of Oct1 in toxicity of pyroplatin was determined by comparing the toxicity profile of pyroplatin between *Oct1+/+* and *Oct1-/-* mice. The initial dose of pyroplatin started with 120 mg/kg, which later was reduced to 90 mg/kg due to death or moribundity observed in *Oct1-/-* mice at 120 mg/kg.

3.2.1 Pyroplatin resulted in much greater body weight loss in *Oct1-/-* mice. Compared with the saline control group, pyroplatin treatment caused body weight loss in both *Oct1+/+* and *Oct1-/-* mice (Figure 3.7). However, the body weight loss was much greater in *Oct1-/-* mice than in *Oct1+/+* mice. The greater decrease in body weight in

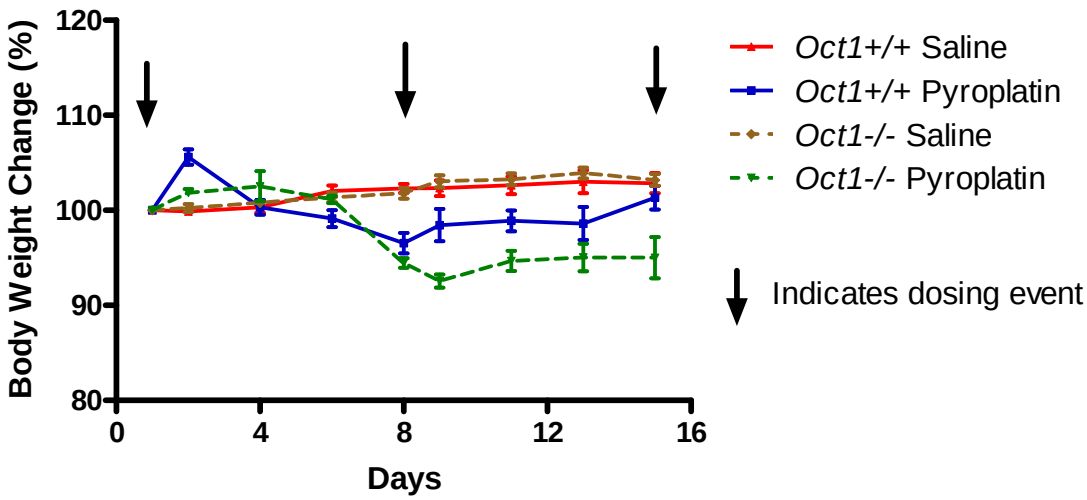

Figure 3.7. Pyroplatin results in greater body weight loss in *Oct1*-/- mice. *Oct1*-/- and *Oct1*+/+ mice were treated with saline or pyroplatin (120/90 mg/kg) via tail vein injection once weekly for a total of three weeks (at least 9 animals per group). Body weight was monitored three times per week. The mice were fasted for at least 16 hours before sacrifice. Data are presented as the mean ± SD.

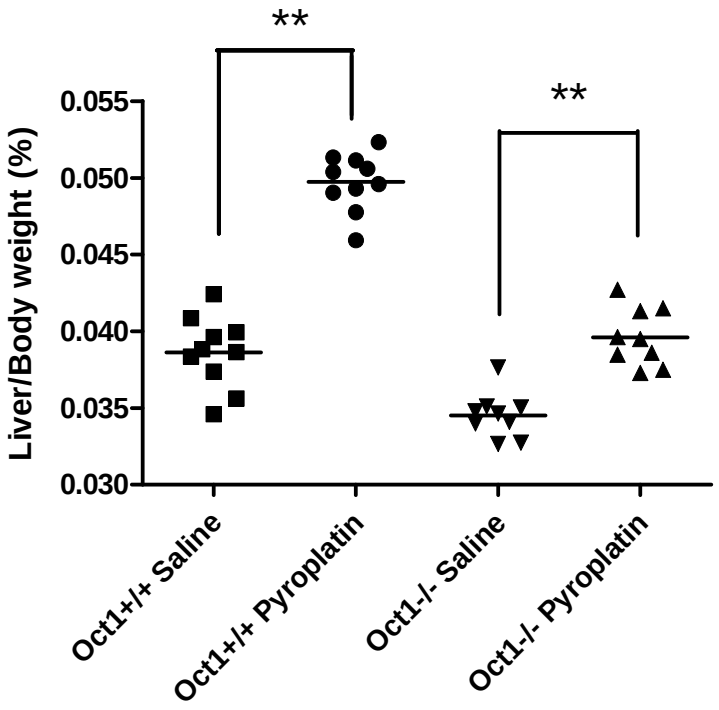

Figure 3.8. Pyroplatin induces more severe hepatomegaly in *Oct1*+/+ mice. *Oct1*-/- and *Oct1*+/+ mice were treated with saline or pyroplatin (120/90 mg/kg) via tail vein injection once weekly for a total three weeks (at least 9 animals per group). The mice were fasted for at least 16 hours before sacrifice. Liver was collected 24 hrs after the last dose, liver weight was measured. Liver to body weight ratio was compared among groups. Data are presented as the mean ± SD. ** $p < 0.0001$ compared with saline control group.

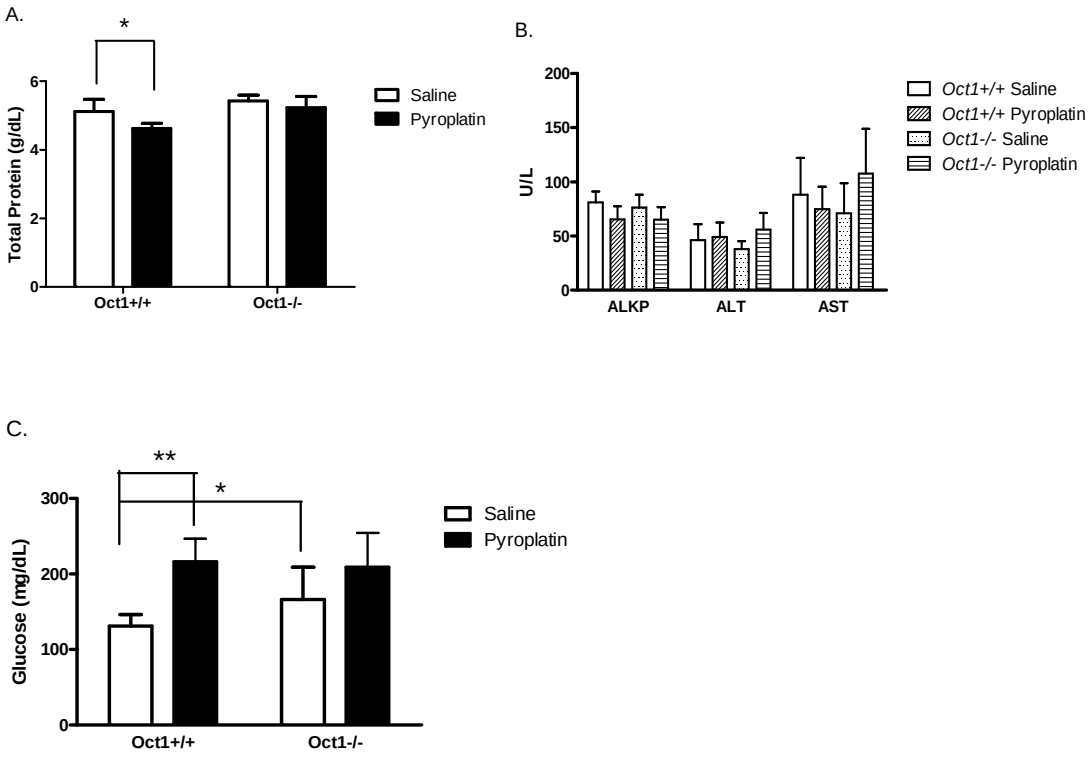

Figure 3.9. Effects of pyroplatin on liver function of *Oct1*+/+ and *Oct1*-/- mice. *Oct1*-/- and *Oct1*+/+ mice were treated with saline or pyroplatin (120/90 mg/kg) via tail vein injection once weekly for a total three weeks (at least 9 animals per group). The mice were fasted for at least 16 hours before sacrifice. Blood was collected 24 hrs after the last dose; Total protein (A) and the activities of three-liver associated enzymes, alkaline phosphatase (ALKP), alanine aminotransferase (ALT), and aspartate aminotransferase(AST) (B) and glucose level (C) in serum were measured. Data are presented as the mean ± SD. * $p < 0.05$ compared with saline control group. ** $p < 0.001$ compared with saline control group.

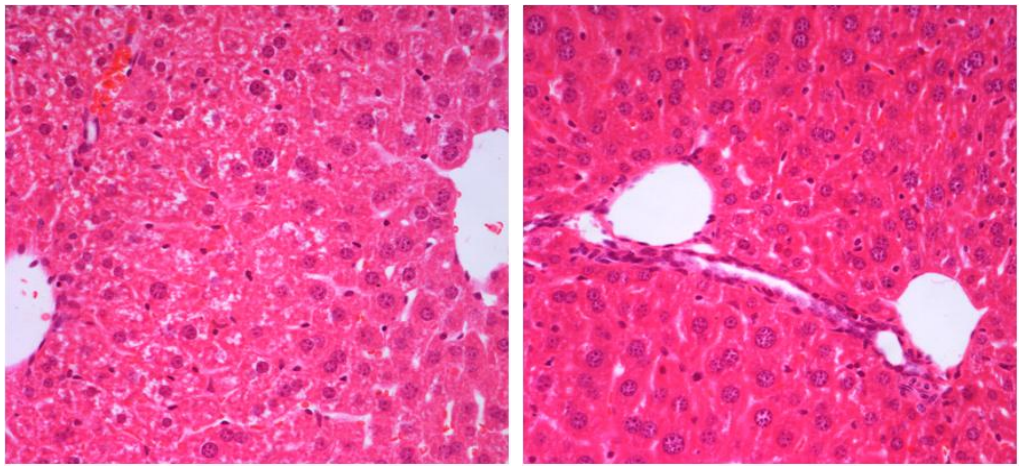

***Oct1*+/+** ***Oct1*-/-**

Figure 3.10. Representative hepatic histopathology of *Oct1*+/+ and *Oct1*-/- mice treated with pyroplatin. *Oct1*-/- and *Oct1*+/+ mice were treated with saline or pyroplatin (120/90 mg/kg) via tail vein injection once weekly for a total three weeks (at least 9 animals per group). The mice were fasted for at least 16 hours before sacrifice. Liver was collected 24 hrs after the last dose and fixed in 4% paraformaldehyde. The paraffin-embedded liver is sliced and stained with hematoxylin and eosin. The magnification is 40X.

Oct1-/- mice treated with pyroplatin was consistent with the higher plasma platinum concentration in these mice ($p < 0.005$; Figure 3.15A).

3.2.2 Hepatic toxicity of pyroplatin was enhanced in *Oct1+/+* mice. Similar to the dose-range-finding toxicity study, we observed that following treatment with pyroplatin, the liver to body weight ratio was significantly increased compared to saline control in both *Oct1+/+* and *Oct1-/-* mice (Figure 3.8). However, the liver to body weight ratio change in *Oct1+/+* mice, which was 28.8% increase in pyroplatin-treated mice compared with saline-treated mice, was more striking than that in *Oct1-/-* mice, which was 14.7% increase in pyroplatin-treated mice compared with saline-treated mice. To exclude the confounding effect of less body weight decrease in *Oct1+/+* mice on the liver to body weight ratio, the actual liver weights between *Oct1+/+* and *Oct1-/-* mice treated with pyroplatin and saline were also compared, our data showed that the actual liver weight was increased by pyroplatin treatment in *Oct1+/+* mice but not in *Oct1-/-* mice (pyroplatin vs saline: 1.23 vs 0.973 g in *Oct1+/+* mice, $p < 0.00001$; 1.02 vs 1.00 g in *Oct1-/-* mice, $p > 0.05$), indicating that pyroplatin indeed resulted in hepatomegaly in *Oct1+/+* mice.

The effect of pyroplatin on the liver function was compared between *Oct1+/+* and *Oct1-/-* mice. As shown in Figure 3.9, the level of total protein was significantly reduced by pyroplatin in *Oct1+/+* mice, but not affected in *Oct1-/-* mice. The activities of ALT, AST and ALKP were not affected in either *Oct1+/+* or *Oct1-/-* mice; however, glucose levels were significantly increased by pyroplatin in *Oct1+/+* mice, but not in *Oct1-/-* mice, the mechanism for the increased glucose levels are unclear at this point.

Histopathological examination of liver from *Oct1-/-* mice treated with either saline or pyroplatin showed no clear signs of toxicity, while the liver from *Oct1+/+* mice treated with pyroplatin appeared to have enlarged and rounded hepatocytes, which are normally hexagonal (Figure 3.10). The irregular white spots, which were considered to be aqueous materials inside the hepatocytes pushed the nucleus aside, indicating pyroplatin resulted in liver edema in Oct1+/+ mice. The hepatic lesion was more striking in portal vein area than in other regions of the liver (Figure 3.10), which is similar to the hepatotoxicity produced by oxaliplatin. The greater hepatic toxicity in *Oct1+/+* mice was consistent with the higher hepatic platinum accumulation in these mice (Figure 3.15B; $p < 0.005$). These data strongly suggest that *Oct1*deletion protects animals from developing liver toxicity and that *Oct1* plays a role not only in pyroplatin disposition but also in pyroplatin target organ toxicity.

3.2.3. Renal toxicity of pyroplatin was more pronounced in *Oct1-/-* mice. In both *Oct1+/+* and *Oct1-/-* mice administered with pyroplatin, serum creatinine levels were not significantly different from mice administered with saline ($p > 0.05$; Figure 3.11). Serum BUN levels were significantly reduced in pyroplatin-treated *Oct1+/+* mice compared with saline-treated *Oct1+/+* mice ($p < 0.05$), while serum BUN was not affected by pyroplatin in *Oct1-/-* mice ($p > 0.05$; Figure 3.11). Pyroplatin treatment increased renal mRNA levels of Kim-1, a more sensitive and quantitative renal biomarker of early tubular damage, by 19.3-fold over control values in *Oct1+/+* mice. However, the elevation of renal Kim-1 expression in *Oct1-/-* mice following pyroplatin treatment was much more striking than in *Oct1+/+* mice, the fold difference over saline control was 117 (Figure 3.12).

Histologic evaluation of kidneys from pyroplatin-treated mice demonstrated tubular cast formation, which was revealed by eosinophilic amorphous material and pyknotic and karyorhectic debris (Figure 3.13 B) and degeneration of tubular cells including tubular dilatation, tubular cell vacuolation, tubular cell detachment (Figure 3.13C). The renal morphology change seemed to localize to the outer medulla (Figure3.13B and Figure 3.13C). Consistent with the Kim-1 expression study, the kidney tubular lesions were most prominent in *Oct1-/-* mice treated with pyroplatin compared with *Oct1+/+* mice treated with pyroplatin (Figure 3.13A) and saline-treated control animals. The kidney platinum accumulation in *Oct1-/-* mice was remarkably greater than that in *Oct1+/+* mice (Figure 3.15C; $p < 0.05$). These data indicate that pyroplatin is more toxic to the kidney in *Oct1-/-* mice.

3.2.4. Hematological toxicity of pyroplatin was more pronounced in *Oct1-/-* mice. Figure 3.14 showed the hematological parameters affected by pyroplatin in both *Oct1+/+* and *Oct1-/-* mice. The significant changes in white blood cell parameters including neutrophil (%) and lymphocytes (%), and in platelet parameter, i.e. mean platelet volume (MPV) were observed in pyroplatin-treated *Oct1-/-* mice but not in *Oct1+/+* mice ($p <0.05$). The higher plasma platinum concentration in *Oct1-/-* mice supported greater hematological toxicity of pyroplatin in these mice (Figure 3.15A; $p < 0.005$). Significant changes in red blood cell parameters including red blood cell count, hemoglobin (Hb), hematocrit (HCT) and red blood cell width (RDW), all of these changes, which indicated anemia, were observed in both *Oct1+/+* and *Oct1-/-* mice following pyroplatin treatment ($p < 0.05$).

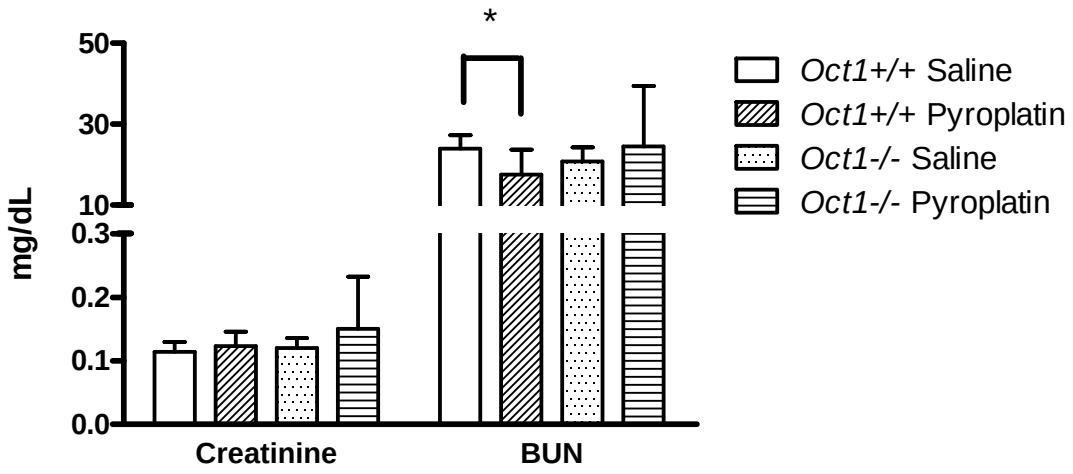

Figure 3.11. Effects of pyroplatin on creatinine and blood urea nitrogen (BUN) in *Oct1*+/+ and *Oct1*-/- mice. *Oct1*+/+ and *Oct1*-/- mice were treated with saline or pyroplatin (120/90 mg/kg) via tail vein injection once weekly for a total three weeks (at least 9 animals per group). The mice were fasted for at least 16 hours before sacrifice. Blood was collected 24 hrs after the last dose; Creatinine and BUN in serum were measured. Data are presented as the mean ± SD. * $p < 0.05$ compared with corresponding saline control group.

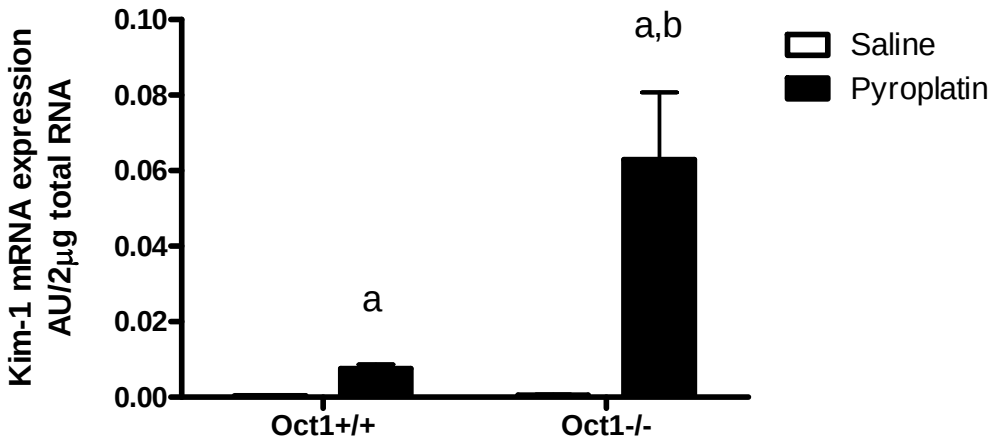

Figure 3.12. Pyroplatin results in more striking Kim-1 expression in *Oct1*-/- in comparison to *Oct1*+/+ mice. *Oct1*+/+ and *Oct1*-/- mice were treated with saline or pyroplatin (120/90 mg/kg) via tail vein injection once weekly for a total three weeks (at least 9 animals per group). The mice were fasted for at least 16 hours before sacrifice. Kidneys were collected 24 hrs after the last dose; Total RNA from kidney was reverse-transcribed and the synthesized cDNA was subject to qRT-PCR using Kim-1 probe. The amplification of glyceraldehydes-3-phosphate dehydrogenase (GAPDH) mRNA was used as an internal control. Data are presented as the mean ± SD. a: $p < 0.01$ pyroplatin treatment compared with saline control for *Oct1*+/+ and *Oct1*-/- mice, respectively; b: $p < 0.05$ *Oct1*+/+ compared with *Oct1*-/- mice for pyroplatin treatment.

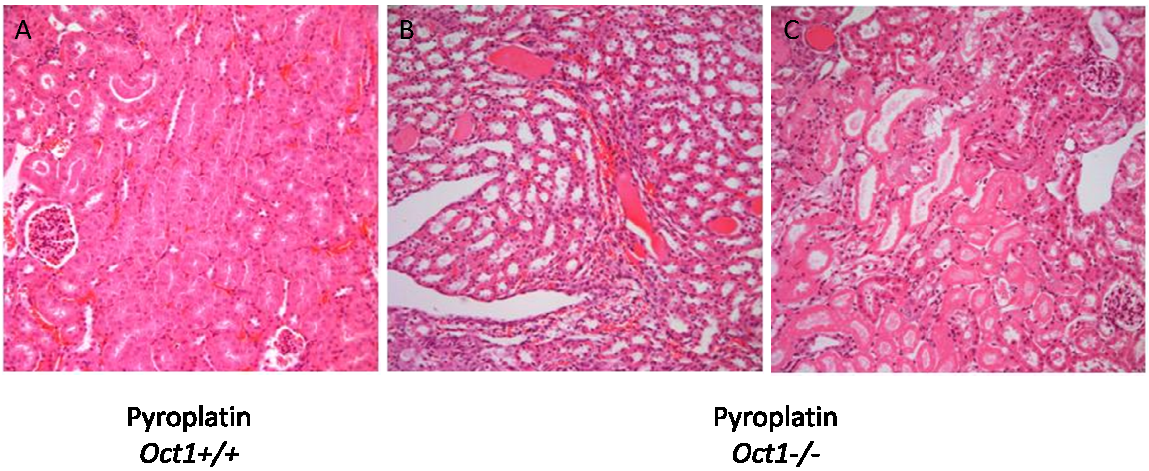

Figure 3.13. Representative kidney histopathology of *Oct1*+/+ and *Oct1*-/- mice treated with pyroplatin. *Oct1*+/+ and *Oct1*-/- mice were treated with saline or pyroplatin (120/90 mg/kg) via tail vein injection once weekly for a total three weeks (at least 9 animals per group). The mice were fasted for at least 16 hours before sacrifice. Kidney was collected 24 hrs after the last dose and fixed in 4% paraformaldehyde. The paraffin-embedded kidney is sliced and stained with hematoxylin and eosin. The magnification is 20X.

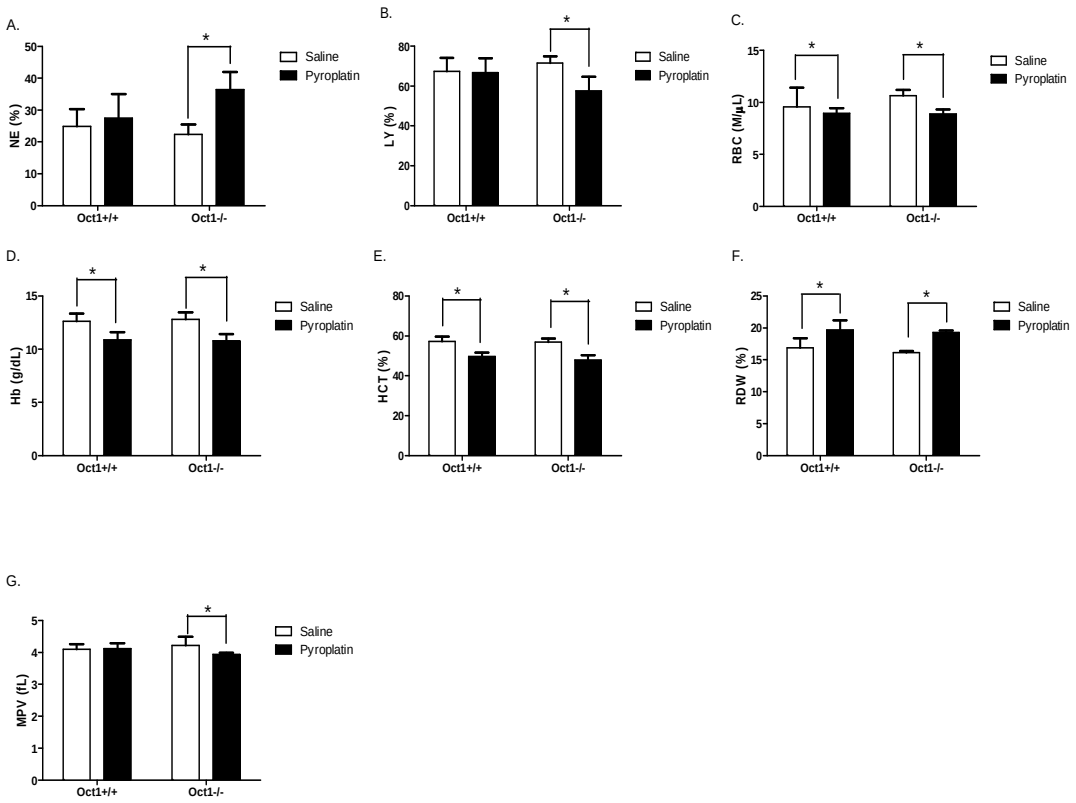

Figure 3.14. Effect of Oct1 deletion on hematological toxicity of pyroplatin. *Oct1+/+* and *Oct1-/-* mice were treated with saline or pyroplatin (120/90 mg/kg) via tail vein injection once weekly for a total three weeks (at least 9 animals per group). The mice were fasted for at least 16 hours before sacrifice. Blood was collected via tail vein bleeding 24 hrs after the last dose; CBC was measured within 24 hr after collection. Data are presented as the mean ± SD. * $p < 0.05$ compared with corresponding saline control group.

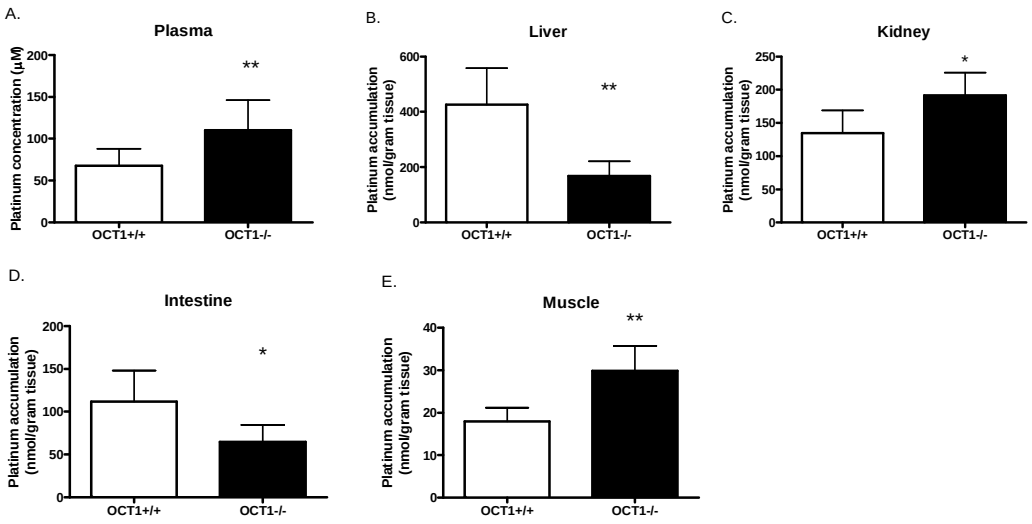

Figure 3.15. Platinum concentrations in plasma and various tissues collected from *Oct1*+/+ and *Oct1*-/- mice. *Oct1*+/+ and *Oct1*-/- *1*-/- mice were treated with saline or pyroplatin (120/90 mg/kg) via tail vein injection once weekly for a total three weeks (at least 9 animals per group). The mice were fasted for at least 16 hours before sacrifice. Blood (A), liver (B), kidney (C), intestine (D) and muscle (E) were harvested 24 hrs after the last dose. Platinum was measured by ICP-MS. Data are presented as the mean ± SD. * $p < 0.05$ compared with saline control group; ** $p < 0.005$ compared with saline control group.

3.2.5. No intestinal histological change was observed. Histological examination of intestine showed no signs of intestinal toxicity in either *Oct1*+/+ or *Oct1*-/- mice following pyroplatin treatment, although significantly higher intestinal accumulation of pyroplatin in *Oct1*+/+ mice was observed (Figure 3.15D, $p < 0.05$).

3.3. Pyroplatin is substrate of hOCT3. The cellular platinum accumulation rate after 1-hour of exposure to 10 µM pyroplatin in HEK-hOCT3 cells [59.7 ± 1.95 pmol/mg protein/hr] was 3.2-fold ($p < 0.0001$) of that in HEK-MOCK cells [18.6 ± 1.20 pmol/mg protein/hr] (Figure 3.16A). Coincubation with corticosterone (10 µM) resulted in a 4.1-fold decrease in the rate of platinum accumulation in HEK-hOCT3 cells [control versus corticosterone treated, 59.7 ± 1.95 pmol/mg protein/hr versus 14.7 ± 0.66 pmol/mg protein/hr; $p < 0.0001$] with no effect in HEK-MOCK cells [control versus corticosterone treated, 18.6 ± 1.20 pmol/mg protein/hr versus 17.3 ± 0.89 pmol/mg protein/hr; $p > 0.05$; Figure 3.16A]. The platinum-DNA adduct level in HEK-hOCT3 cells [0.0509 ± 0.0097 pmol/µg DNA] was 6.21-fold greater ($p < 0.005$) than that in HEK-MOCK cells [0.0082 ± 0.0016 pmol/µg DNA] after incubation with pyroplatin (Figure 3.16B) and was markedly reduced by corticosterone (10 µM) [control versus corticosterone treated, 0.0509 ± 0.0097 pmol/µg DNA versus 0.0047 ± 0.0019 pmol/µg DNA; $p < 0.005$]. Corticosterone produced only a small decrease in platinum-DNA adduct level in HEK-MOCK cells [control versus corticosterone treated, 0.0082 ± 0.0016 pmol/µg DNA versus 0.0053 ± 0.0008 pmol/µg DNA; $p > 0.05$; Figure 3.16B]. These results indicate that human OCT3 contributes substantially to the uptake of pyroplatin and subsequently the formation of platinum-DNA adduct.

3.4. Pyroplatin is good substrate of hMATE1 and weak substrate of hMATE2K.

Because the MATE transporters are activated by the oppositely generated H^+-gradient across the plasma membrane, the transporter-expressing cells were incubated with basic buffer containing pyroplatin to stimulate the uptake of pyroplatin. The platinum accumulation rate in HEK-hMATE1 and HEK-hMATE2K [53.6 ± 8.19 pmol/mg protein/hr and 23.5 ± 1.17 pmol/mg protein/hr, respectively] was significantly higher (3.6-fold and 1.6-fold, respectively; $p < 0.005$) than that in HEK-MOCK cells [14.8 ± 1.14 pmol/mg protein/hr] (Figure 3.17A), suggesting that pyroplatin is a substrate of hMATE1 and hMATE2K.

4. Discussion

Previous studies in collaboration with the Lippard laboratory indicated that pyroplatin, a new generation platinum analog effectively blocks transcription from DNA templates carrying adducts of the complex and yet largely escapes repair [12]. These exceptional characteristics support the candidacy of this unique monofunctional cationic complex as an anticancer drug. The studies also showed that the drug is an excellent substrate of OCT1; therefore, the toxicity profile associated with pyroplatin and the role of OCT1 in regulating the toxicity of pyroplatin warranted further investigation.

We determined the role of Oct1 in the overall mortality produced by pyroplatin. The initial dose of pyroplatin used was 120 mg/kg, which caused mortality in *Oct1-/-* but not in *Oct1+/+* mice. Because Oct1 deletion resulted in markedly higher plasma platinum concentrations in *Oct1-/-* mice compared with wildtype mice as determined in Chapter 2, the mortality in *Oct1-/-* mice is likely due to a greater systemic exposure to platinum.

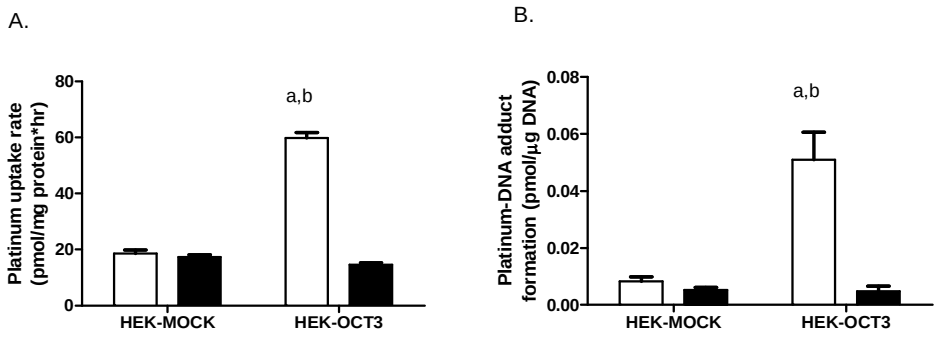

Figure 3.16. Uptake of pyroplatin and platinum-DNA adduct formation after 1-hour exposure to pyroplatin in hOCT3-transfected cells. Intracellular platinum accumulation rates (A) and platinum-DNA adduct formation (B) in hOCT3-transfected cells and in MOCK cells after 1 hour exposure to 10 µM pyroplatin in the presence (black columns) or absence (white columns) of OCT3 inhibitor (corticosterone) were determined as described in Materials and Methods. Briefly, HEK-293 cells were incubated in PBS containing 10 µM pyroplatin at 37^{o}C and 5% CO_2 for 1 hour. For the inhibitor studies, the incubation medium also contained corticosterone (10 µM). Total platinum concentration inside the cells and DNA-bound platinum were determined using ICP-MS. Total platinum concentration was normalized for protein content, and DNA-bound platinum was normalized for DNA content. Data are presented as the mean ± SD. a: significantly greater than in MOCK cells, $p<0.001$; b: significantly greater than in the presence of corticosterone, $p<0.001$.

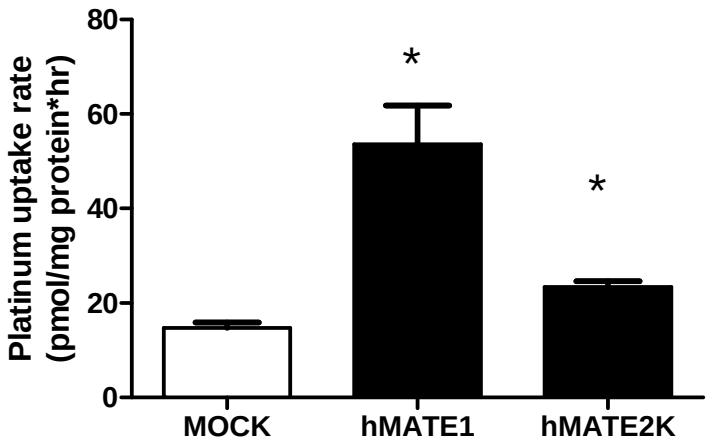

Figure 3.17. Uptake of pyroplatin by HEK-293 cells stably expressing hMATE1, hMATE2K and empty vector (MOCK). Intracellular platinum accumulation rates in hMATE1, hMATE2K-transfected cells and in the corresponding MOCK cells after 1 hour exposure to 10 µM pyroplatin and in HEK293 cells were determined as described in Materials and Methods. Briefly, HEK-293 cells were incubated in uptake buffer containing 10 µM pyroplatin at 37^{o}C and 5% CO_2 for 1 hour. Total platinum concentration inside the cells was determined using ICP-MS. Total platinum concentration was normalized for protein content. Data are presented as the mean ± SD. * $p<0.005$ compared with MOCK cells.

Consistent with higher plasma platinum concentrations in *Oct1-/-* mice, the body weight decreased more in *Oct1-/-* mice and the hematological effects of pyroplatin was more severe in *Oct1-/-* mice compared with *Oct1+/+* mice.

Because of its huge abundance in the liver, OCT1 facilitates the hepatic accumulation of drugs and other xenobiotics and accordingly may play an important role in mediating the hepatic toxicity of its substrates. A more than two-fold increase in the activity of ALT in pyroplatin-treated animals (120 mg/kg) was considered to indicate hepatocyte damage with clinical significance. Histological examination revealed swelling of the liver at 90 mg/kg in the Oct1 wildtype, but not the knockout mice, consistent with the increased liver to body weight ratio in the wildtype mice. These data suggest that at 90 mg/kg, pyroplatin exhibits hepatotoxicity and that Oct1 deletion protects against this toxicity. The low BUN in the wildtype mice is also consistent with hepatotoxicity in these mice. A low BUN usually has little significance, but its causes include liver problems, malnutrition (insufficient dietary protein), or excessive alcohol consumption. Although there was greater hepatic toxicity in *Oct1+/+* mice, the level of toxicity was still considered as mild and reversible. If pyroplatin is developed as an anticancer drug, the hepatic toxicity may not be a concern. In addition, our work also demonstrated that pyroplatin is a substrate of MATE1, which is expressed on the canalicular membrane of the hepatocyte. MATE1 may facilitate the removal of pyroplatin from the liver and thus prevent excessive accumulation of the drug.

The glucose level was significantly increased in pyroplatin treated (90 mg/kg) wildtype but not knockout mice though the exact mechanism for this increase is not clear.

Since plasma glucose levels in fasting mice are determined primarily by gluconeogenesis, it is possible that pyroplatin inhibits gluconeogenesis in the liver. Because it did not accumulate substantially in the liver of *Oct1-/-* mice, it did not affect glucose levels as much. However this explanation is highly speculative; and further studies examining the mechanisms of the pyroplatin-induced increase in glucose levels are clearly needed.

Similar to other platinum agents, pyroplatin also exhibited hematological toxicity, which was obvious at a dose of 120 mg/kg; however the effect of Oct1 on hematologic toxicities was variable. The markedly increased % neutrophil in the *Oct1* knockout but not wildtype mice cannot be explained. It might indicate possible acute inflammation associated with dosing manipulation, which is modulated by Oct1. However, no role of Oct1 in hematologic toxicity has been reported. The markedly decreased % lymphocyte in the *Oct1-/-*, but not the *Oct1* wildtype mice, is consistent with higher plasma levels of pyroplatin in the knockout mice. In general, abnormally high MPV values correlate primarily with thrombocytopenia. Pyroplatin decreased, rather than increased, MPV in the *Oct1* knockout mice, and had no effect on MPV in wildtype mice suggesting that it will not produce thrombocytopenia at doses of 90 mg/kg.

In this study, we made a striking and unexpected observation that *Oct1* deletion markedly increased the renal toxicity of pyroplatin in *Oct1-/-* mice, which were revealed by much greater Kim-1 mRNA expression and histological changes of tubular cast formation and degeneration of tubular cells in *Oct1-/-* mice (Figure 3.12, Figure 3.13B, and Figure 3.13C). The increase in Oct2 expression in the kidney of *Oct1-/-* mice and the fact that pyroplatin is an excellent substrate of Oct2 [12] may explain the greater renal

toxicity of the drug in *Oct1-/-* mice. In addition, the differential localization of organic cation transporters Oct1 and Oct2 in the basolateral membrane of rat kidney proximal tubules may further account for the greater kidney toxicity in *Oct1-/-* mice. In particular, Oct1 was shown to be concentrated in the proximal tubules in the renal cortex, whereas Oct2 was abundant in the proximal tubules in the outer stripe of the outer medulla [16, 17]. The increase in Oct2 expression observed in the kidney of Oct1-/- mice is likely to localize in the outer strip of the outer medulla and may produce a localized accumulation of pyroplatin in this region. The outer medulla was the region most damaged by pyroplatin (Figure 3.13B). Because our data suggest that pyroplatin is also a substrate of MATE1 and MATE2K (Figure 3.17), these apical transporters may work in concert with Oct1 and Oct2 in mouse kidney to control regional levels of pyroplatin. Further studies sorting out the role of MATEs in pyroplatin induced kidney toxicity are clearly needed.

Pyroplatin has been shown to have significant anti-cancer activity in a mouse tumor model. According to the study, pyroplatin at 40 mg/kg resulted in a 103% increase in mean survival time over untreated mice when tested against Sarcoma 180 ascites (S180). Pyroplatin at 80 mg/kg resulted in a 72% increase in mean survival time over control when tested against P388 leukemia [18]. The doses used in our toxicity studies covered the efficacious doses used in the mouse tumor model. Pyroplatin at 90 mg/kg only showed mild and reversible hepatic toxicity in *Oct1+/+* mice without nephrotoxicity, a major concern associated with cisplatin treatment.

In summary, pyroplatin appears to possess a favorable toxicity profile, and Oct1 plays an important role in determining the toxicity profile of pyroplatin. Our study

supported the concept that by targeting drug influx transporters, off-target toxicities can be greatly spared. The study also suggests that genetic variants in pyroplatin transporters will modulate toxicity. Whether pyroplatin can be used for targeted therapy of various cancers is worthy of further investigation.

References

1. Bosl, G.J., Bajorin, D.F., and Sheinfeld, J., *Cancer of the testis*, in *Cancer: Principles and practice of oncology*, Devita, V.T., Hellman, S, Rosenberg S.A Editor. 2000, Lippincott, Williams and Wilkins. p. 1491.

2. Rabik, C.A. and Dolan, M.E., *Molecular mechanisms of resistance and toxicity associated with platinating agents.* Cancer Treatment Reviews, 2007. **33**(1): p. 9-23.

3. Harrap, K.R., *Preclinical studies identifying carboplatin as a viable cisplatin alternative.* Cancer Treatment Reviews, 1985. **12**: p. 21-33.

4. Kelland, L., *The resurgence of platinum-based cancer chemotherapy.* Nature Reviews Cancer, 2007. **7**(8): p. 573-584.

5. Wagstaff, A.J., Ward, A., Benfield, P., and Heel, R.C., *Carboplatin: A preliminary review of its pharmacodynamic and pharmacokinetic properties and therapeutic efficacy in the treatment of cancer.* Drugs, 1989. **37**(2): p. 162-190.

6. Misset, J.L., Bleiberg, H., Sutherland, W., Bekradda, M., and Cvitkovic, E., *Oxaliplatin clinical activity: A review.* Critical Reviews in Oncology Hematology, 2000. **35**(2): p. 75-93.

7. Urakami, Y., Okuda, M., Masuda, S., Saito, H., and Inui, K.I., *Functional characteristics and membrane localization of rat multispecific organic cation transporters, OCT1 and OCT2, mediating tubular secretion of cationic drugs.*

Journal of Pharmacology and Experimental Therapeutics, 1998. **287**(2): p. 800-805.

8. Yonezawa, A., Masuda, S., Nishihara, K., Ikuko, Y., Katsura, T., and Inui, K., *Organic cation transporter Oct2 (Slc22a2) as a determinant of the cisplatin-induced nephrotoxicity in the rat.* Yakugaku Zasshi-Journal of the Pharmaceutical Society of Japan, 2005. **125**: p. 46-47.

9. Yonezawa, A., Masuda, S., Nishihara, K., Yano, I., Katsura, T., and Inui, K., *Association between tubular toxicity of cisplatin and expression of organic cation transporter rOCT2 (Slc22a2) in the rat.* Biochemical Pharmacology, 2005. **70**(12): p. 1823-1831.

10. Muggia, F., *Platinum compounds 30 years after the introduction of cisplatin: Implications for the treatment of ovarian cancer.* Gynecologic Oncology, 2009. **112**(1): p. 275-281.

11. Jonker, J.W. and Schinkel, A.H., *Pharmacological and physiological functions of the polyspecific organic cation transporters: OCT1, 2, and 3 (SLC22A1-3).* Journal of Pharmacology and Experimental Therapeutics, 2004. **308**(1): p. 2-9.

12. Lovejoy, K.S., Todd, R.C., Zhang, S.Z., McCormick, M.S., D'Aquino, J.A., Reardon, J.T., Sancar, A., Giacomini, K.M., and Lippard, S.J., *Cis-diammine(pyridine)chloroplatinum(ii), a monofunctional platinum(ii) antitumor agent: Uptake, structure, function, and prospects.* Proceedings of the National

Academy of Sciences of the United States of America, 2008. **105**(26): p. 8902-8907.

13. Jonker, J.W., Wagenaar, E., Mol, C., Buitelaar, M., Koepsell, H., Smit, J.W., and Schinkel, A.H., *Reduced hepatic uptake and intestinal excretion of organic cations in mice with a targeted disruption of the organic cation transporter 1 (Oct1 [Slc22a1]) gene.* Molecular and Cellular Biology, 2001. **21**(16): p. 5471-5477.

14. Chen, Y., Teranishi, K., Li, S., Yee, S.W., Hesselson, S., Stryke, D., Johns, S.J., Ferrin, T.E., Kwok, P., and Giacomini, K.M., *Genetic variants in multidrug and toxic compound extrusion-1, hMATE1, alter transport function.* Pharmacogenomics J, 2009. **9**(2): p. 127-136.

15. Zhang, S.Z., Lovejoy, K.S., Shima, J.E., Lagpacan, L.L., Shu, Y., Lapuk, A., Chen, Y., Komori, T., Gray, J.W., Chen, X., Lippard, S.J., and Giacomini, K.M., *Organic cation transporters are determinants of oxaliplatin cytotoxicity.* Cancer Research, 2006. **66**(17): p. 8847-8857.

16. Sugawara-Yokoo, M., Urakami, Y., Koyama, H., Fujikura, K., Masuda, S., Saito, H., Naruse, T., Inui, K., and Takata, K., *Differential localization of organic cation transporters rOct1 and rOct2 in the basolateral membrane of rat kidney proximal tubules.* Histochemistry and Cell Biology, 2000. **114**(3): p. 175-180.

17. Urakami, Y., Okuda, M., Masuda, S., Akazawa, M., Saito, H., and Inui, K., *Distinct characteristics of organic cation transporters, Oct1 and Oct2, in the*

basolateral membrane of renal tubules. Pharmaceutical Research, 2001. **18**(11): p. 1528-1534.

18. Hollis, L.S., Amundsen, A.R., and Stern, E.W., *Chemical and biological properties of a new series of cis-diammineplatinum(ii) antitumor agents containing 3 nitrogen donors - cis-[pt(nh3)2(n-donor)cl]+*. Journal of Medicinal Chemistry, 1989. **32**(1): p. 128-136.

CHAPTER 4

ROLE OF OCT1 IN THE ANTITUMOR EFFECT OF PYROPLATIN IN MICE

Introduction

Liver cancer (mainly hepatocellular carcinoma, aka HCC) is a major health problem worldwide. It is the sixth most common cancer and the third leading cause of cancer related death worldwide with more than 600,000 new cases per year [1]. This cancer is more frequent among Native Americans, Asians, Pacific Islanders, and Hispanics than among Caucasians. Diseases that predispose patients to HCC include chronic viral hepatitis, alcoholism and cirrhosis (scarring of the liver). There is no effective treatment for most of the individuals who succumb to this neoplasm, and difficulties in treatment of HCC appear to be due to insufficient drug accumulation or extensive drug inactivation (metabolism) by the liver cancer cells. Sorafenib, an oral multikinase inhibitor that blocks tumor cell proliferation by targeting the Raf/mitogen-activated protein kinase/extracellular signal-regulated kinase (Raf/MEK/ERK) signaling pathway and exerts antiangiogenic effects was approved by the FDA in 2007 as a result of the SHARP trial (Sorafenib HCC Assessment Randomized Protocol). Data from SHARP indicated that sorafenib significantly improved survival from a median of 34.4 weeks to 46.3 weeks and prolonged the median time to progression from 12.3 weeks to 24 weeks among patients with advanced HCC [2]. However, sorafenib does not induce tumor involution or radiologic remission typical of cytotoxic chemotherapeutics. Therefore, there is an urgent need to develop novel cytotoxic agents, which can be used in combination with targeted agents such as sorafenib, for better treatment outcome, or

even cure of this deadly disease. Problems with the traditional cytotoxic agents such as cisplatin and doxorubicin are their lack of tumor specificity, and therefore their toxicity to normal tissues.

In previous studies we determined that the novel platinum analog, pyroplatin, was an excellent substrate of the liver organic cation transporter, OCT1 [3]. In Chapter 2, using *Oct1-/-* mice, we showed that Oct1 played an important role *in vivo* in determining the disposition of pyroplatin and importantly, in facilitating the accumulation of pyroplatin in the liver, the tissue in which it is most highly expressed. Further, studies in the literature [4] and our unpublished data indicate that OCT1 is abundantly expressed in hepatocellular carcinoma, suggesting that pyroplatin may be useful in the treatment of HCC. The goal of the current study was to test the hypothesis that Oct1 mediates the antitumor effect of pyroplatin, in particular, the efficacy of pyroplatin in HCC. Firstly, we assessed the role of Oct1 in tumor responsiveness of pyroplatin *in vivo* to establish the link between OCT1 expression and antitumor efficacy of pyroplatin using a xenograft model of stably transfected HEK-OCT1 cell lines. Further, we investigated the effect of pyroplatin in hepatocellular carcinoma (HCC) and the role of Oct1 on pyroplatin response in *Oct1+/+* and *Oct1-/-* mice bearing HCC that was induced by hydrodynamic transfection of oncogenes.

Materials and Methods

Synthesis of pyroplatin *cis*-[Pt(NH$_3$)$_2$(Pyr)Cl]NO$_3$. Pyroplatin was synthesized as previously described (refer to Chapter 2).

Constructs. Plasmids encoding the Sleeping Beauty transposase and transposons with wild-type human *MET*, a constitutively active version of *CTNNB1* (Δ*N90-CTNNB1*) were provided by Dr. Xin Chen of UCSF; all plasmids were purified using the Plasmid Maxi Kit (QIAGEN) before injecting into mice.

Cell lines and cell culture. All human HCC cell lines (SNU449, SNU398, HuH7, Hep3B and HepG2) used in the present study were from the American Type Culture Collection (Manassas, VA). The culture medium is DMEMH21 medium supplemented with 10% FBS, 100 units/ml penicillin and 100 µg/ml streptomycin. All cell lines were grown at 37 °C in a humidified atmosphere with 5% CO_2.

Transfection. The day before transient expression, HepG2 and SNU398 cells were seeded onto 100 mm poly-D-lysine coated dishes. The cells were transfected with 1 µg of pcDNA5/FRT empty vector, pcDNA5/FRT vector containing the full-length hOCT1 using Lipofectamine 2000 (Invitrogen) according to the manufacturer's instructions. Forty-eight hours after transfection, the cells were used for the experiments.

Cytotoxicity assay. The cytotoxicity of pyroplatin was measured by the 3-(4,5-dimethylthiazol-2-yl)-2,5-diphenyltetrazolium bromide (MTT) assay in 96-well plates as previously described [5]. Drug exposure time was 7 hours followed by 65 hour incubation in drug free medium.

Reaction of platinum agents with glutathione. The reaction of platinum agents with glutathione was determined as described previously [6]. In brief, reactions were carried out at 37 ± 0.1°C in a total volume of 5.0 ml. In a typical experiment, the mixture

contained 60 mM Tris-NO_3, 100 μM platinum drug, and 16.5 mM GSH (pH 7.4). For all reactions, the final concentration of NaCl was adjusted to 4.62 mM, the approximate concentration of NaCl in the cytoplasm, by the addition of appropriate amounts of 154 mM NaCl solution. Reactions were initiated by mixing platinum drug with the buffer and NaCl followed by immediate addition of the GSH. The UV absorbance at 260 nm as a function of time (which reflects the Pt-S and S-S bond formation reactions) was measured using a single beam spectrophotometer (Secomam). Each reaction was followed for 24 h. Two control mixtures were incubated along with each reaction. One control mixture contained the same additions without GSH (which showed negligible absorbance changes over 24 h); the other control mixture contained the same additions without the Pt drug for measuring the rate of disulfide formation. The absorbance changes due to disulfide formation were subtracted from that of the reactions.

Animals. *Oct1*-/- mice were generated as described elsewhere [7]. *Oct1*-/- and *Oct1*+/+ (wild-type) mice were in FVB background and were housed in a virus-free, temperature-controlled facility on a 12-h light–dark cycle. They were allowed standard mouse food and water *ad libitum*. For xenografts mode antitumor assay, seven-week old female athymic mice (nu/nu genotype, BALB/c background) were purchased from Taconic Inc. (Frederick, MD, USA) through a contract with the UCSF Cancer Center and housed under aseptic conditions, which included filtered air and sterilized food, water, bedding, and cages. All experiments on mice were approved by the Institutional Animal Care and Use Committee of University of California at San Francisco.

Xenograft model antitumor study. 10^7 HEK 293 cells stably expressing OCT1 (HEK-OCT1) or HEK 293 cells stably expressing the empty vector (HEK-MOCK) were transplanted subcutaneously into nude mice. Serial tumor measurements were obtained every 3-4 days by caliper in three dimensions. Tumor volumes were calculated according to the following formula: volume = height x width x length x 0.5236. When tumor size reached ~ 100 to 150 mm^3 (about two weeks later), mice were separated into four groups (n = 6/group), two groups for each cell line. For each cell type, one group was treated with saline and the other with pyroplatin (50 mg/kg) through tail vein injections once a week for three weeks. Tumor and body weight measurements were performed twice a week. Relative tumor volume (%) was calculated by dividing the tumor volume at each measurement by initial tumor volume. All surviving animals were sacrificed 24 hours after the last treatment. On the day of the terminal sacrifice, blood was collected by heart puncture and centrifuged for 30 min at 1000 X g at 4^oC. The plasma was decanted and frozen at -80^oC until analysis. Tumor tissues were collected and snap frozen in liquid nitrogen.

Hydrodynamic transfection. The procedures were described previously [8, 9]. In brief, 0.4 µg of the plasmids encoding the Sleeping Beauty transposase and 10 µg of transposons with wild-type human *MET*, a constitutively active version of *CTNNB1* (Δ*N90-CTNNB1*) were suspended in 2 mL 0.9% NaCl, filtered, and injected into the lateral tail vein of 6-week-old to 8-week- old *Oct1*+/+ and *Oct1*-/- mice in ≤10 sec. All mice were monitored once weekly for the appearance of HCC.

Anti-HCC study. Mice bearing HCC were divided into two groups for each *Oct1* genotype, and treated with pyroplatin (50 mg/kg) or saline by tail vein injection once weekly until the animals were moribund or until unacceptable adverse effects occurred. A subset of animals from each group (n=6) was sacrificed 24 hrs after the first dose, blood was collected by heart puncture and centrifuged for 30 min at 1000 X g at 4^{o}C. The plasma was decanted and frozen at -80^{o}C until analysis. Tumor tissues were collected and divided into two halves, one half of the tissues was fixed in 4% paraformaldehyde for histopathology examination, the other half of the tissues was snap frozen in liquid nitrogen. The rest of the animals were closely monitored three times a week and sacrificed when moribund; the survival data were recorded.

Plasma and tissue platinum measurement. Plasma and tissue powder were dissolved in 70% nitric acid and incubated at 65°C for at least 2.5 hours. Distilled water containing 10 ppb of iridium (Sigma) and 0.1% Triton X-100 was added to the samples to dilute nitric acid to 7%. 5 μl of plasma and about 10-30 mg of tissue powders were used for total platinum measurement by ICP-MS.

Caspase-3/7 assay. Caspase-3/7 activity in HCC tissue was measured using a Caspase-Glo®3/7 Assay kit (Promega) according to the manufacturer's instructions. Cytosolic extracts from HCC tissue were prepared by Dounce homogenization in hypotonic extraction buffer [25 mm HEPES, pH 7.5, 5 mm $MgCl_2$, 1 mm EGTA, 1X protease inhibitor cocktail (Sigma-Aldrich)] and subsequently centrifuged (15 min, 13,000 rpm, 4 °C) [10]. The supernatant was stored at -80 °C until use. An equal volume of Caspase-Glo®3/7 reagent and 10 μg/ml cytosolic proteins were added to a white-

walled 96-well plate and incubated at room temperature for 1 h. The luminescence of each sample was measured in a plate-reading luminometer.

Isolation of total RNA and quantitative real-time polymerase chain reaction (qRT-PCR) analysis. Total RNA from each cell line was isolated using an RNeasy Mini Kit (QIAGEN) according to the manufacturer's instructions. Total RNA from HCC tissue was extracted using Trizol (Invitrogen). During the RNA purification procedure, DNase I was treated to digest residual genomic DNA. RNA was quantified spectrophotometrically at 260 nm. Extracted RNA was stored at -80^{o}C until use.

Total RNA from each sample was reverse transcribed into cDNA using a superscript first-strand cDNA synthesis kit (Invitrogen, Carlsbad, Calif., USA) according to the manufacturer's protocol. qRT-PCR was carried out in a 96-well plate in a total volume of 10 µl reaction solution that includes a cDNA equivalent of 2 µg total RNA, specific probe and Taqman Universal Master Mix (Applied Biosystems, Foster City, CA). Reactions were run on an AABI Prism 7700, and the thermal cycling conditions were 95 ^{o}C for 20 seconds followed by 40 cycles of 95 ^{o}C for 3 seconds and 60 ^{o}C for 30 seconds. The amplification of glyceraldehydes-3-phosphate dehydrogenase (GAPDH) mRNA was used as an internal control.

Statistical analysis. All experimental data except survival were expressed as mean ± standard deviation (SD). Data were analyzed statistically using the unpaired Student's t test. Multiple comparisons were performed with Dunnett's two-tailed test after one-way ANOVA. A log rank test was used for analysis of survival. A P value of less than 0.05 was considered statistically significant.

Results

OCT1 did not affect the cytotoxicity of pyroplatin in HCC cell lines. Five human HCC cell lines (SNU449, SNU398, HuH7, Hep3B and HepG2) were examined for the expression of OCT1 by qRT-PCR. As indicated in Figure 4.1, in all cell lines tested, the expression of OCT1 was very low, with the highest expression in HepG2, the lowest in SNU398.

To delineate the potential role of OCT1 in the cytotoxicity of pyroplatin, HepG2 and SNU398 were transiently tranfected with hOCT1 or empty vector. The sensitivity of these HCC cell lines to pyroplatin in the presence or absence of an OCT1 inhibitor, disopyramide was determined. The mRNA levels of OCT1 in cells transfected with OCT1 were remarkably increased [about 2000-fold for HepG2 cells and 5000-fold for SNU398 cells (data not shown)). However, there was no significant change in IC_{50} values of pyroplatin when HepG2 and SNU398 cells were transfected with hOCT1 (Figure 4.2). The IC_{50} values ranged from 57.7 to 82.3 µM for HepG2 cells and from 36.9 to 50.6 µM for SNU398. Coincubation with disopyramide did not increase the IC_{50} values in the cells as well ($p > 0.05$).

OCT1 appeared to enhance the antitumor effects of pyroplatin in mice with xenografts of HEK293 cells. A proof-of-concept *in vivo* antitumor study using xenografts of stably transfected OCT1 or empty vector cell lines was conducted to examine the role of OCT1 in the antitumor efficacy of pyroplatin. The dose of pyroplatin used was 50 mg/kg, which was determined in dose-range finding study (see Chapter 3). The dose of 50 mg/kg was considered well-tolerated over three weeks. We first examined

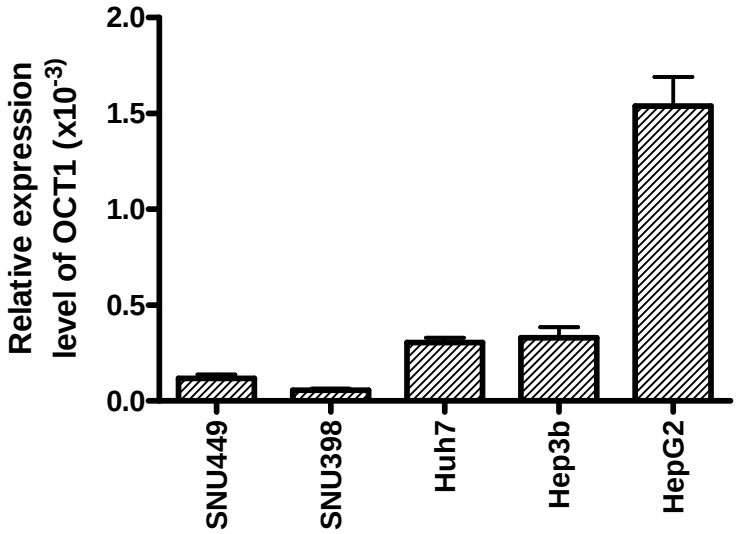

Figure 4.1. mRNA level of OCT1 in human hepatocellular carcinoma-derived cell lines. Total RNA from the cell lines was reverse-transcribed, and the OCT1 expression level was measured by qRT-PCR. The amplification of glyceraldehydes-3-phosphate dehydrogenase (GAPDH) mRNA was used as an internal control. Data are presented as the mean ± SD.

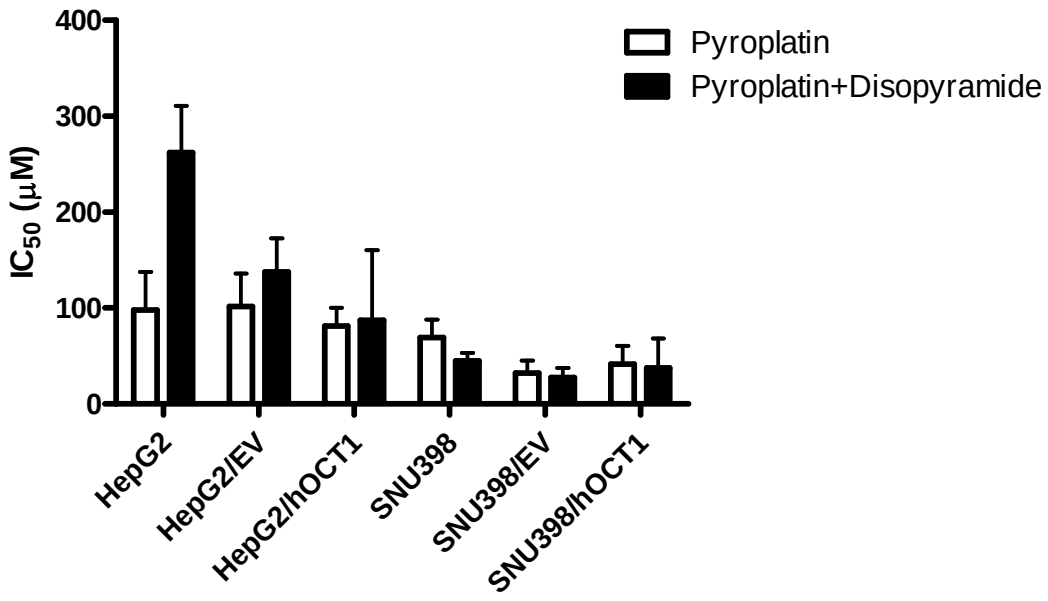

Figure 4.2. Role of hOCT1 expression in pyroplatin-induced cytotoxicity. HepG2 and SNU398 cells or these cells transiently expressing hOCT1, or empty vector were treated with pyroplatin in the presence or absence of an OCT1 inhibitor, disopyramide for 7 hrs. Then the cells were incubated in the normal culture medium for another 65 hrs. The cytotoxicity of pyroplatin was determined with a MTT assay. Data are presented as the mean ± SD.

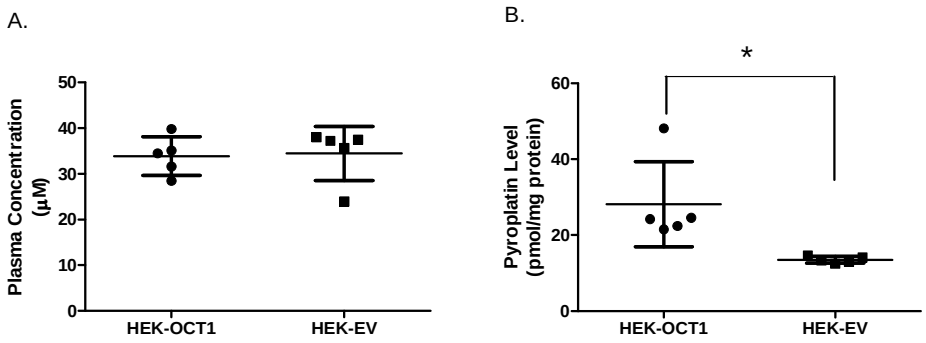

Figure 4.3. Pyroplatin levels in plasma and xenografts of HEK cells. Nude mice bearing xenografts of HEK-hOCT1 or HEK-MOCK were treated with pyroplatin (50 mg/kg) or saline once weekly for a total of three doses once the tumor volume reached ~ 100 to 150 mm^3 (about two weeks later). All surviving animals were sacrificed 24 hours after the last treatment. The platinum levels in plasma (A) and tumor mass (B) were determined by ICP-MS. Data are presented as the mean ± SD. * $p < 0.05$.

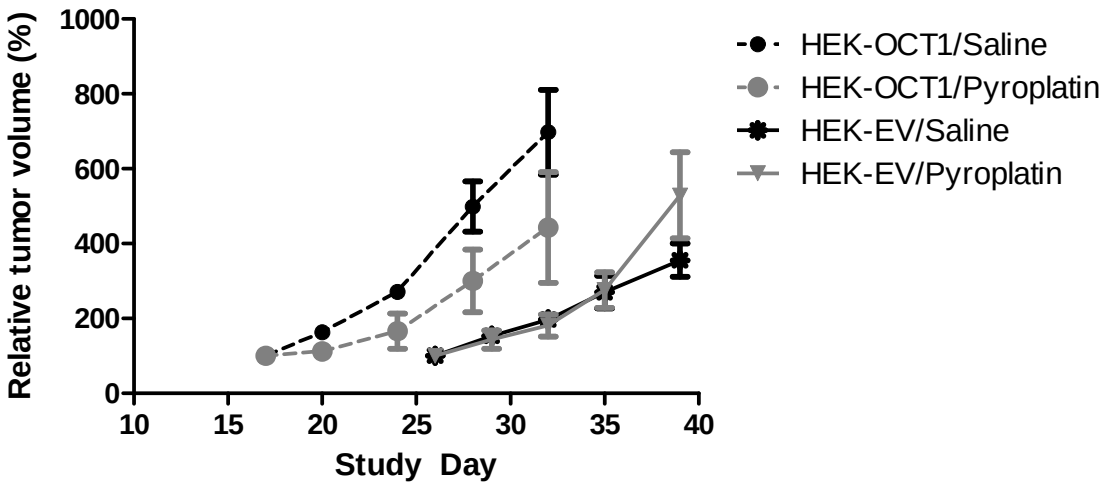

Figure 4.4. Role of hOCT1 expression in the antitumor activity of pyroplatin. Nude mice bearing xenografts of HEK-hOCT1 or HEK-MOCK were treated with pyroplatin (50 mg/kg) or saline once weekly for a total of three doses once the tumor volume reached ~ 100 to 150 mm^3 (about two weeks later). The tumor volume was monitored twice weekly. Relative tumor volume (%) was calculated by dividing the tumor volume at each measurement by initial tumor volume. Data are presented as the mean ± SD.

the pyroplatin levels in tumor mass and observed that the pyroplatin levels in HEK-hOCT1 tumor mass was significantly higher than that in HEK-MOCK tumor mass (Figure 4.3B; $p < 0.05$). However, the plasma pyroplatin concentrations were comparable between mice bearing HEK-hOCT1 xenografts and HEK-MOCK xenografts (Figure 4.3A). These results indicate that OCT1 indeed enhances pyroplatin accumulation in tumor mass. Relative tumor volume was compared to demonstrate whether the increased pyroplatin accumulation in mice bearing HEK-hOCT1 xenografts could translate into the greater antitumor activity of pyroplatin in these mice. As shown in Figure 4.4, pyroplatin produced a trend toward slowing tumor growth, and the relative tumor volume in pyroplatin-treated HEK-OCT1 tumors was lower than the corresponding saline-treated tumors at all monitored points with more obvious divergence at later points, although the difference in relative tumor volume did not reach statistical significance ($p > 0.05$). In HEK-MOCK tumors, pyroplatin treatment had no effect on reducing the relative tumor volume in comparison to saline treatment ($p > 0.05$).

HCC was induced in *Oct1*+/+ and *Oct1*-/- mice by hydrodynamic transfection. Hydrodynamic transfection of the combination of human *MET* and activating mutations of β-catenin (Δ*N90-CTNNB1)* gave rise to tumor in about 70% of surviving animals, which was similar to previous studies [9]. The appearance of tumor was observed at around 7 weeks at earliest by palpation. The tumor type induced in both *Oct1*+/+ and *Oct1*-/- mice was HCC confirmed by histological examination. The HCCs were multifocal as indicated in Figure 4.5. The Oct1 expression levels were also examined in HCC induced in *Oct1*+/+ mice. Similar levels of OCT1 mRNAs were evident in both

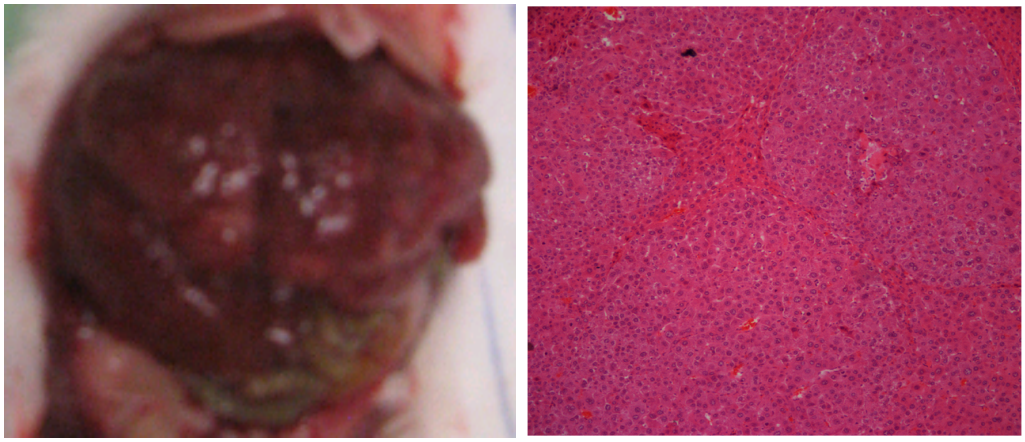

Figure 4.5. HCC was induced by hydrodynamic transfection of the combination of human *MET* and Δ*N90-CTNNB1*. 0.4 µg of the plasmids encoding the Sleeping Beauty transposase and 10 µg of transposons with wild-type human *MET*, a constitutively active version of *CTNNB1* (Δ*N90-CTNNB1*) were suspended in 2 mL 0.9% NaCl, filtered, and injected into the lateral tail vein of 6-week-old to 8-week- old Oct1+/+ and Oct1-/- mice in ≤10 sec. All mice were monitored once weekly for the appearance of tumor. (A) Representative gross image of liver tumor. Note that there are numerous tumor nodules in liver. (B) Histological examination of liver tumors that are multifocal.

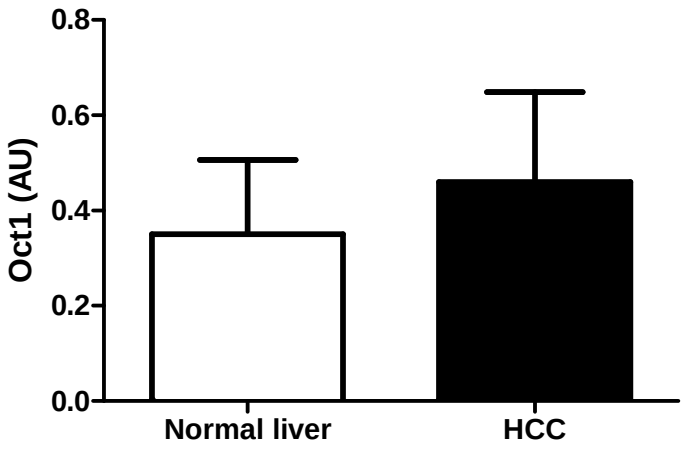

Figure 4.6. Oct1 expression was not altered during hepatocarcinogenesis. Total RNAs from normal liver and HCC induced in *Oct1*+/+ mice were reverse-transcribed, and the Oct1 expression level was measured by qRT-PCR. The amplification of glyceraldehydes-3-phosphate dehydrogenase (GAPDH) mRNA was used as an internal control. Data are presented as the mean ± SD.

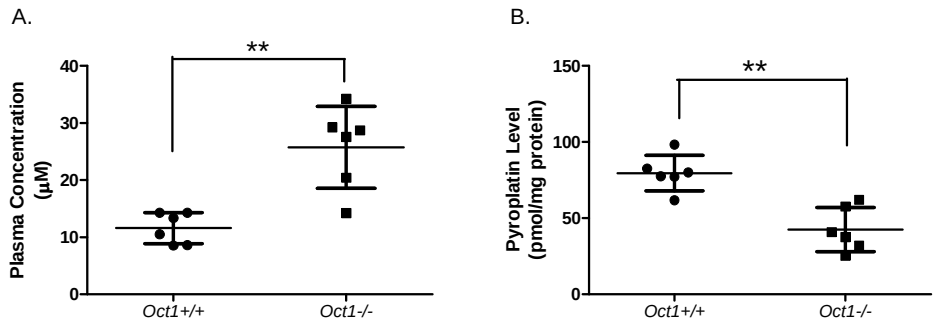

Figure 4.7. Pyroplatin levels in plasma and HCC tumor mass in *Oct1*+/+ and *Oct1*-/- mice. *Oct1*+/+ and *Oct1*-/- mice bearing HCC were treated with a single dose of pyroplatin (50 mg/kg) or saline via tail vein injection. All animals were sacrificed 24 hours. The platinum levels in plasma (A) and HCC tumor mass (B) were determined by ICP-MS. Data are presented as the mean ± SD. ** $p < 0.005$.

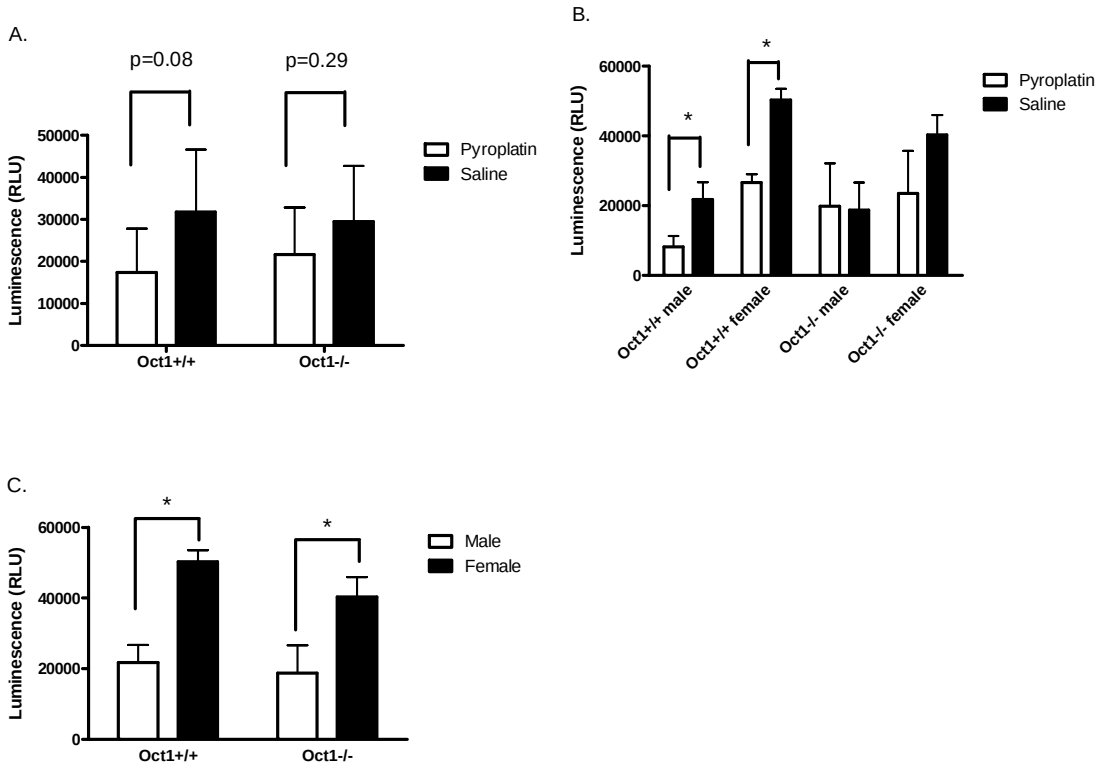

Figure 4.8. Effect of pyroplatin on caspase-3/7 activity in HCC tissues harvested from *Oct1*+/+ and *Oct1*-/- mice. *Oct1*+/+ and *Oct1*-/- mice bearing HCC were treated with a single dose of pyroplatin (50 mg/kg) or saline via tail vein injection. All animals were sacrificed at 24 hours. The HCC tissues were harvested. Caspase-3/7 activity was determined as described in Materials and Methods. (A) caspase-3/7 activity in Oct1+/+ and Oct1-/- mice; (B) caspase-3/7 activity in Oct1+/+ and Oct1-/- mice categorized by sex; (C) Sex difference of caspase-3/7 activity in saline treated mice. Data are presented as the mean ± SD. * $p < 0.05$.

normal liver and HCC induced in *Oct1*+/+ mice indicating that hepatocarcinogenesis does not alter Oct1 expression in the liver of *Oct1*+/+ mice (Figure 4.6).

Oct1 enhanced pyroplatin accumulation in HCC. To prove the concept that Oct1 presented in HCC could lead to increased pyroplatin accumulation, we compared the platinum levels in plasma and in HCC tissues between *Oct1*+/+ and *Oct1*-/- mice bearing HCC after a single dose of pyroplatin. Compared to *Oct1*-/- mice, *Oct1*+/+ mice exhibited significantly reduced pyroplatin concentrations in plasma (*Oct1*+/+ versus *Oct1*-/- mice, 11.6 ± 2.7 μM versus 25.7 ± 7.2 μM; Fig 4.7A; $p < 0.005$), which is consistent with our previous study (refer to Chapter 2). The platinum levels in HCCs harvested from *Oct1*+/+ mice were 1.9-fold greater than that in HCCs from *Oct1*-/- mice (*Oct1*+/+ versus *Oct1*-/- mice, 79.6 ± 11.7 pmol/mg protein versus 42.6 ± 14.5 μM; Fig 4.7B; $p < 0.005$). The difference between *Oct1*+/+ and *Oct1*-/- mice in terms of pyroplatin accumulation in HCC tissues was even greater after normalization with corresponding plasma concentration. HCC tissues from *Oct1*+/+ mice accumulated pyroplatin 4.1-fold greater than that from *Oct1*-/- mice (*Oct1*+/+ versus *Oct1*-/- mice, 7.1 ± 1.2 ml/g protein versus 1.7 ± 0.7 μM; $p < 0.0001$). These results suggest that Oct1 greatly facilitate pyroplatin uptake into the HCCs and set the foundation for further studies.

Necrosis, instead of apoptosis, was more likely to be responsible for cell death secondary to pyroplatin treatment. Many cytotoxic agents have been found to cause cell death through both necrosis and apoptosis. The specific mechanism of death may be related to the concentration, as well as the duration of exposure to the toxic agents. For

example, the induced caspase-3 activities in LLC-PK_1 cells began to decline as the cisplatin concentration was increased beyond 50 μM, which suggests that necrosis, instead of apoptosis, might be responsible for cell death after treatment with higher concentrations of cisplatin [11]. In our current study, we observed no significant differences in caspase-3/7 activity in pyroplatin-treated compared with saline treated *Oct1*+/+ mice (pyroplatin treated versus saline treated, 17400 ± 10400 RLU versus 31800 ± 14800 RLU; Figure 4.8A; $p > 0.05$), though a trend was present. Pyroplatin only resulted in a slight decrease in caspase-3/7 activity in *Oct1-/-* mice (pyroplatin treated versus saline treated, 21600 ± 11200 RLU versus 29500 ± 13300 RLU; Figure 4.8A; $p > 0.05$). However, when caspase-3/7 activity was categorized based on sex, we found that in both *Oct1*+/+ male and *Oct1*+/+ female mice, pyroplatin produced a notable reduction in caspase-3/7 activity compared to saline, the fold differences were 2.7 and 1.9-fold for *Oct1*+/+ male and *Oct1*+/+ female mice, respectively (pyroplatin treated versus saline treated, 8180 ± 3150 RLU versus 21800 ± 4930 RLU for *Oct1*+/+ male mice; 26600 ± 2430 RLU versus 50300 ± 3240 RLU for *Oct1*+/+ female mice Figure 4.8B; $p < 0.05$). There was no significant change in caspase-3/7 activity in either *Oct1-/-* male or female mice (Figure 4.8B; $p > 0.05$). The caspase-3/7 activity was affected by sex. Female mice had significantly higher caspase-3/7activity than male in both *Oct1*+/+ and *Oct1-/-* mice (Figure 4.8C; $p < 0.05$). These results indicate that the Oct1 may play a role in the cell death caused by pyroplatin, and pyroplatin concentration was high enough to induce necrosis, instead of apoptosis, which is the typical mechanism of cytotoxic agent-induced cancer cell death, in HCCs.

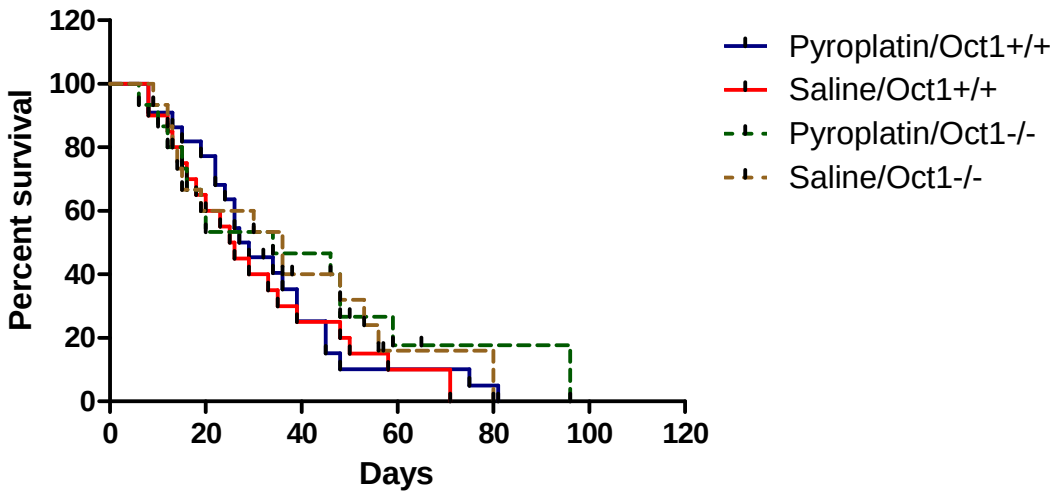

Figure 4.9. Effect of pyroplatin on survival of tumor-bearing mice. *Oct1*+/+ and *Oct1*-/- mice bearing HCC were treated with pyroplatin (50 mg/kg) or saline via tail vein injection. The animals were closely monitored three times a week and sacrificed when moribund; the survival data were recorded and analyzed.

Pyroplatin did not prolong survival of tumor-bearing *Oct1+/+* and *Oct1-/-* mice. To assess whether the increased pyroplatin accumulation in HCCs translated into greater anti-HCC activity in *Oct1+/+* mice, the survival of tumor-bearing mice was compared between the wild-type and knockout mice after administration of pyroplatin or saline. The majority of animals died within 3 months. There was no significant survival advantage in pyroplatin-treated mice over saline treated mice with either *Oct1+/+* or *Oct1-/-* backgrounds (Figure 4.9) suggesting that pyroplatin was not effective in the treatment of HCC at the tested dose. In addition, the survival of pyroplatin-treated *Oct1+/+* mice was not strikingly different from pyroplatin-treated *Oct1-/-* mice (Figure 4.9). The role of Oct1 is moot, since the drug did not produce an anti-cancer effect.

Pyroplatin exhibited lower reactivity with glutathione in comparison to cisplatin and oxaliplatin. The reactions of platinum agents (100 μM) with GSH (6.75 mM) were investigated in 60 mM Tris-NO_3 (pH 7.4) and 4.62 mM NaCl. The reaction mixtures (at 37 °C) and their initial rates (calculated by linear fit of the data from 0 to 2 hr) are shown in Table 4.1. The rank order of the reactivity with GSH was cisplatin > oxaliplatin > picoplatin > pyroplatin. The initial rate of change of absorbance for the reaction of GSH with pyroplatin was 40 fold slower than that with cisplatin ($p < 0.001$), and 8.3 fold slower than that with picoplatin ($p < 0.001$).

Discussion

There were five major findings of the current study: 1. Oct1 was expressed at significant levels in HCC; 2. Mouse and human OCT1 facilitated the accumulation of

Table 4.1. Reactivity of platinum agents with glutathione. The reactions were carried out at 37°C and pH 7.4 with 60 mM Tris-NO_3. The initial rates were calculated from linear fits to the data for 0.5–2.0 h. The significantly low initial rate indicates that pyroplatin interacts poorly with glutathione. *R*, regression coefficient.

Platinum Drug (100 µM)	**[GSH] (mM)**	**[NaCl] (mM)**	**Initial Rate Absorption units / hr**	**R**
Cisplatin	6.75	4.62	0.1759	>0.99
Oxaliplatin	6.75	4.62	0.1364	>0.99
Picoplatin	6.75	4.62	0.0364	>0.99
Pyroplatin	6.75	4.62	0.0044	>0.98

pyroplatin in HCC and in xenografts of HEK293 cells, respectively; 3. Pyroplatin acted by necrosis in HCC; 4. Pyroplatin stimulated caspase-3/7 activity in HCC from *Oct1*+/+ but not *Oct1*-/- mice; and 5. Pyroplatin, as monotherapy, did not prolong survival of mice with HCC.

Currently, platinum-based therapies are widely used in the treatment of a variety of tumors, including testicular cancer, ovarian cancer, small cell lung cancer, and head and neck cancers [12]. In these therapies, cisplatin is often the drug of choice because other platinum agents, such as carboplatin and oxaliplatin, are not superior. However, the issue with cisplatin is its lack of tumor specificity, and therefore its toxicity to normal tissues, especially nephrotoxicity.

Recently, OCT1, OCT2 and OCT3 expression has been observed in several human cancer cell lines [13, 14]. Selective transport by these transporters could possibly contribute to tumor sensitivity/resistance to anticancer agents. For example, the uptake of imatinib, a tyrosine kinase inhibitor effective in the treatment of chronic myeloid leukemia, was mediated by hOCT1 [15] and hOCT1 expression level was a determinant of outcome in imatinib-treated chronic myeloid leukemia [16, 17]. Patients with a high level of hOCT1 had a greater probability of achieving a cytogenetic response and superior progression-free and overall survival [16]. In addition, the superior anticolorectal cancer activity of oxaliplatin over cisplatin has been attributed to its interactions with OCT1 and OCT3 [5, 14], whereas cisplatin, which is poorly transported by OCT1 and OCT3, shows little activity in colorectal cancer [5, 18, 19]. Therefore, we hypothesized

that OCT1 is a key determinant of the therapeutic effects of pyroplatin. More specifically, the abundant expression of OCT1 in liver contributed to its anti-HCC activity.

Expression levels of drug metabolizing enzymes and drug transporters are normally lost in liver cells in culture as a consequence of the adaptation of cells to the *in vitro* environment. Previous reports showed that the expression of OCT1 either decreased or was undetectable in rat HCC cell lines [4, 20]. The expression of OCT1 in human HCC cell lines tested in this study was remarkably low; that is, OCT1 expression was about 10 - 1000 fold lower than its expression in normal liver tissues. Therefore, the HCC cell lines were not considered a good cellular model to determine the role of OCT1 in the cytotoxicity of pyroplatin. When HepG2 and SNU398 cells were transiently transfected with hOCT1, the mRNA of OCT1 was significantly increased compared to the cells without transfection or the cells transfected with empty vector. However, the cytotoxicity of pyroplatin was not remarkably changed, the possible reasons might be due to 1) a trafficking problem such that hOCT1 is not able to localize to the cell plasma membrane and functions as an influx transporter; or 2) a significant deactivation of pyroplatin in the cytoplasm, rendering it inaccessible to the pharmacological target-DNA. Other reasons might be that platinum resistance mechanisms, e.g., DNA repair mechanisms, are active in HCC.

HEK293 cells were chosen for the proof-of-concept *in vivo* xenograft antitumor study because of their modest tumor growth-rates and their well-documented ability to readily express transfected mammalian proteins [21]. In the present study, we demonstrated that OCT1 facilitated pyroplatin accumulation in tumor xenografts and the

increased pyroplatin levels appeared to reduce the rate of tumor growth. However, the tumor growth inhibition was not statistically significant. Pyroplatin has been shown to be cytotoxic to MDCK cells. That is, the IC_{50} value was significantly decreased in MDCK cells that overexpressed hOCT1 (MDCK-MOCK versus MDCK-hOCT1, 709 μM versus 8.09 μM), suggesting OCT1 sensitized these cells to pyroplatin cytotoxicity [3]. The plasma concentration of pyroplatin was greater than 30 μM in mice with both HEK-hOCT1 and HEK-MOCK xenografts, which was much greater than the IC_{50} value of 8.09 μM observed previously in MDCK-hOCT1 cells. It is possibly that HEK-293 cells have lower sensitivity to pyroplatin than MDCK cells, and that free platinum concentrations in the HEK xenografts were not high enough to kill the cells. Pyroplatin has been found to have antitumor activity against Sarcoma 180 ascites at 40 mg/kg and P388 murine leukemia at 80 mg/kg [3]. Therefore, the dose of 50 mg/kg used in our study was considered appropriate. The lack of significant antitumor activity of pyroplatin against HEK-293 xenografts with or without hOCT1 transfection in the present study may indicate that there was a species difference to pyroplatin response. Murine xenografts might be more sensitive to pyroplatin than human-derived xenografts. In addition, HEK-293 is not considered to be a real tumor model physiologically.

It has been reported that ≈ 20% of human HCC may arise through the cooperation of Met and β-catenin. Therefore, the HCC model employed in our study was appropriate for the preclinical testing of therapeutics. Platinum agents, as well as many chemotherapeutic agents, have been recognized to cause cancer cell death through apoptosis. The hallmark of apoptosis is the cleavage of nuclear chromatin by DNases that can be activated by caspase-3. It should be noted that the activity of caspase-3/7 in HCCs

was significantly lower in pyroplatin-treated *Oct1*+/+ male and female mice than saline-treated mice. This result was opposite to what we expected. It suggested that necrosis, instead of apoptosis, was more likely to be responsible for cell death due to pyroplatin treatment in the current study. In *Oct1*-/- mice, the activity of caspase-3/7 was not significantly affected by pyroplatin as observed in *Oct1*+/+ mice. Studies had shown that cisplatin resulted in cell death through both necrosis and apoptosis. The appearance of the specific mechanism was concentration-dependent [11, 22]. Lieberthal et al. [22] found that high concentrations (200- 800 μM) of cisplatin induced necrosis in primary culture of mouse tubular cells, whereas substantially lower concentrations of cisplatin (2-8 μM) induced cell death with the biochemical and morphological features typical of apoptosis. Lau [11] determined the role of caspase-3 in cisplatin-induced renal cell apoptosis and found that the elevation of caspase-3 activity in LLC-PK_1 cells declined as the cisplatin concentration increased beyond 50 μM. Although the plasma concentration of pyroplatin in *Oct1*+/+ mice was lower than in *Oct1*-/- mice, the hepatic platinum level was opposite to the plasma concentration, i.e. *Oct1*+/+ mice had higher pyroplatin accumulated in HCCs than *Oct1*-/- mice. The actual pyroplatin levels in HCCs are likely to determine the mechanisms of cell death induced by pyroplatin. The pyroplatin level of HCC in *Oct1*+/+ mice was high enough to trigger cell death through necrosis, which was reflected by decreased caspase3/7 activity. Together with the lack of change in the activity of caspase-3/7 between pyroplatin treatment and saline treatment in *Oct1*-/- mice, these results indicate that OCT1 regulates the mechanisms of cell death by regulating the pyroplatin concentration in HCC.

Oct1 expression was not altered during hepatocarcinogenesis, which validated the feasibility of the HCC mouse model in different Oct1 backgrounds to assess the role of Oct1 in the anti-HCC activity of pyroplatin. As shown in Chapters 2 and 3, OCT1 contributed to the higher hepatic accumulation of pyroplatin. We also observed that in *Oct1*+/+ mice pyroplatin accumulated in HCC to greater levels than in *Oct1*-/- mice. However, pyroplatin did not prolong survival time of mice bearing HCC in either *Oct1*+/+ or *Oct1*-/- mice. The most likely reasons for its lack of efficacy on survival are that 1) pyroplatin is not potent as a cytotoxic agent, the concentration of pyroplatin in HCCs is not sufficient to kill the tumor cells; 2) there is extensive deactivation of pyroplatin by liver tumor cells, which renders it ineffective in the treatment of HCC; 3) starting time of treatment was not well-controlled due to the difficulty in detecting the appearance of HCC by palpation; the variable starting time of treatment confounded the results; and 4) platinum resistance mechanisms are present in HCC. In the future, new HCC models or tumor detection by quantitative methods, such as ^{13}C labeled magnetic resonance (MR) technique [23], should be further explored.

One of the major mechanisms of resistance to platinum agents is interaction with thiols, which limits the amount of platinum available for binding to DNA. Picoplatin was primarily designed to overcome one of the known mechanisms of platinum resistance: detoxification by binding to intracellular thiols, through the introduction of a bulky methylpyridine ring to provide steric hindrance to direct interaction with platinum [24]. Comparing the reactivity of platinum compounds with GSH, we found that the reactivity of pyroplatin with GSH was even lower than that of picoplatin. So deactivation of

pyroplatin by GSH is minimal compared with other platinum compounds and may not explain the lack of efficacy of pyroplatin in our mouse models of HCC.

Our study demonstrated that OCT1 can control pyroplatin concentrations in tumor tissues. Furthermore, our study has provided a promising direction to currently ineffective HCC treatments. Development of new platinum-based anticancer agents with modification in pyroplatin structure would be an interesting avenue to explore to obtain a clinical candidate with improved safety and efficacy profiles. Platinum analogues with high OCT1 specificity and high potency may be used for targeted therapy of liver cancer. Our study has also provided the basis for personalized therapies with platinum-based compounds. That is, in the future, individuals whose tumors express OCT1 could be prescribed platinum analogs, whereas those with tumors with low OCT1 expression could be given alternative therapies.

References

1. Parkin, D.M., Bray, F., Ferlay, J., and Pisani, P., *Global cancer statistics, 2002.* CA: A Cancer Journal for Clinicians, 2005. **55**(2): p. 74-108.

2. Lau, W.Y. and Lai, E.C.H., *Hepatocellular carcinoma: Current management and recent advances.* Hepatobiliary & Pancreatic Diseases International, 2008. **7**(3): p. 237-257.

3. Lovejoy, K.S., Todd, R.C., Zhang, S.Z., McCormick, M.S., D'Aquino, J.A., Reardon, J.T., Sancar, A., Giacomini, K.M., and Lippard, S.J., *Cis-diammine(pyridine)chloroplatinum(II), a monofunctional platinum(II) antitumor agent: Uptake, structure, function, and prospects.* Proceedings of the National Academy of Sciences of the United States of America, 2008. **105**(26): p. 8902-8907.

4. Lecureur, V., Guillouzo, A., and Fardel, O., *Differential expression of the polyspecific drug transporter OCT1 in rat hepatocarcinoma cells.* Cancer Letters, 1998. **126**(2): p. 227-233.

5. Zhang, S.Z., Lovejoy, K.S., Shima, J.E., Lagpacan, L.L., Shu, Y., Lapuk, A., Chen, Y., Komori, T., Gray, J.W., Chen, X., Lippard, S.J., and Giacomini, K.M., *Organic cation transporters are determinants of oxaliplatin cytotoxicity.* Cancer Research, 2006. **66**(17): p. 8847-8857.

6. Hagrman, D., Goodisman, J., and Souid, A.K., *Kinetic study on the reactions of platinum drugs with glutathione.* Journal of Pharmacology and Experimental Therapeutics, 2004. **308**(2): p. 658-666.

7. Jonker, J.W., Wagenaar, E., Mol, C., Buitelaar, M., Koepsell, H., Smit, J.W., and Schinkel, A.H., *Reduced hepatic uptake and intestinal excretion of organic cations in mice with a targeted disruption of the organic cation transporter 1 (Oct1 [Slc22a1]) gene.* Molecular and Cellular Biology, 2001. **21**(16): p. 5471-5477.

8. Carlson, C.M., Frandsen, J.L., Kirchhof, N., McIvor, R.S., and Largaespada, D.A., *Somatic integration of an oncogene-harboring sleeping beauty transposon models liver tumor development in the mouse.* Proceedings of the National Academy of Sciences of the United States of America, 2005. **102**(47): p. 17059-17064.

9. Tward, A.D., Jones, K.D., Yant, S., Cheung, S.T., Fan, S.T., Chen, X., Kay, M.A., Wang, R., and Bishop, J.M., *Distinct pathways of genomic progression to benign and malignant tumors of the liver.* Proceedings of the National Academy of Sciences of the United States of America, 2007. **104**(37): p. 14771-14776.

10. Liu, D.Y., Li, C.S., Chen, Y.L., Burnett, C., Liu, X.Y., Doens, S., Collins, R.D., and Hawiger, J., *Nuclear import of proinflammatory transcription factors is required for massive liver apoptosis induced by bacterial lipopolysaccharide.* Journal of Biological Chemistry, 2004. **279**(46): p. 48434-48442.

11. Lau, A.H., *Apoptosis induced by cisplatin nephrotoxic injury.* Kidney International, 1999. **56**(4): p. 1295-1298.

12. Lebwohl, D. and Canetta, R., *Clinical development of platinum complexes in cancer therapy: An historical perspective and an update.* European Journal of Cancer, 1998. **34**: p. 1522-1534.

13. Hayer-Zillgen, M., Bruss, M., and Bonisch, H., *Expression and pharmacological profile of the human organic cation transporters hOCT1, hOCT2 and hOCT3.* British Journal of Pharmacology, 2002. **136**(6): p. 829-836.

14. Yokoo, S., Masuda, S., Yonezawa, A., Terada, T., Katsura, T., and Inui, K.I., *Significance of organic cation transporter 3 (SLC22A3) expression for the cytotoxic effect of oxaliplatin in colorectal cancer.* Drug Metabolism and Disposition, 2008. **36**(11): p. 2299-2306.

15. Thomas, J., Wang, L.H., Clark, R.E., and Pirmohamed, M., *Active transport of imatinib into and out of cells: Implications for drug resistance.* Blood, 2004. **104**(12): p. 3739-3745.

16. Wang, L., Giannoudis, A., Lane, S., Williamson, P., Pirmohamed, M., and Clark, R.E., *Expression of the uptake drug transporter hOCT1 is an important clinical determinant of the response to imatinib in chronic myeloid leukemia.* Clinical Pharmacology and Therapeutics, 2007. **83**(2): p. 258-264.

17. White, D.L., Saunders, V.A., Dang, P., Engler, J., Venables, A., Zrim, S., Zannettino, A., Lynch, K., Manley, P.W., and Hughes, T., *Most CML patients who have a suboptimal response to imatinib have low OCT-1 activity: Higher doses of imatinib may overcome the negative impact of low OCT-1 activity.* Blood, 2007. **110**: p. 4064-4072.

18. Yokoo, S., Yonezawa, A., Masuda, S., Fukatsu, A., Katsura, T., and Inui, K.-I., *Differential contribution of organic cation transporters, OCT2 and MATE1, in platinum agent-induced nephrotoxicity.* Biochemical Pharmacology, 2007. **74**(3): p. 477-487.

19. Yonezawa, A., Masuda, S., Yokoo, S., Katsura, T., and Inui, K., *Cisplatin and oxaliplatin, but not carboplatin and nedaplatin, are substrates for human organic cation transporters (SLC22A1-3 and multidrug and toxin extrusion family).* Journal of Pharmacology and Experimental Therapeutics, 2006. **319**(2): p. 879-886.

20. Le Vee, M., Jigorel, E., Glaise, D., Gripon, P., Guguen-Guillouzo, C., and Fardel, O., *Functional expression of sinusoidal and canalicular hepatic drug transporters in the differentiated human hepatoma HepaRG cell line.* European Journal of Pharmaceutical Sciences, 2006. **28**(1-2): p. 109-117.

21. Cheng, J.D., Valianou, M., Canutescu, A.A., Jaffe, E.K., Lee, H.O., Wang, H., Lai, J.H., Bachovchin, W.W., and Weiner, L.M., *Abrogation of fibroblast*

activation protein enzymatic activity attenuates tumor growth. Molecular Cancer Therapeutics, 2005. **4**(3): p. 351-360.

22. Lieberthal, W., Triaca, V., and Levine, J., *Mechanisms of death induced by cisplatin in proximal tubular epithelial cells: Apoptosis vs. Necrosis.* American Journal of Physiology-Renal Physiology, 1996. **270**(4): p. F700-F708.

23. Kohler, S.J., Yen, Y., Wolber, J., Chen, A.P., Albers, M.J., Bok, R., Zhang, V., Tropp, J., Nelson, S., Vigneron, D.B., Kurhanewicz, J., and Hurd, R.E., *In vivo 13 carbon metabolic imaging at 3T with hyperpolarized 13C-1-pyruvate.* Magnetic Resonance in Medicine, 2007. **58**(1): p. 65-69.

24. Holford, J., Sharp, S.Y., Murrer, B.A., Abrams, M., and Kelland, L.R., *In vitro circumvention of cisplatin resistance by the novel sterically hindered platinum complex AMD473.* British Journal of Cancer, 1998. **77**(3): p. 366-373.

CHAPTER 5

ROLE OF OCT1 AND OCT2 IN THE DISPOSITION OF OXALIPLATIN IN MICE

Introduction

Oxaliplatin (*cis*-[(1*R*,2*R*)-1,2-cyclohexanediamine-*N*,*N*′] oxalato (2-)-*O*,*O*′] platinum; Eloxatine) is a platinum coordination complex in the same family as cisplatin and carboplatin. That is, all three platinum compounds share similar mechanisms of action. In particular, their cytotoxicity arises primarily from covalent binding to DNA after aquation to form monoaqua and diaqua complexes [1]. This chemistry initiates a biochemical cascade, eventually leading to cell death [2]. However, oxaliplatin exhibits a different pattern of sensitivity to that of cisplatin in the NCI60-cell human tumor panel and in combination with 5-FU/leucovorin produces response rates twice that of 5-FU/leucovorin regimens alone in the treatment of colorectal cancer, against which cisplatin is inactive [3-5]. Efforts to understand the differences in oxaliplatin versus cisplatin antitumor activity have focused mainly on the difference in DNA-adduct formation and the cellular processing of cisplatin-DNA and oxaliplatin-DNA adducts [6-9]. Oxaliplatin-DNA adducts are bulkier and more hydrophobic than those formed from cisplatin or carboplatin, leading to different effects in the cell [3]; defects in mismatch repair cause moderate resistance to cisplatin but not to oxaliplatin [6]. Recently, the differences in the mechanism(s) controlling cellular uptake and efflux of these platinum compounds have gained attention and are now considered to be one of the major mechanisms of contributing to their disparate activities.

The organic cation transporters (OCT/SLC22A) are considered electrogenic facilitative transporters driven by the chemical gradient and intracellular negative potential. In recent studies we and others demonstrated that oxaliplatin (but not cisplatin or carboplatin) is a substrate of OCTs using human colorectal cancer-derived cell lines and genetically engineered immortal cell lines, in which hOCTs were overexpressed [10, 11]. The studies also demonstrated that OCTs were highly expressed in colorectal cancer cell lines and tumor samples suggesting that the interactions with OCTs are likely to be important contributors to the sensitivity of colorectal cancer to oxaliplatin [10, 11]. Further, OCTs may play a role in the toxicity of oxaliplatin. The most common adverse effects associated with oxaliplatin are neuropathy, hematological toxicity and GI toxicity [12]. Recently, use of oxaliplatin has been associated with development of hepatic lesions, which include sinusoidal alteration, portal hypertension, increase in transaminases, gammaglutamyl transpeptidase and alkaline phosphatase, and steatohepatitis [13, 14]. Since the development of liver injuries may limit the ability to perform an extensive hepatectomy and can contribute to postoperative patient morbidity and mortality, hepatic toxicity presents major problems for optimal use of oxaliplatin. Because of its high expression in the liver, OCT1 may contribute to the hepatotoxicity of oxaliplatin. Moreover, OCT2, which is expressed at high levels in the kidney, may contribute to its renal elimination and therefore, to dose-dependent toxicities.

The major goals of the present study were to determine the role of Oct1 and Oct2 in the disposition of oxaliplatin using genetically engineered mouse models. Our experiments suggest that Oct1 and Oct2 have slight effects on the disposition of oxaliplatin; Oct1 deletion mainly affected the distribution phase of oxaliplatin, whereas

Oct1 and Oct2 double deletion mainly affected the terminal elimination phase of oxaliplatin. Although Oct1 enhanced the hepatic accumulation after multiple dosing, the increase hepatic platinum levels did not result in obvious liver toxicity.

Materials and Methods

Drugs and reagents. Oxaliplatin was purchased from Sigma (St. Louis, MO). Solutions of oxaliplatin (5 mmol/L) were freshly prepared in saline or PBS. The stock solutions were stored frozen at -20^{o}C and discarded after one month of preparation. The cell culture media DMEM, William's E, and heat inactivated fetal bovine serum (FBS), ITS and L-glutamine were purchased from the Cell Culture Facility of the University of California, San Francisco (San Francisco, CA).

Cell lines and culture. Human embryonic kidney (HEK) 293 cells stably transfected with the full length reference human OCT1 cDNA (HEK-hOCT1), OCT2 cDNA (HEK-hOCT2), mutant OCT1 and OCT2 cDNA inserts and with the empty vector (HEK-MOCK) were established previously in our laboratory [10, 14]. The culture medium for stably transfected cells is DMEM H21 medium supplemented with 10% FBS, 100 units/ml penicillin and 100 µg/ml streptomycin and 60 µg/ml hygromycin B. All cell lines were grown at 37 °C in a humidified atmosphere with 5% CO_2.

Cellular accumulation of platinum. The cellular accumulation of platinum was determined as described previously [10] with some modifications. Briefly, the cells were incubated in the serum-free culture medium containing the indicated platinum compounds with or without a specific inhibitor at 37^{o}C in 5% CO_2 for 1 hour. After

incubation, cells were washed with ice-cold PBS three times. Then the cells were dissolved in 100 µl of 70% nitric acid at 65°C for at least 2.5 hours. Distilled water containing 10 ppb of iridium (Sigma) and 0.1% Triton X-100 was added to the samples to dilute nitric acid to 7%. The platinum content was measured by inductively coupled plasma mass spectrometry (ICP-MS) in the Analytical Facility at the University of California at Santa Cruz (Santa Cruz, CA). Cell lysates from a set of identical cultures were used for BCA protein assay. Cellular platinum accumulation was normalized to the protein content.

Intracellular accumulation of oxaliplatin in primary hepatocytes. Primary hepatocytes were isolated from *Oct1*+/+ and *Oct1*-/- mice by the UCSF Liver Center using a standard collagenase method [15]. The intracellular accumulation of platinum was determined after exposure to oxaliplatin as described previously [10] with some modifications. Briefly, the freshly isolated hepatocytes were incubated in suspension (1.5 x 10^5 cells/tube) in serum-free William's E culture medium containing different concentrations of oxaliplatin at 37°C in 5% CO_2 for different times. During the incubation, the tubes were mixed several times by gentle vortex. After incubation, cells were washed three times with ice-cold PBS. The cell pellets were dissolved in 100 µl of 70% nitric acid at 65°C for at least 2.5 hours. Distilled water containing 10 ppb of iridium (Sigma) and 0.1% Triton X-100 was added to the samples to dilute nitric acid to 7%. The platinum content was measured by ICP-MS. Cellular platinum accumulation was normalized to the protein content from a set of identical cultures.

Animals. *Oct1-/-* and *Oct1/2-/-*mice were generated as described elsewhere [14, 16, 17]. The animals used in all experiments were in FVB background and were age-matched *Oct1-/-* , *Oct1/2-/-* and *Oct1+/+* (wild-type) mice between 8-10 weeks of age. All animals were housed in a virus-free, temperature-controlled facility on a 12-h light–dark cycle. They were allowed standard mouse food and water *ad libitum*. All experiments on mice were approved by the Institutional Animal Care and Use Committee of University of California at San Francisco.

Tissue accumulation study of oxaliplatin in mice: Eight week old mice (wild-type, *Oct1-/-*, and *Oct1/2 -/-)* were given oxaliplatin (6 mg/kg) in saline via tail vein injection. The animals were sacrificed at different time points after oxaliplatin treatment. Blood samples were collected by heart puncture and transferred into heparinized BD vacutainer blood collection tubes. Blood was centrifuged for 30 min at 1000 x g and the plasma was decanted and frozen at -80^{o}C. Tissues (liver, kidney, heart, lung, intestine, spleen and muscle) were collected as quickly as possible and snap frozen in liquid nitrogen. Bone marrow was isolated from femur bone using 1 ml of 10% BSA and frozen at -80^{o}C until analysis.

Total platinum content in plasma and various tissues. Plasma, bone marrow and tissue powders were dissolved in 70% nitric acid and incubated at 65°C for at least 2.5 hours. Distilled water containing 10 ppb of iridium (Sigma) and 0.1% Triton X-100 was added to the samples to dilute nitric acid to 7%. 5 µl of plasma, bone marrow and about 10-30 mg of tissue powders were used for total platinum measurement by ICP-MS.

Platinum-DNA adduct formation in various tissues. The platinum content associated with genomic DNA in various tissues was determined as described previously [10] with some modifications. Briefly, genomic DNA was isolated from the tissues harvested from tissue accumulation study using Wizard Genomic DNA Purification kit (Promega, Madison, WI) according to the manufacturer's protocol. The DNA-bound platinum was determined by ICP-MS. The DNA content from the same DNA preparation was measured by absorption spectroscopy at 260 nm. Platinum-DNA adduct level was normalized to total DNA content.

Pharmacokinetics study of oxaliplatin in mice: Eight weeks old mice (wild-type, *Oct1-/-*, and *Oct1/2 -/-)* were administered oxaliplatin (8 mg/kg) in saline via tail vein injection and placed in metabolic cages for 24 hrs. Blood samples (20 µl) were collected at different time points by tail vein bleeding into heparinized micro-hematocrit capillary tubes (Fisher, Pittsburg, PA). Blood was centrifuged for 5 min using Microhematocrit Centrifuge (Thermo Fisher Scientific Inc. Waltham, MA) and the plasma was decanted and frozen at -80^{o}C until analysis. An aliquot of plasma was diluted with PBS and filtered through a Millipore multiscreen filter plate with Ultracel-10 membrane containing a 10kDa cutoff filter by centrifugation at 2000 x g for 30 minutes at 4 ^{o}C. The plasma ultrafiltrates (PUF) were stored at -80 ^{o}C until analysis. Urine was collected from tubes attached to the cages. Tissues (liver, kidney, intestine, muscle) were collected as quickly as possible upon the last time point and snap frozen in liquid nitrogen. Plasma, PUF, urine and tissue powder were dissolved in 70% nitric acid and incubated at 65°C for at least 2.5 hours. Distilled water containing 10 ppb of iridium (Sigma) and 0.1% Triton X-100 was added to the samples to dilute nitric acid to 7%. 5 µl

of plasma, PUF, urine and about 10-30 mg of tissue powders were used for total platinum measurement by ICP-MS. The pharmacokinetics parameters were obtained by two-compartmental analysis using WinNonlin 4.0 (Pharsight Corporation, Mountain view, CA).

Toxicity study. Eight weeks old *Oct1-/-* and *Oct1+/+* mice were randomized and treated with saline or oxaliplatin (6 mg/kg) via tail vein injection once daily for a total of five days (n = 5 animals per group). The animals were closely monitored and sacrificed at the onset of moribundity. Body weight was monitored and recorded daily. All surviving animals were sacrificed 24 hours after the last treatment. On the day of the terminal sacrifice, the animals were anesthetized with isoflurane, and blood (500 – 1000 µl) was collected by heart puncture and centrifuged for 30 min at 1000 X g at 4^{o}C. The serum was decanted and frozen at -80^{o}C until analysis. Tissues (liver, kidney, intestine, and muscle) were collected and divided into two halves; one half of the tissues were fixed in 4% paraformaldehyde for histopathology examination, the other half of the tissues were snap frozen in liquid nitrogen.

Clinical chemistry evaluation. Alanine transaminase (ALT), aspartate transaminase (AST), alkaline phosphatase (ALP) in serum were measured by the Clinical Laboratory of the San Francisco General Hospital.

Histopathological examination. The liver tissues fixed in 4% paraformaldehyde were embedded in paraffin, cut into thin sections and mounted on glass slides. The tissue sections were stained with hematoxylin and eosin for microscopic examination.

Plasma and tissue platinum measurement. Plasma and tissue powder were dissolved in 70% nitric acid and incubated at 65°C for at least 2.5 hours. Distilled water containing 10 ppb of iridium (Sigma) and 0.1% Triton X-100 was added to the samples to dilute nitric acid to 7%. 5 μl of plasma and about 10-30 mg of tissue powders were used for total platinum measurement by ICP-MS.

Statistical analysis. Unless specified, data are expressed as mean ± standard deviation (SD). Data were analyzed statistically using the unpaired Student's t test. Multiple comparisons were performed with Dunnett's two-tailed test after one-way ANOVA. A P value of less than 0.05 was considered statistically significant.

Results

Polymorphisms of OCT1 and OCT2 were associated with different rates of intracellular accumulation of oxaliplatin. Previously, we and others showed that human OCT1 is a highly polymorphic gene [18-20]. Several OCT1substrates have been shown to have altered uptake in the OCT1 variants, such as metformin, MPP+ and paraquat [14, 21]. To determine whether OCT1 polymorphisms modulate the uptake, we measured the intracellular total platinum in stable cells expressing empty vector, OCT1-reference and twelve OCT1 variants (Figure 1A). Compared to OCT1-reference, seven out of twelve OCT1 variants exhibited significantly reduced oxaliplatin uptake ($p < 0.005$; Figure 1A), of which five are common in human populations with allele frequencies >= 1%. For example, the allele frequencies of OCT1-420del are 19% and 5% in Caucasians and African Americans, respectively.

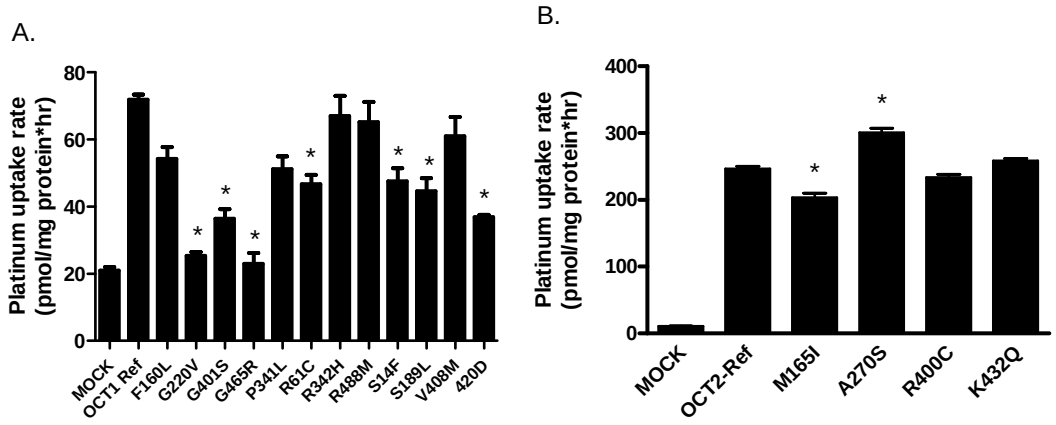

Figure 5.1. Genetic variants of OCT1 and OCT2 were associated with different intracellular uptake rates of oxaliplatin in stably transfected HEK293 cells.

Intracellular platinum accumulation rates in cell lines stably expressing human OCT1 and its variants (A) and cell lines stably expressing human OCT2 and its variants (B) were determined as described in Materials and Methods. Briefly, the cells were incubated with oxaliplatin (10 μM) at 37^{o}C and 5% CO_2 for 2 hours. Total platinum concentration inside the cells was determined using ICP-MS. Total platinum concentration was normalized to the protein content. Data are presented as the mean ± SD (n = 3). * $P < 0.005$.

Leabman et al. functionally characterized four non-synonymous cSNPs of OCT2 (M165I, A270S, R400C and K432Q) that have ethnic-specific allele frequencies >= 1% and found the these genetic variants had altered transporter activity when assayed in Xenopus laevis oocytes [22]. In our current study, we determined the intracellular accumulation rate of oxaliplatin in these four genetic variants. Compared to hOCT2-reference, M165I variant had significantly decreased uptake. However, A270S exhibited significantly increased uptake ($p < 0.001$; Figure 1B), which was consistent with the study result for metformin [23].

Effect of Oct1 on the intracellular accumulation rate of oxaliplatin in primary mouse hepatocytes. Since the isolation procedure and subsequent cell culture significantly decreased the expression of Oct1 in primary hepatocytes as indicated by our unpublished data, cells in suspension instead of attached cells were used to examine the role of Oct1 in the cellular platinum accumulation rate after exposure to oxaliplatin in an attempt to minimize the loss of Oct1 expression. As shown in Figure 5.2, the intracellular accumulation rate of oxaliplatin increased proportionally with increasing concentrations of oxaliplatin in hepatocytes isolated from both *Oct1*+/+ and *Oct1*-/- mice. In all hepatocytes isolated from *Oct1*+/+ and *Oct1*-/- mice, the accumulation rate of oxaliplatin was similar between 30 minute exposure and 120 minute exposure. Compared to hepatocytes isolated from *Oct1*-/- mice, hepatocytes isolated from *Oct1*+/+ mice had significantly higher platinum accumulation rates after incubation with 1 μM and 5 μM of oxaliplatin for 30 minutes and 120 minutes. The hepatocellular accumulation rate of oxaliplatin after 30 minute exposure in hepatocytes from *Oct1* wild-type mice (1 μM versus 5 μM, 1.54 ± 0.30 pmol/mg protein/hr versus 5.55 ± 0.38 pmol/mg protein/hr) was

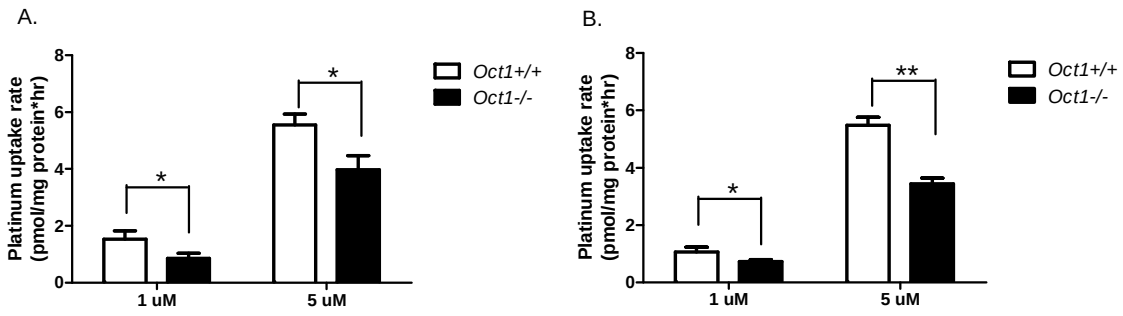

Figure 5.2. Effect of Oct1 on the intracellular accumulation rate of oxaliplatin in primary mouse hepatocytes. Intracellular platinum accumulation rates in hepatocytes from *Oct1* wild-type and *Oct1-/-* mice after 30 minute (A) and 120 minute (B) exposure to 1 µM and 5 µM of oxaliplatin were determined as described in Materials and Methods. Briefly, freshly isolated hepatocytes from *Oct1* wild-type and *Oct1-/-* mice were suspended and incubated in serum-free William's E medium containing different concentrations of oxaliplatin at 37^{o}C and 5% CO_2 for 30 minutes or 120 minutes. Total platinum concentration inside the cells was determined using ICP-MS. Total platinum concentration was normalized to the protein content. Data are presented as the mean ± SD (n = 3). * $P < 0.05$, ** $P < 0.005$.

1.8-fold and 1.4-fold that in hepatocytes from *Oct1* -/- mice (1 μM versus 5 μM, 0.86 ± 0.18 pmol/mg protein/hr versus 3.97 ± 0.50 pmol/mg protein/hr), respectively ($p < 0.05$; Figure 5.2A). The hepatocellular accumulation rate of oxaliplatin after 120 minute exposure in hepatocytes from *Oct1* wild-type mice (1 μM versus 5 μM, 1.06 ± 0.17 pmol/mg protein/hr versus 5.48 ± 0.28 pmol/mg protein/hr) was 1.5-fold and 1.6-fold that in hepatocytes from *Oct1* -/- mice (1 μM versus 5 μM, 0.72 ± 0.07 pmol/mg protein/hr versus 3.44 ± 0.20 pmol/mg protein/hr), respectively ($p < 0.05$; Figure 5.2B). These data indicate that Oct1 is likely to play a role in facilitating oxaliplatin across hepatocytes, however, the extent of the effect is not as great as it played in pyroplatin uptake (refer to Chapter 2).

Effect of *Oct1* deletion on mouse pharmacokinetics of oxaliplatin. Consistent with the previous reports of oxaliplatin pharmacokinetics following a single bolus intravenous dose in rodents[24, 25], the concentration versus time course of total platinum following i.v. administration of oxaliplatin (8 mg/kg) exhibited a biexponential decline in both *Oct1* wild-type and *Oct1*-/- mice (Figure 5.3). Though similar, the plasma concentrations of platinum tended to be slightly higher in *Oct1*-/- mice than in *Oct1*+/+ mice. This was most obvious at the distribution phase (0 - 0.5 hr) of oxaliplatin. The pharmacokinetics parameters were not statistically significantly different between *Oct1*+/+ and *Oct1*-/- mice as shown in Table 5.1. The clearance and volume of distribution in both *Oct1*+/+ and *Oct1*-/- mice were similar to that reported in BD2F1 mice [24].

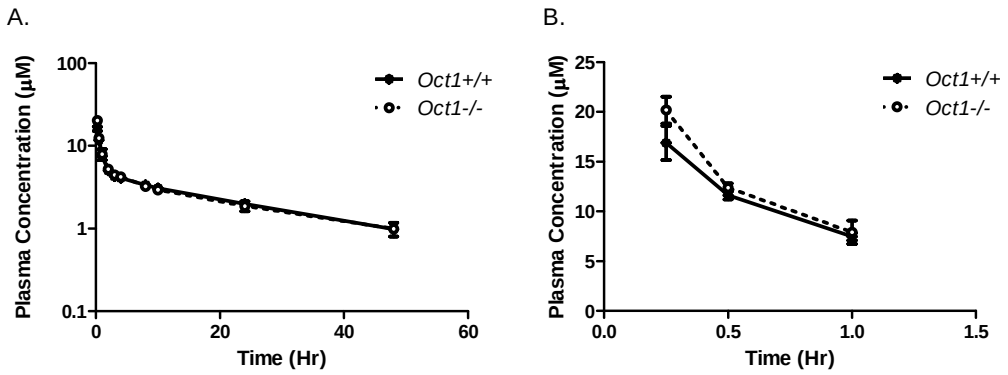

Figure 5.3. Pharmacokinetics of total platinum levels in *Oct1*+/+ and *Oct1*-/- mice after i.v. bolus dose of oxaliplatin. The mice (n = 3 per group) were treated with oxaliplatin (8 mg/kg) by tail vein injection. Blood samples (20 µl) were collected at 15, 30 min, 1, 2, 3, 4, 8, 10, 24, 48 hr after oxaliplatin treatment by tail vein bleeding and immediately spun at 1000 x g for 30 min. Platinum levels in plasma were determined by ICP-MS. (A) The plasma concentration –time curve from 0 to 48 hours; (B) the plasma concentration-time curve for the first one hour after oxaliplatin administration. Data are presented as the mean ± SD (n = 3).

Table 5.1. Plasma platinum pharmacokinetic parameters following a single intravenous dose of oxaliplatin (8 mg/kg) in *Oct1+/+* and *Oct1-/-*mice (3 per group). Blood samples for pharmacokinetic analysis were drawn up to 48 hours. The pharmacokinetic parameters were obtained by two compartmental analysis using WinNonlin 4.0.

	Oct1WT	*Oct1KO*		
	Mean ± SD	Mean ± SD	*Oct1KO/ Oct1WT*	P value
AUC_{0-48} (μM*hr)	118.7±4.4	118.5±7.7	1.00	> 0.05
AUC_{inf} (μM*hr)	146.5 ±5.9	143.8 ±16.0	0.98	> 0.05
CL (ml/min*kg)	2.29 ±0.09	2.35 ±0.27	1.03	> 0.05
CL_R(ml/min*kg)	0.76 ±0.36	1.09 ±0.58	1.43	> 0.05
V_{SS} (L/kg)	3.80 ±0.10	3.56 ±0.17	0.94	> 0.05
C_{max} (uM)	23.9 ±3.4	30.4 ±4.4	1.28	> 0.05
$T_{1/2,\alpha}$ (hr)	0.37 ±0.04	0.33 ±0.08	0.89	> 0.05
$T_{1/2,\beta}$ (hr)	20.6 ±0.8	19.2 ±2.4	0.93	> 0.05

Note: $T_{1/2,\alpha}$: distribution half life; $T_{1/2,\beta}$: terminal half life; C_{max}: maximal plasma concentration; AUC_{inf}: area under the curve of plasma concentration from time 0 to infinity; V_{SS}: volume of distribution at steady state; CL: clearance; CL_R: renal clearance. *Oct1 KO: Oct1-/-; Oct1 WT: Oct1+/+*.

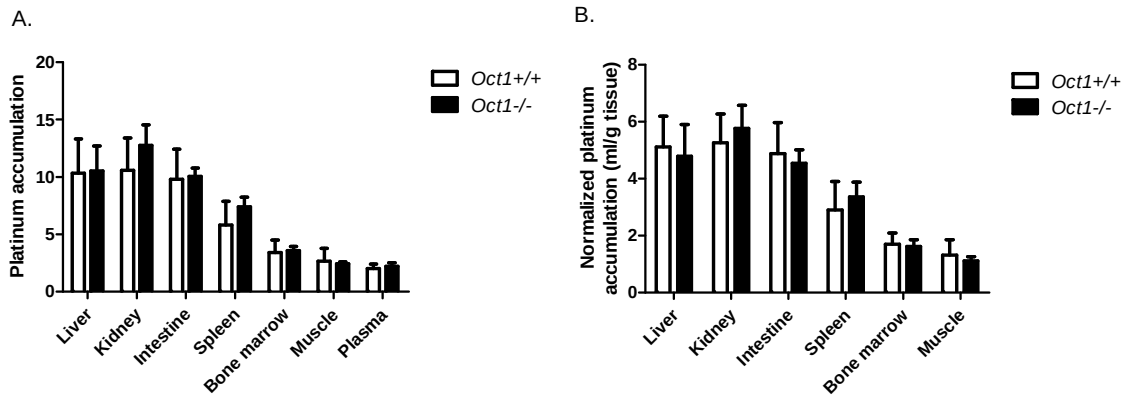

Figure 5.4. Tissue accumulation of total platinum in *Oct1*+/+ and *Oct1*-/- mice six hours after dosing of oxaliplatin. (A) Absolute platinum accumulation levels, and (B) normalized platinum accumulation levels in various tissues were measured six hours post dosing in *Oct1* wild-type and *Oct1*-/- mice. Briefly, the mice (at least 7 mice each group) were given 6 mg/kg of oxaliplatin in PBS via tail vain. Blood, liver, intestine, kidney, spleen, bone marrow and muscle were harvested six hour post dosing. Plasma was isolated from whole blood by centrifugation at 1000 x g for 30 min. Bone marrow was isolated by flushing femur bone with 1ml of 10% BSA. The unit of absolute platinum accumulation for all tissues except bone marrow is nmol/gram tissue, the unit for bone marrow and plasma is μM. The platinum levels in plasma and various tissues were determined using ICP-MS. Data are presented as the mean ± SD ($n \geq 7$).

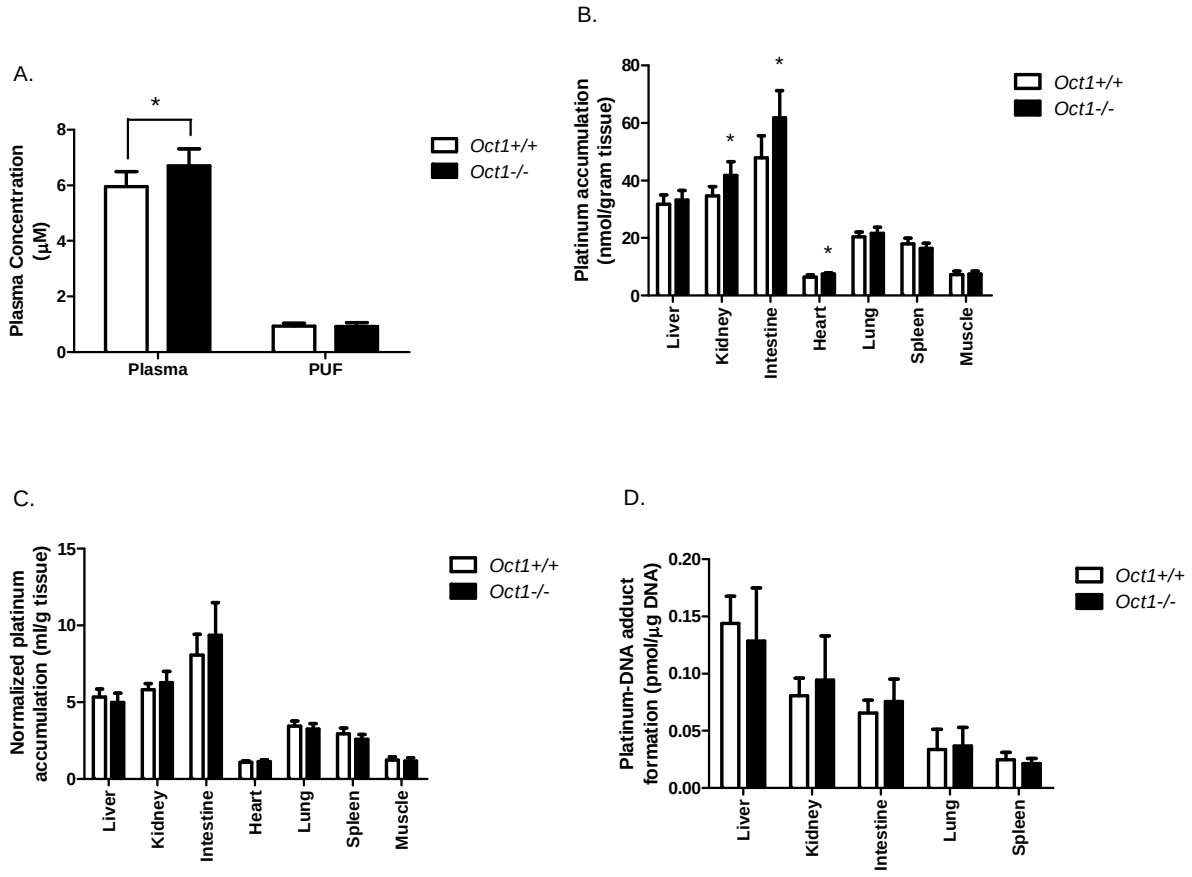

Figure 5.5. Tissue accumulation of total platinum in *Oct1*+/+ and *Oct1*-/- mice one hour after intravenous dosing of oxaliplatin. (A) Platinum accumulation levels in plasma and plasma ultrafiltrate matrix (PUF), (B) absolute platinum accumulation levels, (C) normalized platinum accumulation levels and (D) platinum-DNA adduct formation in various tissues were measured one hour post dosing in *Oct1* wild-type and *Oct1*-/- mice. Briefly, the mice (n = 8 per group) were given 10 mg/kg of oxaliplatin in PBS via tail vein. Blood, liver, intestine, kidney, heart, lung, spleen and muscle were harvested one hour post dosing. Plasma, PUF and genomic DNA were prepared as described in Materials and Methods. The platinum levels in plasma and various tissues and DNA-bound platinum were determined using ICP-MS. Data are presented as the mean ± SD (n = 8). * $P < 0.05$.

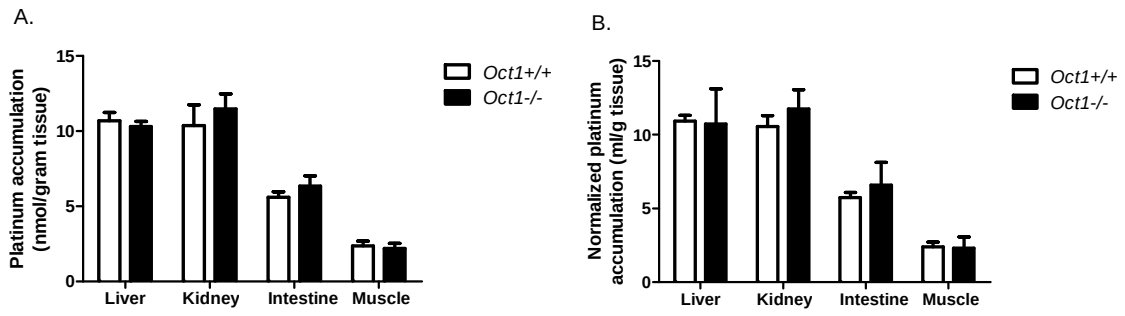

Figure 5.6. Tissue accumulation of total platinum in *Oct1*+/+ and *Oct1*-/- mice 48 hours after intravenous dosing of oxaliplatin. (A) Absolute platinum accumulation levels, and (B) normalized platinum accumulation levels in various tissues were measured 48 hours post dosing in *Oct1* wild-type and *Oct1*-/- mice. Briefly, the mice (n = 3 per group) were given 8 mg/kg of oxaliplatin in PBS via tail vein. Liver, intestine, kidney and muscle were harvested at the end of pharmacokinetics study (48 hours post dosing). The platinum levels in various tissues were determined using ICP-MS. The platinum levels in various organs were normalized to the plasma concentration of platinum at 48 hr. Data are presented as the mean ± SD (n = 3).

Effect of *Oct1* deletion on tissue accumulation of oxaliplatin was time-dependent in mice. The effect of OCT1 on the tissue distribution of oxaliplatin was first examined six hours after intravenous dosing of oxaliplatin. The absolute platinum levels (Figure 5.4A) and the platinum levels normalized to plasma platinum concentrations (Figure 5.4B) in various tissues including liver, kidney, intestine, spleen, bone marrow and muscle showed no significant difference between *Oct1*+/+ and *Oct1*-/- mice ($p > 0.05$). The effect of Oct1 on the tissue distribution of oxaliplatin was reexamined after a shorter treatment duration. After one hour treatment with oxaliplatin, the plasma concentration of oxaliplatin in *Oct1*+/+ was slightly but significantly lower than that in *Oct1*-/- mice (*Oct1*+/+ versus *Oct1*-/-, 5.96 ± 0.54 µM versus 6.69 ± 0.62 µM; $p < 0.05$; Figure 5.5A). However, the platinum concentration in plasma ultrafiltrate (PUF) was not significantly different between *Oct1*+/+ mice and *Oct1*-/- mice ($p > 0.05$; Figure 5.5A). Consistent with the previous tissue accumulation study of pyroplatin (refer to Chapter 2), we observed that the absolute oxaliplatin levels in kidney and heart in *Oct1*-/- mice were significantly higher than that in *Oct1*+/+ mice (Figure 5.5B; $p < 0.05$). In contrast to pyroplatin, oxaliplatin accumulated significantly higher in intestine of *Oct1*-/- mice than in *Oct1*+/+ mice. No difference in absolute accumulation of oxaliplatin was observed in other tissues one hour post dosing. After normalization with corresponding plasma concentrations, the differences in renal, cardiac, and intestinal accumulation between *Oct1*+/+ and *Oct1*-/- mice were not observed. The platinum-DNA adduct formation in liver, kidney, intestine, lung and spleen was not significantly different between *Oct1*+/+ and *Oct1*-/- mice (Figure 5.5D; $p > 0.05$).

Platinum levels in various tissues were also measured at the end of the pharmacokinetic study, i.e. 48 hours post dosing. We observed that the absolute platinum accumulation levels and the normalized platinum accumulation levels in all tissues harvested 48 hr post dosing were not significantly different between *Oct1+/+* and *Oct1-/-* mice ($p > 0.05$; Figure 5.6). Collectively, these data indicate that Oct1 does not play a substantial role in the disposition of oxaliplatin *in vivo.*

Effect of *Oct1* and *Oct2* double deletion on the pharmacokinetics of total platinum and ultrafilterable platinum after oxaliplatin administration. Previously, we showed that Oct2 expression in various tissues was increased in *Oct1-/-* mice (refer to Chapter 2). This increase in expression level may be one explanation for the lack of effect of Oct1 deletion on the pharmacokinetics and tissue accumulation of oxaliplatin in mice. To further determine the role of Octs in the disposition of oxaliplatin, we characterized the pharmacokinetic profile of oxaliplatin in *Oct1/2-/-* mice. The Oct1/2 double deletion had a small but significant effect on the pharmacokinetics of total platinum following an i.v. dose of oxaliplatin (Figure 5.7). Though no differences in plasma platinum concentrations at early time points were observed, from 4 hr after dosing, plasma platinum concentrations were significantly higher in *Oct1/2-/-* mice than in *Oct* WT mice at all time points except 10 hr ($p < 0.05$). As shown in Table 5.2, the *Oct1/2-/-* mice had a significantly greater total platinum AUC_{inf} than the Oct WT mice (*Oct1/2-/-* versus *Oct* WT, 193.4 ± 13.4 µM versus 164.1 ± 5.6 µM; $p = 0.025$) with a significantly lower clearance (*Oct1/2-/-* versus *Oct* WT, 2.05 ± 0.13 ml/min/kg versus 2.42 ± 0.08 ml/min/kg, $p = 0.013$). There was no difference in the maximal plasma concentration (C_{max}), the volume of distribution at steady state (Vss) and the distribution half-life ($T_{1/2,\alpha}$) between

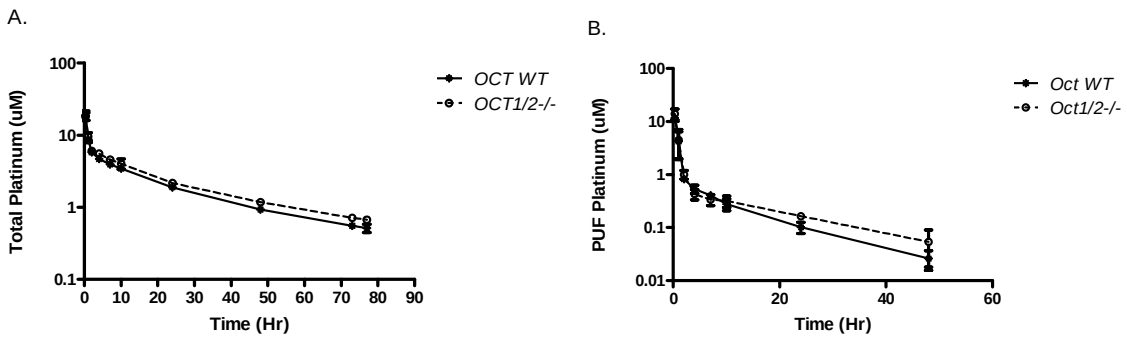

Figure 5.7. Pharmacokinetics of platinum in *Oct WT* and *Oct1/2-/-* mice after intravenous administration of oxaliplatin. (A) Total platinum concentrations in plasma, (B) platinum in plasma ultrafiltrate (PUF). The mice (n = 3 per group) were treated with oxaliplatin (10 mg/kg) by tail vein injection. Blood samples (20 µl) were collected at 30 min, 1, 2, 3, 4, 7, 10, 24, 48, 73 and 77 hr after oxaliplatin treatment by tail vein bleeding and immediately spun at 1000 x g for 30 min. Diluted plasma was filtered through a Millipore multiscreen filter plate with ultracel-10 membrane containing a 10 kDa cutoff filter and centrifuged at 2000 x g for 30 minutes to obtain PUF sample. Platinum levels in plasma and PUF were determined by ICP-MS. Data are presented as the mean ± SD (n =3).

Table 5.2. Plasma platinum pharmacokinetic parameters following a single intravenous dose of oxaliplatin (10 mg/kg) in *Oct WT* and *Oct1/2-/-* mice (3 per group). Blood samples for pharmacokinetic analysis were drawn up to 77 hours. The pharmacokinetic parameters were obtained by two compartmental analysis using WinNonlin 4.0.

	Oct WT	*Oct1/2 KO*		
	Mean ± SD	Mean ± SD	*Oct1/2 KO/Oct WT*	P value
AUC_{inf} (μM*hr)	164.1 ± 5.6	193.4 ± 13.4	1.18	0.025
C_{max} (μM)	28.3 ± 5.3	26.4 ± 4.5	0.93	0.665
CL (ml/min*kg)	2.42 ± 0.08	2.05 ± 0.13	0.85	0.013
V_{SS} (L/kg)	4.26 ± 0.19	3.94 ± 0.30	0.92	0.192
$T_{1/2,\alpha}$ (hr)	0.41 ± 0.06	0.44± 0.11	1.08	0.676
$T_{1/2,\beta}$ (hr)	20.9 ± 0.9	22.3 ± 0.2	1.07	0.057
MRT (hr)	27.7 ± 1.5	30.1 ± 0.4	1.09	0.059

Note: $T_{1/2,\alpha}$: distribution half life; $T_{1/2,\beta}$: terminal half life; C_{max}: maximal plasma concentration; AUC_{inf}: area under the curve of plasma concentration from time 0 to infinity; V_{SS}: volume of distribution at steady state; CL: clearance; MRT: mean residence time. *Oct1/2 KO: Oct1/2-/-*.

Table 5.3. Pharmacokinetic parameters of platinum in plasma ultrafiltrate of *Oct WT* and *Oct1/2-/-* mice following a single intravenous dose of oxaliplatin (10 mg/kg). Blood samples for pharmacokinetic analysis were drawn up to 77 hours. The PUF samples were prepared from plasma samples up to 48 hours. The pharmacokinetic parameters were obtained by two compartmental analysis using WinNonlin 4.0.

	Oct WT	*Oct1/2 KO*		
	Mean ± SD	Mean ± SD	*Oct1/2 KO/Oct WT*	P value
AUC_{inf} (μM*hr)	19.0 ± 2.6	22.4 ± 5.1	1.18	0.359
C_{max} (μM)	21.3 ± 4.2	24.6 ± 5.2	1.15	0.445
CL (ml/min*kg)	22.5 ± 2.8	18.9 ± 4.3	0.84	0.302
V_{SS} (L/kg)	8.76 ± 0.48	10.0 ± 2.1	1.14	0.368
$T_{1/2,\alpha}$ (hr)	0.36 ± 0.10	0.37 ± 0.07	1.02	0.908
$T_{1/2,\beta}$ (hr)	9.98 ± 2.52	13.4 ± 1.4	1.34	0.115
MRT (hr)	6.60 ± 1.01	8.62 ± 0.08	1.31	0.026

Note: $T_{1/2,\alpha}$: distribution half life; $T_{1/2,\beta}$: terminal half life; C_{max}: maximal plasma concentration; AUC_{inf}: area under the curve of plasma concentration from time 0 to infinity; V_{SS}: volume of distribution at steady state; CL: clearance; MRT: mean residence time. *Oct1/2 KO: Oct1/2-/-*.

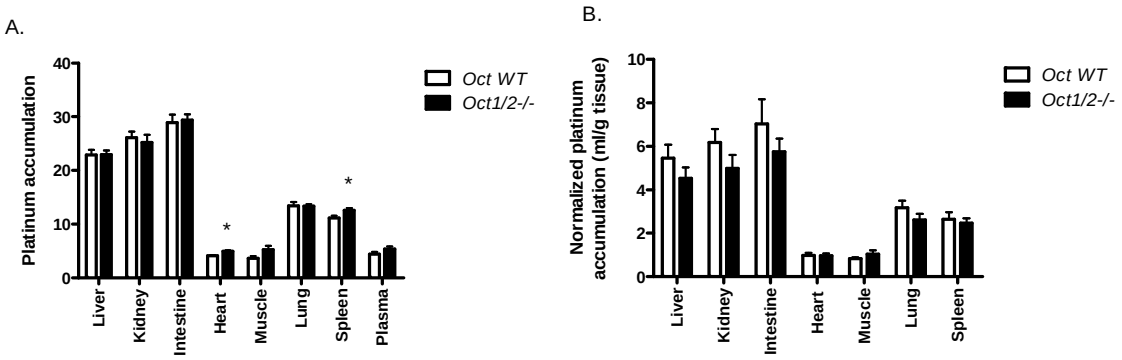

Figure 5.8. Tissue accumulation of total platinum in *Oct WT* and *Oct1/2-/-* mice one hour after intravenous dosing of oxaliplatin. (A) Absolute platinum accumulation levels and (B) normalized platinum accumulation levels in various tissues were measured one hour post dosing in *Oct WT* and *Oct1/2-/-* mice. Briefly, the mice (n = 6 per group) were given 10 mg/kg of oxaliplatin in PBS via tail vein. Blood, liver, intestine, kidney, heart, lung, spleen and muscle were harvested one hour post dosing. Plasma was isolated from whole blood by centrifugation at 1000 x g for 30 min. The unit for absolute platinum levels in various tissues is nmol/gram tissue, the unit for plasma is μM. The platinum levels in plasma and various tissues were determined using ICP-MS. Data are presented as the mean ± SD (n = 6). * $P < 0.05$.

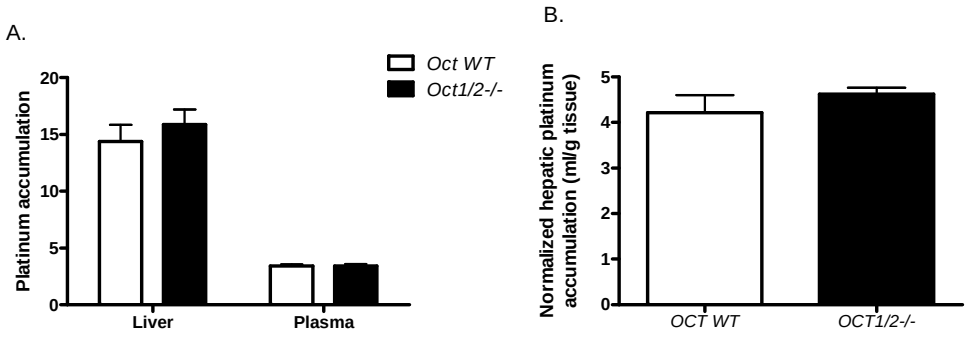

Figure 5.9. Effect of liver perfusion on the hepatic accumulation of total platinum in *Oct WT* and *Oct1/2-/-* mice one hour after intravenous dosing of oxaliplatin. (A) Absolute platinum accumulation levels in liver and plasma and (B) normalized hepatic platinum accumulation levels were measured one hour post dosing in *Oct1 wild-type* and *Oct1/2-/-* mice. Briefly, the mice (n = 3 per group) were given 10 mg/kg of oxaliplatin in PBS via tail vein. Blood was collected by heart puncture and liver was harvested after perfusion with PBS one hour post dosing. Plasma was isolated from whole blood by centrifuging at 1000 x g for 30 minutes. The unit for hepatic accumulation of platinum is nmol/gram tissue, the unit for plasma is μM. The platinum levels in plasma and liver were determined using ICP-MS. Data are presented as the mean ± SD (n = 3). * $P < 0.05$.

Oct WT and *Oct1/2-/-* mice. The terminal half-life ($T_{1/2,\beta}$) tended to be greater in *Oct1/2-/-* mice, although not significantly different from *Oct* WT mice ($p = 0.057$).

Ultrafilterable platinum (comprising nonprotein bound drug and biotransformation products in plasma water) is thought to reflect more of the platinum species with antitumor and toxic properties in the circulation. Consistent with the results in plasma matrix, *Oct1/2-/-* mice had greater platinum concentrations in the plasma ultrafiltrate during terminal elimination phase than Oct wild-type mice at 24 and 48 hr, respectively (Figure 5.7, $p < 0.05$). The mean residence time (MRT) for *Oct1/2-/-* mice was significantly different compared with *Oct* wild-type mice ($p = 0.026$, Table 5.3).

Effect of *Oct1* and *Oct2* double deletion on tissue accumulation of platinum in mice after administration of oxaliplatin. The absolute platinum levels in heart and spleen were slightly but significantly higher in *Oct1/2-/-* than in *Oct* WT mice 1 hr after intravenous administration of oxaliplatin (Figure 5.8A; $p < 0.05$). However, this significant difference disappeared when the absolute platinum levels were normalized with corresponding plasma concentrations (Figure 5.8B; $p > 0.05$). No accumulation difference was observed in other major tissues. To eliminate the confounding effect of platinum in whole blood left in liver, we performed extensive liver perfusion before tissue collection. As shown in Figure 5.9, the liver perfusion did not affect the study results. That is, the absolute and normalized hepatic accumulation did not exhibit significant differences between *Oct1/2-/-* and *Oct* WT mice ($p > 0.05$).

Role of Oct1 in oxaliplatin toxicities in mice. To assess the role of Oct1 in the toxicities associated with oxaliplatin treatment, especially the hepatotoxicity, *Oct1+/+*

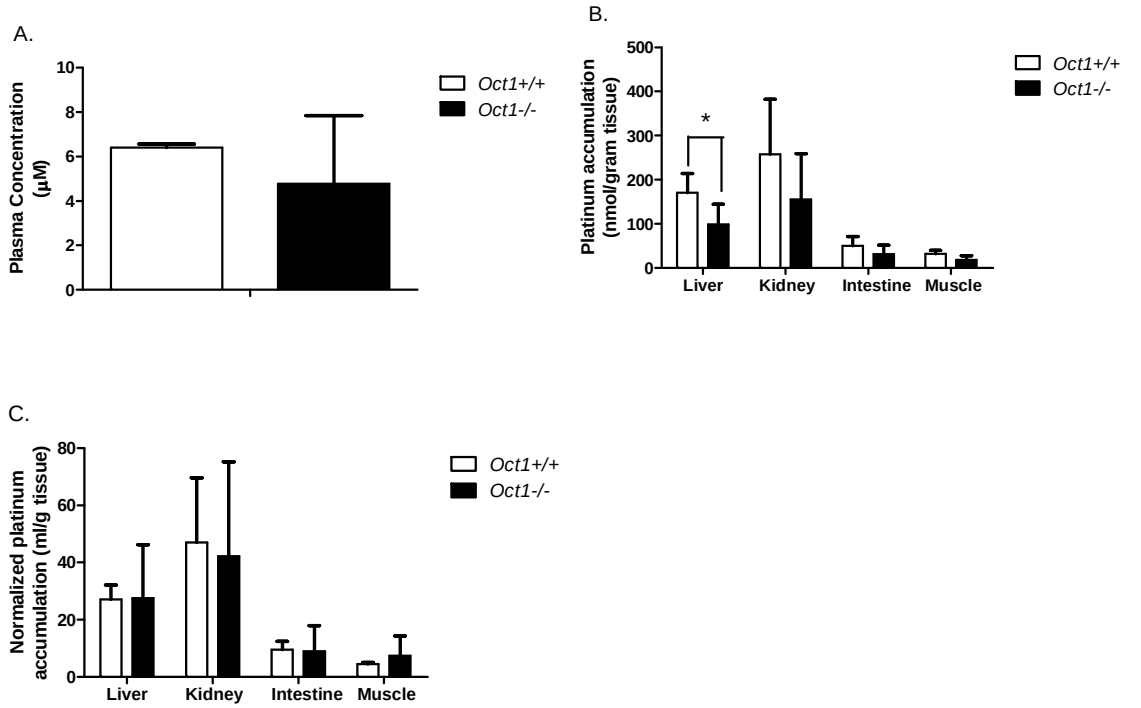

Figure 5.10. Effect of multiple doses of oxaliplatin on tissue accumulation of platinum in *Oct1*+/+ and *Oct1*-/- mice. (A) Plasma concentration, (B) absolute platinum levels in various tissues, (C) normalized platinum accumulations in various tissues. *Oct1*+/+ and *Oct1*-/- mice were treated with saline or oxaliplatin (6 mg/kg) via tail vein injection daily for a total five days (n = 5 animals per group). The mice were fasted for at least 16 hours before sacrifice. Blood and various tissues (liver, kidney, intestine and muscle) were collected 24 hrs after the last dose. Plasma was isolated from whole blood by centrifuging at 1000 x g for 30 minutes. The platinum levels in plasma and various tissues were determined using ICP-MS. Data are presented as the mean ± SD (n = 5). * $P < 0.05$.

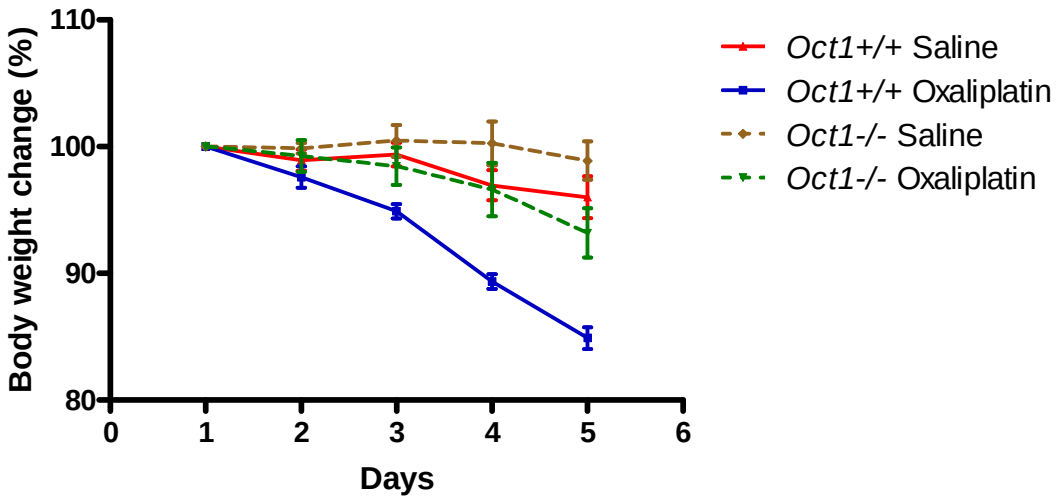

Figure 5.11. Oxaliplatin results in greater body weight loss in *Oct1*+/+ mice.

Oct1+/+ and *Oct1*-/- mice were treated with saline or oxaliplatin (6 mg/kg) via i.p. injection once daily for a total five days (n = 5 animals per group). Body weight was monitored daily. The mice were fasted for at least 16 hours before sacrifice. Data are presented as the mean ± SD (n = 5).

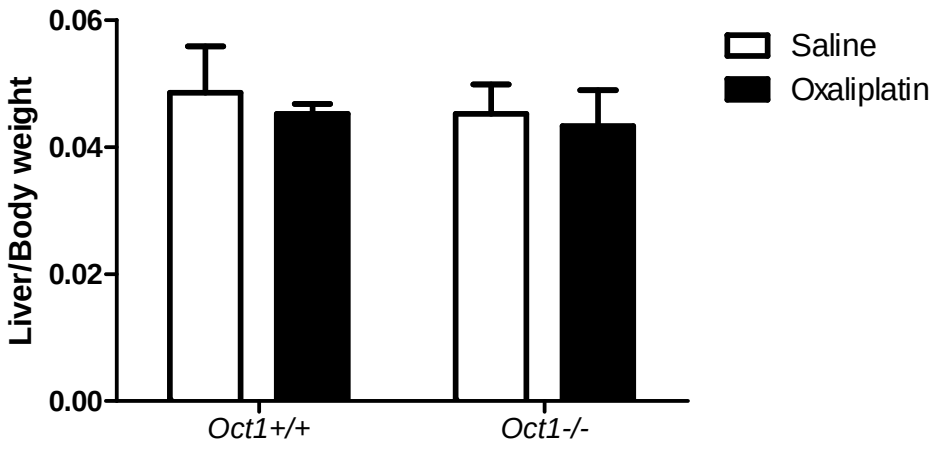

Figure 5.12. Oxaliplatin has no effect on liver over body weight ratio in *Oct1*+/+ and *Oct1*-/- mice. *Oct1*+/+ and *Oct1*-/- mice were treated with saline or oxaliplatin (6 mg/kg) via tail vein injection daily for a total five days (n = 5 animals per group). The mice were fasted for at least 16 hours before sacrifice. Liver was collected 24 hrs after the last dose, liver weight was measured. Liver to body weight ratio was compared among groups. Data are presented as the mean ± SD (n = 5).

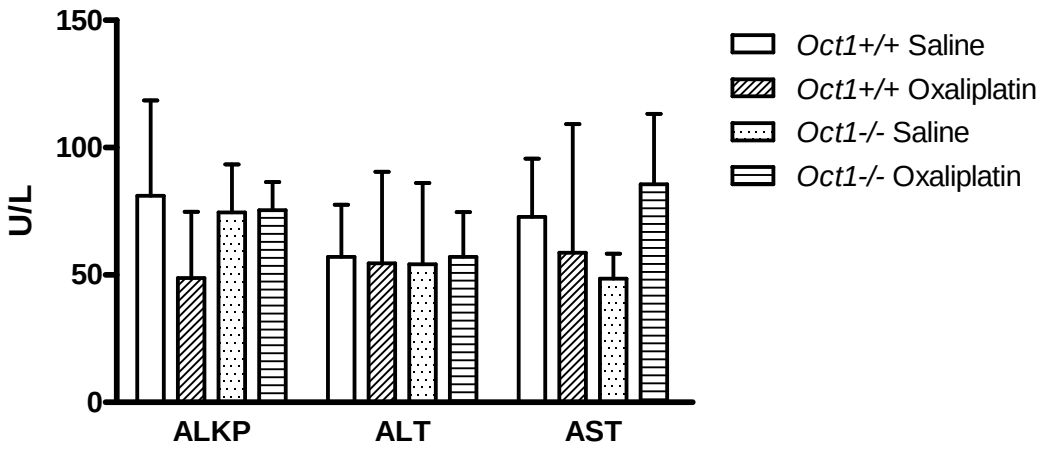

Figure 5.13. Oxaliplatin has no effect on liver function of *Oct1+/+* and *Oct1-/-* mice. *Oct1+/+* and *Oct1-/-* mice were treated with saline or oxaliplatin (6 mg/kg) via tail vein injection daily for a total five days (n = 5 animals per group). The mice were fasted for at least 16 hours before sacrifice. Blood was collected 24 hrs after the last dose; The activities of three-liver associated enzymes, alkaline phosphatase (ALKP), alanine aminotransferase (ALT), and aspartate aminotransferase(AST) in serum were measured. Data are presented as the mean ± SD (n = 5).

and *Oct1-/-* mice (n =5 per group) were treated with 6 mg/kg oxaliplatin or saline via i.p. injection once daily for a total five days. The platinum concentrations in plasma were not significantly different between *Oct1+/+* mice and *Oct1-/-* mice after multiple doses (Figure 5.10A; $p > 0.05$). However, *Oct1+/+* mice had significantly higher hepatic platinum accumulation than in *Oct1-/-* mice (Figure 5.10B; $p < 0.05$); the difference disappeared after normalization with corresponding plasma concentration (Figure 5.10C; $p > 0.05$). Oxaliplatin caused more severe body weight loss in *Oct1+/+* mice than in *Oct1-/-* mice, the relative body weight loss in *Oct1+/+* was 15.1%, whereas the relative body weight loss in *Oct1-/-* mice was 6.8% (Figure 5.11). Although there was a significantly greater hepatic accumulation of oxaliplatin in *Oct1+/+* mice, no difference was observed in liver size and the activities of three liver associated enzymes: ALT, AST and ALKP between *Oct1+/+* and *Oct1-/-* mice (Figure 5.12 and Figure 5.13). The liver histopathology examination showed no clear sign of liver damage associated with oxaliplatin treatment in both*Oct1+/+* and *Oct1-/-* mice. The data suggest that the hepatic toxicity of oxaliplatin observed in humans was not observed under the conditions used in this study and a clear role for Oct1 in oxaliplatin-induced hepatotoxicity could not be evaluated. The effect of Oct1 deletion on body weight was striking and suggests that Oct1 plays a role in the overall toxicity of oxaliplatin in the mice.

Discussion

Oxaliplatin is an outstanding substrate of OCTs as revealed by increased intracellular accumulation in cells that overexpress these critical transporters compared to those lacking them[10, 11]. The dramatic increases in cellular accumulation and

corresponding cell sensitization together with abundant expression of OCTs in colorectal cancer cell lines and tumor samples support a role for OCTs in the superior anti-colorectal cancer effect of oxaliplatin in comparison to cisplatin [26], which is a much weaker substrate of OCTs. In the present study, we investigated the role of OCT1 at physiological expression levels in the disposition of oxaliplatin in an attempt to identify the molecular mechanism(s) that contribute to its unique anticancer activity *in vivo* and provide the scientific foundations for its potential use in the treatment of hepatocellular carcinoma (HCC).

Organic cation transporters 1 and 2 genes are highly polymorphic, and the polymorphisms of OCT1 and OCT2 have been associated with the altered activity for their substrates [14, 21-23]. In the current study, the common OCT1 variants 420Del, G465R, G401S, R61C and S14F and OCT2 variants M165I and A270S showed significant differences in cellular uptake of oxaliplatin when compared to the reference transporters. These data might, in part, help to explain the variability in oxaliplatin response and toxicity in colorectal cancer patients.

Compared to the *in vitro* uptake result, the cellular platinum accumulation rate of oxaliplatin in hOCT1 transfected cells was 5.6 fold of that in MOCK cells [10]; the intracellular platinum accumulation rate of oxaliplatin in *Oct1*+/+ hepatocytes ranged from 1.4 to 1.8 fold of that in *Oct1*-/- hepatocytes. The difference in the cellular platinum accumulation rate of oxaliplatin between hOCT1 transfected cells, which overexpress the transporter, and mouse primary hepatocytes is likely to be due to differences in the expression levels of OCT1. In primary hepatocytes, the OCT1 expression level is

reduced upon isolation and culture procedure, as showed in our unpublished data. The kinetics of oxaliplatin uptake between mouse and human OCT1 were similar suggesting that kinetic differences between human and mouse Oct1 could not account for differences observed in the effect of OCT1 on oxaliplatin uptake between the human transfected cell lines and primary hepatocytes from mouse (unpublished data).

The pharmacokinetic profiles of oxaliplatin were similar to previous reports in rodents [24, 25]. The studies showed that platinum levels in plasma of mice after intravenous administration of oxaliplatin exhibited a short initial distribution phase ($t_{1/2}$, 0.33 – 0.44 hr) and long terminal elimination phase ($t_{1/2}$, 19.2 – 22.3 hr). The long terminal half-life of plasma platinum probably represents the slow turn-over rate of degradation of cellular macromolecules such as proteins. The clearance of platinum in the ultrafiltrate of plasma was much higher than the clearance of total platinum in plasma (Tables 5.1, 5.2 and 5.3), probably reflecting the covalent binding of platinum to plasma proteins. The renal clearance of oxaliplatin in *Oct1*+/+ and *Oct1*-/- mice was about half of the total clearance of plasma platinum, which is consistent with the oxaliplatin pharmacokinetics in human [27]. In humans, oxaliplatin is rapidly cleared from plasma by covalent binding to tissues and renal elimination. Urinary excretion represents about half of the total clearance.

Oct1 deletion did not affect the pharmacokinetics of platinum after oxaliplatin administration. In addition, no differences were observed in platinum accumulation in various tissues 6 hours after oxaliplatin administration to *Oct1* wild-type and knockout mice (Figure 5.4). However, further studies demonstrated that the effect of Oct1 on

tissue accumulation was time-dependent, and at early times, there were significant differences in plasma, renal, intestinal, and cardiac accumulation between *Oct1-/-* and *Oct1+/+* mice. When the data were normalized to plasma concentration, the differences disappeared suggesting that the differences in tissue accumulation reflected differences in plasma concentrations at early times.

Since the expression of Oct2 was increased in various tissues from *Oct1-/-* mice, we conducted the tissue accumulation study in *Oct1/2-/-* mice one hr post dosing (Figure 5.8). Though slight differences were observed in platinum levels in heart and spleen, no differences were observed when the tissue levels were normalized to plasma concentrations. Confounding effects of blood platinum retained in tissues were not apparent (Figure 5.9). Collectively, our data demonstrated small effects of *Oct1* and *Oct2* on the tissue distribution of oxaliplatin in mice.

It is noteworthy that the result of the absolute oxaliplatin accumulation in intestine of *Oct1-/-* mice was opposite to that for pyroplatin (refer to Chapter 2). This may be due to increased expression of Oct2 and Oct3 in the intestine of mice. In particular, pyroplatin is a more selective substrate for OCT1 than for OCT2 and OCT3; thus, increased expression of these transporters in *Oct1-/-* mice is not likely to compensate for the effect of Oct1 deletion. In contrast, oxaliplatin is an equally good substrate for OCT1, OCT2 and OCT3, therefore, enhanced expression of these cation transporters may have obscured the effect of the Oct1 deletion.

In rodents, Oct1 and Oct2 are both expressed in kidney and localized at the basolateral membrane of epithelial cells of the proximal tubules [28], and these two

transporters also share extensive overlap with respect to substrate and inhibitor specificities. Double deletion of Oct1 and Oct2 in mice results in impaired renal secretion of substrate organic cations [17], which may result in increased drug exposure. The effect of Oct1 and Oct2 double deletion on plasma concentration of total platinum was most obvious in the terminal elimination phase (Figure 5.7). The total platinum clearance in *Oct1/2-/-* mice was significantly lower than in wild-type mice, which resulted in an increased AUC in the double knockout mice. These data suggest that the elimination of oxaliplatin from the kidney may be impaired to some degree by deleting both organic cation transporters. Unlike rodents, which express both Oct1 and Oct2 in the kidney, humans express only OCT2 in the kidney [29]. Therefore, it is likely that the Oct1/2-/- mouse model better reflects the effect of an OCT2 deficiency on kidney function in humans. Patients with reduced function variants of OCT2 may have decreased renal clearance of oxaliplatin, which may result in oxaliplatin toxicities.

To establish the link between Oct1 and oxaliplatin associated toxicities, we compared the differences in the toxicities of oxaliplatin between *Oct1-/-* and *Oct1+/+* mice, with a special focus on hepatic toxicity. Although there was significantly greater platinum accumulation in liver of *Oct1+/+* mice after chronic administration of oxaliplatin, liver toxicity in these animals, reflected by liver size and liver enzyme activities, was not apparent. All tissues including plasma in *Oct1+/+* mice tended to have higher platinum levels compared to *Oct1-/-* mice, which likely reflected a greater extent of absorption of oxaliplatin following intraperitoneal dosing of oxaliplatin. The higher tissue and plasma levels of platinum in *Oct1+/+* mice were consistent with greater body weight decreases in these animals. However, since oxaliplatin was not hepatotoxic

under the conditions used in this study, we could not assess the effect of Oct1 on hepatotoxicity. The dosing regimen or dosing route used in our study might not be appropriate to elicit the hepatic toxicity.

In summary, our studies indicate that Oct1 does not play a major role in the tissue distribution or plasma levels of total platinum following oxaliplatin administration. However, total plasma platinum levels may not reflect platinum complexes available for DNA binding, anti-tumor effects and toxicity of the oxaliplatin. The fact that oxaliplatin administration resulted in much greater reduction in body weight in the wild-type mice in comparison to the Oct1 knockout mice, may suggest that Oct1 plays a role in the systemic toxicities of oxaliplatin.

References

1. Zamble, D.B. and Lippard, S.J., *Cisplatin and DNA-repair in cancer-chemotherapy*. Trends in Biochemical Sciences, 1995. **20**(10): p. 435-439.

2. Wang, D. and Lippard, S.J., *Cellular processing of platinum anticancer drugs.* Nature Reviews Drug Discovery, 2005. **4**(4): p. 307-320.

3. Misset, J.L., Bleiberg, H., Sutherland, W., Bekradda, M., and Cvitkovic, E., *Oxaliplatin clinical activity: A review.* Critical Reviews in Oncology Hematology, 2000. **35**(2): p. 75-93.

4. Kelland, L., *The resurgence of platinum-based cancer chemotherapy.* Nature Reviews Cancer, 2007. **7**(8): p. 573-584.

5. Rixe, O., *Oxaliplatin, tetraplatin, cisplatin, and carboplatin: Spectrum of activity in drug-resistant cell lines and in the cell lines of the national cancer institute's anticancer drug screen panel.* Biochemical Pharmacology, 1996. **52**: p. 1855-1865.

6. Rabik, C.A. and Dolan, M.E., *Molecular mechanisms of resistance and toxicity associated with platinating agents.* Cancer Treatment Reviews, 2007. **33**(1): p. 9-23.

7. Chaney, S.G., Campbell, S.L., Bassett, E., and Wu, Y.B., *Recognition and processing of cisplatin- and oxaliplatin-DNA adducts.* Critical Reviews in Oncology Hematology, 2005. **53**(1): p. 3-11.

8. Vaisman, A., *Effect of DNA polymerases and high mobility group protein 1 on the carrier ligand specificity for translesion synthesis past platinum-DNA adducts.* Biochemistry, 1999. **38**: p. 11026-11039.

9. Fink, D., Nebel, S., Aebi, S., Zheng, H., Cenni, B., Nehme, A., Christen, R.D., and Howell, S.B., *The role of DNA mismatch repair in platinum drug resistance.* Cancer Research, 1996. **56**(21): p. 4881-4886.

10. Zhang, S.Z., Lovejoy, K.S., Shima, J.E., Lagpacan, L.L., Shu, Y., Lapuk, A., Chen, Y., Komori, T., Gray, J.W., Chen, X., Lippard, S.J., and Giacomini, K.M., *Organic cation transporters are determinants of oxaliplatin cytotoxicity.* Cancer Research, 2006. **66**(17): p. 8847-8857.

11. Yokoo, S., Masuda, S., Yonezawa, A., Terada, T., Katsura, T., and Inui, K.I., *Significance of organic cation transporter 3 (SLC22A3) expression for the cytotoxic effect of oxaliplatin in colorectal cancer.* Drug Metabolism and Disposition, 2008. **36**(11): p. 2299-2306.

12. Ramanathan, R.K., Clark, J.W., Kemeny, N.E., Lenz, H.-J., Gococo, K.O., Haller, D.G., Mitchell, E.P., and Kardinal, C.G., *Safety and toxicity analysis of oxaliplatin combined with fluorouracil or as a single agent in patients with previously treated advanced colorectal cancer.* Journal of Clinical Oncology, 2003. **21**(15): p. 2904-2911.

13. Rubbia-Brandt, L., Audard, V., Sartoretti, P., Roth, A.D., Brezault, C., Le Charpentier, M., Dousset, B., Morel, P., Soubrane, O., Chaussade, S., Mentha, G.,

and Terris, B., *Severe hepatic sinusoidal obstruction associated with oxaliplatin-based chemotherapy in patients with metastatic colorectal cancer.* Annals of Oncology, 2004. **15**(3): p. 460-466.

14. Shu, Y., Sheardown, S.A., Brown, C., Owen, R.P., Zhang, S.Z., Castro, R.A., Ianculescu, A.G., Yue, L., Lo, J.C., Burchard, E.G., Brett, C.M., and Giacomini, K.M., *Effect of genetic variation in the organic cation transporter 1 (OCT1) on metformin action.* Journal of Clinical Investigation, 2007. **117**(5): p. 1422-1431.

15. Moldeus, P., Hogberg, J., and Orrenius, S., *Isolation and use of liver cells.* Fleischer, Sidney and Lester Packer (Ed.). Methods in Enzymology, Vol. Lii. Biomembranes. Part C: Biological Oxidations Microsomal, Cytochrome P-450, and Other Hemoprotein Systems. Xxii+595p. Illus. Academic Press, Inc.: New York, N.Y., USA; London, England. Isbn 0-12-181952-3, 1978: p. 60-71.

16. Jonker, J.W., Wagenaar, E., Mol, C., Buitelaar, M., Koepsell, H., Smit, J.W., and Schinkel, A.H., *Reduced hepatic uptake and intestinal excretion of organic cations in mice with a targeted disruption of the organic cation transporter 1 (Oct1 [Slc22a1]) gene.* Molecular and Cellular Biology, 2001. **21**(16): p. 5471-5477.

17. Jonker, J.W., Wagenaar, E., van Eijl, S., and Schinkel, A.H., *Deficiency in the organic cation transporters 1 and 2 (Oct1/Oct2 [Slc22a1/Slc22a2]) in mice abolishes renal secretion of organic cations.* Molecular and Cellular Biology, 2003. **23**(21): p. 7902-7908.

18. Shu, Y., Leabman, M.K., Feng, B., Mangravite, L.M., Huang, C.C., Stryke, D., Kawamoto, M., Johns, S.J., DeYoung, J., Carlson, E., Ferrin, T.E., Herskowitz, I., and Giacomini, K.M., *Evolutionary conservation predicts function of variants of the human organic cation transporter, OCT1*. Proceedings of the National Academy of Sciences of the United States of America, 2003. **100**(10): p. 5902-5907.

19. Kerb, R., Brinkmann, U., Chatskaia, N., Gorbunov, D., Gorboulev, V., Mornhinweg, E., Keil, A., Eichelbaum, M., and Koepsell, H., *Identification of genetic variations of the human organic cation transporter hOCT1 and their functional consequences.* Pharmacogenetics, 2002. **12**(8): p. 591-595.

20. Sakata, T., Anzai, N., Shin, H.J., Noshiro, R., Hirata, T., Yokoyama, H., Kanai, Y., and Endou, H., *Novel single nucleotide polymorphisms of organic cation transporter 1 (SLC22A1) affecting transport functions.* Biochemical and Biophysical Research Communications, 2004. **313**(3): p. 789-793.

21. Chen, Y., Zhang, S.Z., Sorani, M., and Giacomini, K.M., *Transport of paraquat by human organic cation transporters and multidrug and toxic compound extrusion family.* Journal of Pharmacology and Experimental Therapeutics, 2007. **322**(2): p. 695-700.

22. Leabman, M.K., Huang, C.C., Kawamoto, M., Johns, S.J., Stryke, D., Ferrin, T.E., DeYoung, J., Taylor, T., Clark, A.G., Herskowitz, I., Giacomini, K.M., and Pharmacogenetics Membrane, T., *Polymorphisms in a human kidney xenobiotic*

transporter, OCT2, exhibit altered function. Pharmacogenetics, 2002. **12**(5): p. 395-405.

23. Chen, Y., Li, S.L., Brown, C., Cheatham, S., Castro, R.A., Leabman, M.K., Urban, T.J., Chen, L.G., Yee, S.W., Choi, J.H., Huang, Y., Brett, C.M., Burchard, E.G., and Giacomini, K.M., *Effect of genetic variation in the organic cation transporter 2 on the renal elimination of metformin.* Pharmacogenetics and Genomics, 2009. **19**(7): p. 497-504.

24. Rice, J.R., Gerberich, J.L., Nowotnik, D.P., and Howell, S.B., *Preclinical efficacy and pharmacokinetics of AP5346, a novel diaminocyclohexane-platinum tumor-targeting drug delivery system.* Clinical Cancer Research, 2006. **12**(7): p. 2248-2254.

25. Luo, F.R., Wyrick, S.D., and Chaney, S.G., *Pharmacokinetics and biotransformations of oxaliplatin in comparison with ormaplatin following a single bolus intravenous injection in rats.* Cancer Chemotherapy and Pharmacology, 1999. **44**(1): p. 19-28.

26. de Gramont, A., Figer, A., Seymour, M., Homerin, M., Hmissi, A., Cassidy, J., Boni, C., Cortes-Funes, H., Cervantes, A., Freyer, G., Papamichael, D., Le Bail, N., Louvet, C., Hendler, D., de Braud, F., Wilson, C., Morvan, F., and Bonetti, A., *Leucovorin and fluorouracil with or without oxaliplatin as first-line treatment in advanced colorectal cancer.* Journal of Clinical Oncology, 2000. **18**(16): p. 2938-2947.

27. Graham, M.A., Lockwood, G.F., Greenslade, D., Brienza, S., Bayssas, M., and Gamelin, E., *Clinical pharmacokinetics of oxaliplatin: A critical review.* Clinical Cancer Research, 2000. **6**(4): p. 1205-1218.

28. Koepsell, H., Schmitt, B.M., and Gorboulev, V., *Organic cation transporters.* Reviews of Physiology Biochemistry and Pharmacology. Volume 150, 2003: p. 36-90.

29. Gruendemann, D., Koester, S., Kiefer, N., Breidert, T., Engelhardt, M., Spitzenberger, F., Obermueller, N., and Schoemig, E., *Transport of monoamine transmitters by the organic cation transporter type 2, OCT2.* Journal of Biological Chemistry, 1998. **273**(47): p. 30915-30920.

CHAPTER 6

SUMMARY AND CONCLUSIONS

The body is continuously exposed to a variety of environmental toxins and metabolic waste products. To eliminate these compounds, it is equipped with various detoxification mechanisms, such as metabolizing enzymes and transport proteins mediating their inactivation and excretion. Transporter proteins facilitate the transport of certain endogenous and exogenous compounds across cell membranes and have been shown to be key determinants of the ADME (absorption, distribution, metabolism and elimination), and ultimately the efficacy and safety of a drug [1-3]. Efflux transporters, which pump drugs out of cells, are well known to be responsible for multiple drug resistance in cancer chemotherapy [4] and inhibitors of efflux transporters have been developed as potential modulators of anti-cancer drug resistance. In contrast, few studies have focused on influx transporters. Drug targeting using influx transporters expressed in tumors is one effective approach both to increase the pharmacological activity of drugs and to reduce their side effects by enhancing delivery to the target site. Recent research has identified many types of transporters that are expressed selectively in various organs and in tumors, and which, therefore, may be promising targets for drug delivery. The most comprehensively documented case is pravastatin. Pravastatin, a 3-hydroxy-3-methylglutaryl-coenzyme A reductase inhibitor, is taken up by the liver from the portal vein by OATP family proteins located on the sinusoidal (basolateral) membrane for its pharmacological action in the liver [5, 6].

Platinum-based chemotherapies are among the most active anticancer treatments since the clinical introduction of cisplatin in the 1970s and have been used in more than 50% of cancer patients [7]. Cisplatin, carboplatin and oxaliplatin, as well as other platinum compounds, share similar mechanisms of action. However, oxaliplatin showed a different pattern of sensitivity to that of cisplatin in the NCI60-cell human tumor panel and in combination with 5-FU/leucovorin produced response rates twice that of 5-FU/leucovorin regimens alone in the treatment of colorectal cancer, against which cisplatin is inactive [8-10]. In addition, the safety profiles among platinum complexes are different [11]. Recently, the differences in the mechanism(s) controlling cellular uptake and efflux of these platinum compounds have gained more intention and are considered to be one of the major mechanisms of contributing to their disparate activities of anti-tumor and safety [11, 12]. In Chapter 1, platinum-associated drug resistance was discussed in terms of the relevant transporters, such as copper transporters (CTRs), organic cation transporters (OCTs), multidrug and toxic compound extrusion (MATE) and multiple-drug resistance related transporters (MDRs). Among these transporters, OCTs, encoded by SLC22A family are of greatest interest because of their selective expression in normal and tumor tissues and the distinct interactions with different platinum agents[13-15].

Traditional cancer therapy relies on the premise that rapidly proliferating cancer cells are more likely to be killed by a cytotoxic agent. In reality, however, these agents have very little or no specificity, which leads to systemic toxicity, causing undesirable side effects. Therefore, targeted drug-delivery constructs are much desired. Targeted drug-delivery systems using OCTs promise to expand the therapeutic window of platinum complexes, as recently demonstrated for oxaliplatin uptake by colorectal cancer

cells via OCTs and highly expression of OCTs in colorectal cancer cell lines and tumor samples[16, 17]. The overall goal of this dissertation research was to test the hypothesis that OCTs play a role in the targeting, disposition and efficacy of anti-cancer platinum drugs. Oct knockout mice and new anti-cancer platinum analogs were used in the studies. Below, a summary of the findings of each chapter is presented along with the key issues and challenges for OCT targeting of platinum based anti-cancer drugs.

Chapter 2

The resurgence of platinum-based cancer chemotherapy in recent years has resulted in not only the approval of oxaliplatin but also the clinical development of picoplatin and satraplatin [9]. Continuing efforts have also been made in analogue development to broaden the spectrum of activity and to improve the therapeutic properties of platinum-based antitumor agents. Pyroplatin, the antitumor properties of which were established in mice over 20 years ago [18], emerged in our search for platinum anticancer drug candidates with cellular uptake properties superior to those of oxaliplatin in terms of the interaction with OCTs [19]. In Chapter 2, as a first step in evaluating the potential of OCT1 as a valid drug delivery target, the effect of Oct1 on the disposition of pyroplatin under normal physiological Oct1 expression level was investigated *in vivo*. We observed that Oct1 deletion significantly decreased not only the intracellular uptake of pyroplatin but also binding of platinum to DNA, its molecular target in freshly isolated primary hepatocytes from both *Oct1-/-* and wild-type mice *in vitro*. To extend the *in vitro* cellular studies further, we examined the role of OCT1 in the tissue accumulation and pharmacokinetics of pyroplatin in *Oct1* wild-type and *Oct1-/-*

mice. Comparing the platinum accumulation in different tissues, we observed that the highest platinum accumulation levels were found in liver and intestine where Oct1 is highly expressed. In contrast, brain tissue, in which no or low Oct1 is expressed, had the lowest levels in both *Oct1* wild-type and *Oct1-/-* mice. We also observed that Oct1 deletion significantly decreased the hepatic and intestinal accumulation of pyroplatin in the *Oct1-/-* mice compared to *Oct1+/+* mice. Further, deletion of Oct1 resulted in a decreased clearance and apparent volume distribution, which led to an increased systemic exposure in the *Oct1-/-* mice compared to the wildtype mice. Collectively, the data indicate that Oct1 plays a role in the elimination and tissue distribution of pyroplatin. Our study sets the stage for further toxicity and efficacy studies.

Chapter 3

Transporters may regulate the pharmacological and toxicological effects of drugs as they may control their distribution to tissues responsible for the effects. As demonstrated in Chapter 2, Oct1 facilitated the accumulation of pyroplatin to liver and intestine in which Oct1 is highly expressed. However, whether the Oct1 mediated disposition difference of pyroplatin in blood and various tissues would affect the toxicity profile of pyroplatin *in vivo* was worth investigating. Nephrotoxicity and ototoxicity of cisplatin are the dose-limiting side effects of cisplatin and have limited its optimal clinical treatment outcome. The toxicities associated with pyroplatin, the newly emerged anticancer drug candidate, were of great interest and potentially determines the success of pyroplatin as a drug. Studies presented in Chapter 3 were designed to characterize the toxicity profile of pyroplatin and simultaneously determine whether Oct1 can modulate

the toxicities of pyroplatin. To determine the dose to use in the toxicity study, a dose-range finding toxicity study was conducted in *Oct1*+/+ mice with the highest dose of 150 mg/kg. All animals in the 150 mg/kg group died before the second dose. The animals in the lower dose groups survived until the end of the study. Pyroplatin at 90 mg/kg and 120 mg/kg resulted in significant changes in body weight, liver to body weight ratios, liver function and hematology. Therefore, we selected doses between 90 mg/kg to 120 mg/kg for use in evaluating the role of Oct1 in pyroplatin toxicity. The role of Oct1 in the toxicity of pyroplatin was determined by comparing the toxicity profile of pyroplatin between *Oct1*+/+ and *Oct1*-/- mice. The dose of pyroplatin started at 120 mg/kg, which later was reduced to 90 mg/kg due to death or moribundity observed in *Oct1*-/- mice at 120 mg/kg. At the 90 mg/kg dose, pyroplatin resulted in much greater body weight loss and more severe hematological abnormalities in *Oct1*-/- mice than in *Oct1* wildtype mice, which were consistent with higher plasma concentration of pyroplatin in *Oct1*-/- mice. The renal toxicity of pyroplatin, reflected by the increase of Kim-1 mRNA expression and renal tubular lesions was also more pronounced in *Oct1*-/- mice than in *Oct1* +/+ mice. The significantly greater renal pyroplatin accumulation in *Oct1*-/- mice supported more pronounced renal toxicity in *Oct1*-/- mice. However, Oct1 deletion protected animals from developing liver toxicity. In comparison to *Oct1*-/- mice, pyroplatin resulted in more severe hepatomegaly in *Oct1*+/+ mice. Serum protein and glucose level were also significantly increased in *Oct1*+/+ mice, but not affected in *Oct1*-/- mice. Histopathological examination showed that pyroplatin caused apparent liver swelling in *Oct1*+/+ mice, but not in *Oct1*-/- mice. The more apparent hepatic toxicity of pyroplatin in *Oct1*+/+ mice was consistent with greater hepatic pyroplatin accumulation in these

mice. Although there was greater hepatic toxicity in *Oct1+/+* mice, the level of toxicity was considered mild and reversible. If pyroplatin is developed as an anticancer drug, hepatic toxicity may not be a concern. Our study also supports the concept that by targeting drug influx transporters, off-target toxicities can be greatly spared.

Chapter 4

Liver cancer (mainly hepatocellular carcinoma, aka HCC) is a deadly disease. Its mean life expectancy after diagnosis is only 6 months. Before sorafenib was approved in 2007, there was no effective treatment for most of the individuals who succumb to this neoplasm. However, the survival benefit provided by sorafenib was limited, as the mean survival time was only improved by less than 3 months [20]. The difficulties in treatment of HCC appear to be due to insufficient drug accumulation or extensive drug inactivation (metabolism) by the liver cancer cells. Recent studies showed that pyroplatin can largely escape repair and yet inhibit transcription very effectively. Its adducts should persist longer than those of cisplatin yet produce a similar number of downstream consequences that might raise the therapeutic potential of pyroplatin relative to cisplatin [19]. Studies described in Chapter 4 were designed to test the hypothesis that by controlling intracellular uptake of pyroplatin, Oct1 plays a role in the anti-cancer effect of pyroplatin, especially the anti-HCC effect. We found that hOCT1 facilitated the accumulation of pyroplatin in the HEK- hOCT1 xenograft, and the increased pyroplatin accumulation in mice bearing HEK-hOCT1 xenografts appeared to inhibit the tumor growth in these mice. However, because HEK-xenografts are not real tumors and the level of OCT1 expression was super physiological, a more physiological relevant in situ

liver tumor (HCC) model was established by hydrodynamic injection of c-Met and activated β-catenin. Hepatocarcinogenesis did not alter the expression level of Oct1, which was comparable to the normal liver tissue. Comparing the accumulation of pyroplatin in HCC induced in *Oct1-/-* mice with that induced in *Oct1+/+* mice, we observed that Oct1 expressed in HCC induced in *Oct1+/+* mice significantly facilitated the accumulation of pyroplatin in the tumor tissues. However, the increased pyroplatin accumulation in HCC induced in *Oct1+/+* mice did not successfully translate into a better survival benefit. One of the most likely reasons is due to the lower potency of pyroplatin compared to commercially marketed platinum compounds such as cisplatin and oxaliplatin [17]. In addition, pyroplatin reduced the activity of caspase-3/7 of HCCs in both male and female *Oct1+/+* mice, but not in *Oct1-/-* mice suggesting that necrosis, instead of apoptosis, was more likely to be responsible for cell death due to pyroplatin treatment in the current study. The reactivity of pyroplatin with GSH was the lowest compared with cisplatin, oxaliplatin and picoplatin, indicating that deactivation of pyroplatin by GSH is minimal. Although pyroplatin lacked efficacy in the anti-HCC study, our studies demonstrated that mouse and human OCT1 can facilitate the accumulation of pyroplatin in xenografts and HCC tumor tissues. Furthermore, our study provided a potential direction to be explored in the currently ineffective HCC treatments. In the future, we can design and develop anticancer agents with high Oct1 specificity and greater potency for the targeted therapy of liver cancer.

Chapter 5

Compared with pyroplatin, oxaliplatin was considered a moderate substrate of OCT1 [19]. Studies in Chapter 5 were designed to examine the role of Oct1 at physiological expression levels in the disposition of oxaliplatin in an attempt to identify the molecular mechanism(s) that contribute to its unique anticancer activity *in vivo* and provide the scientific foundations for its potential use in the treatment of hepatocellular carcinoma (HCC). The human OCT1 and OCT2 genes are polymorphic, with common polymorphisms causing altered activity in the cellular uptake of oxaliplatin. Our study suggests that genetic variation in these transporters may contribute to the wide variation in response to this critically important therapeutic agent. Oct deletion slightly but significantly decreased the accumulation of oxaliplatin in primary hepatocytes freshly isolated from *Oct1*+/+ and *Oct1*-/- mice. The data indicate that Oct1 is likely to play a role in facilitating oxaliplatin passage into hepatocytes. However, the effect of Oct1 on oxaliplatin uptake is less than its effect on pyroplatin uptake as we expected. *In vivo* pharmacokinetic and tissue accumulation studies in *Oct1*+/+ and *Oct1*-/- mice showed that Oct1 deletion did not affect the pharmacokinetics of platinum after oxaliplatin administration. In addition, no differences were observed in platinum accumulation in various tissues 6 hours after oxaliplatin administration to *Oct1* wild-type and knockout mice. However, further studies demonstrated that the effect of Oct1 on tissue accumulation was time-dependent, and at early times, there were significant differences in plasma, renal, intestinal, and cardiac accumulation between *Oct1*-/- and *Oct1*+/+ mice. When the data were normalized to plasma concentration, the differences disappeared suggesting that the differences in tissue accumulation reflected differences in plasma concentrations at early times. Because Oct2 is up-regulated in Oct1-/- mice as shown in

Chapter 2, we also conducted pharmacokinetic studies of oxaliplatin using the Oct1/2 double knockout in an attempt to minimize the compensatory effect of Oct2 on the disposition of oxaliplatin. The data suggest that Oct1/2 double deletion has no remarkable effect on the tissue accumulation of oxaliplatin. However, Oct1 and Oct2 double deletion increased the plasma concentrations of total platinum in the terminal elimination phase, the total platinum clearance in *Oct1/2-/-* mice was significantly lower than in wild-type mice, which resulted in an increased AUC in the double knockout mice. These data suggest that the elimination of oxaliplatin from the kidney may be impaired to some degree by deleting both organic cation transporters. Unlike rodents, which express both Oct1 and Oct2 in the kidney, humans express only OCT2 in the kidney [21]. Therefore, it is likely that the Oct1/2-/- mouse model better reflects the effect of an OCT2 deficiency on kidney function in humans. Patients with reduced function variants of OCT2 may have decreased renal clearance of oxaliplatin, which may result in oxaliplatin toxicities. Importantly, to truly investigate the effects of OCT1, OCT2 and OCT3 on delivery, efficacy and toxicity of platinum compounds, an Oct1, 2 and 3 triple knockout mouse is needed to prevent compensatory mechanisms that result from enhanced expression of other Octs in Oct knockout mouse models.

Recently, use of oxaliplatin has been associated with development of hepatic lesions, which include sinusoidal alteration, portal hypertension, increases in transaminases, gammaglutamyl transpeptidase and alkaline phosphatase, and steatohepatitis [22, 23]. Studies presented in Chapter 5 also evaluated the role of Oct1 in the toxicity of oxaliplatin, especially focusing on the hepatotoxicity. Although Oct1 enhanced the hepatic accumulation after multiple dosing, the increase hepatic platinum

levels did not result in obvious liver toxicity. The plasma concentrations between *Oct1*+/+ mice and *Oct1*-/- mice were not significantly different. However, the body weight decrease in *Oct1* +/+ mice were more dramatic than in *Oct1*-/- mice. The data suggest that the hepatic toxicity of oxaliplatin observed in humans was not observed under the conditions used in this study and a clear role for Oct1 in oxaliplatin-induced hepatotoxicity could not be evaluated. The effect of Oct1 deletion on body weight was striking and suggests that Oct1 plays a role in the overall toxicity of oxaliplatin in the mice.

Challenges and Future Studies

Research in this dissertation has demonstrated that OCT1 can be used as a drug delivery target for platinum-based anticancer therapy, facilitating the selective accumulation of pyroplatin into tumor tissues and reducing its off-target toxicity. However, due to the lack of potency of pyroplatin, the anti-cancer efficacy of pyroplatin was not achieved in our studies. Further efforts are needed to design new platinum compounds, which have not only high specificity for OCT1 but also high potency for particular tumors that have high OCT1 expression. Further, this study provides another example of a drug distinct from metformin for which OCT1 may play a profound role in its pharmacokinetics and toxicities [24-26]. It has been shown that there is considerable inter-individual variability in drug response and drug-induced toxicity and a significant portion of such variation can be explained by an individual's genes [27]. The highly polymorphic OCT1 and OCT2 are likely to contribute to the variability in oxaliplatin

response and safety profile in colorectal cancer patients and suggest a path for individually optimized treatment choices.

OCT3, the third member of organic cation transporters, has been shown to be significantly involved in oxaliplatin-induced cytotoxicity and accumulation of platinum in colorectal cancer and OCT3-mediated uptake of oxaliplatin into the cancers was suggested to be important for its anti-cancer activity [16]. Investigations of the role of OCT3 in the pharmacokinetics and pharmacodynamics of oxaliplatin *in vivo* using Oct3-/- mice will be of great interest.

References

1. Mizuno, N., Niwa, T., Yotsumoto, Y., and Sugiyama, Y., *Impact of drug transporter studies on drug discovery and development.* Pharmacological Reviews, 2003. **55**(3): p. 425-461.

2. Shitara, Y., Horie, T., and Sugiyama, Y., *Transporters as a determinant of drug clearance and tissue distribution.* European Journal of Pharmaceutical Sciences, 2006. **27**(5): p. 425-446.

3. Giacomini, K.M., Huang, S-M., Tweedie, D. J., Benet, L. Z., Brouwer, K. L.R., Chu, X., Dahlin, A., Evers, R., Fischer, V., Hillgren, K. M., Hoffmaster, K. A., Ishikawa, T., Keppler, D., Kim, R. B., Lee, C. A., Niemi, M., Polli, J. W., Sugiyama, Y., Swaan, P. W., Ware, J. A., Wright, S. H., Yee, S. W., Zamek-Gliszczynski, M. J., & Zhang, L. for the International Transporter Consortium, *Membrane transporters in drug development.* Nature Reviews Drug Discovery, 2010. **9**(3): p. 215-236.

4. Glavinas, H., Krajcsi, P., Cserepes, J., and Sarkadi, B., *The role of ABC transporters in drug resistance, metabolism and toxicity.* Current Drug Delivery, 2004. **1**(1): p. 27-42.

5. Sasaki, M., Suzuki, H., Ito, K., Abe, T., and Sugiyama, Y., *Transcellular transport of organic anions across a double-transfected Madin-Darby canine kidney II cell monolayer expressing both human organic anion-transporting*

polypeptide (OATP2/SLC21A6) and multidrug resistance-associated protein 2 (MRP2/ABCC2). Journal of Biological Chemistry, 2002. **277**(8): p. 6497-6503.

6. Nakai, D., Nakagomi, R., Furuta, Y., Tokui, T., Abe, T., Ikeda, T., and Nishimura, K., *Human liver-specific organic anion transporter, LST-1, mediates uptake of pravastatin by human hepatocytes.* Journal of Pharmacology and Experimental Therapeutics, 2001. **297**(3): p. 861-867.

7. Wong, E. and Giandomenico, C.M., *Current status of platinum-based antitumor drugs.* Chemical Reviews, 1999. **99**(9): p. 2451-2466.

8. Misset, J.L., Bleiberg, H., Sutherland, W., Bekradda, M., and Cvitkovic, E., *Oxaliplatin clinical activity: A review.* Critical Reviews in Oncology Hematology, 2000. **35**(2): p. 75-93.

9. Kelland, L., *The resurgence of platinum-based cancer chemotherapy.* Nature Reviews Cancer, 2007. **7**(8): p. 573-584.

10. Rixe, O., *Oxaliplatin, tetraplatin, cisplatin, and carboplatin: Spectrum of activity in drug-resistant cell lines and in the cell lines of the national cancer institute's anticancer drug screen panel.* Biochemical Pharmacology, 1996. **52**: p. 1855-1865.

11. Rabik, C.A. and Dolan, M.E., *Molecular mechanisms of resistance and toxicity associated with platinating agents.* Cancer Treatment Reviews, 2007. **33**(1): p. 9-23.

12. Choi, M.K. and Kim, D.D., *Platinum transporters and drug resistance.* Archives of Pharmacal Research, 2006. **29**(12): p. 1067-1073.

13. Jonker, J.W. and Schinkel, A.H., *Pharmacological and physiological functions of the polyspecific organic cation transporters: OCT1, 2, and 3 (SLC22A1-3).* Journal of Pharmacology and Experimental Therapeutics, 2004. **308**(1): p. 2-9.

14. Koepsell, H., *Polyspecific organic cation transporters: Their functions and interactions with drugs.* Trends in Pharmacological Sciences, 2004. **25**(7): p. 375-381.

15. Lecureur, V., Guillouzo, A., and Fardel, O., *Differential expression of the polyspecific drug transporter OCT1 in rat hepatocarcinoma cells.* Cancer Letters, 1998. **126**(2): p. 227-233.

16. Yokoo, S., Masuda, S., Yonezawa, A., Terada, T., Katsura, T., and Inui, K.I., *Significance of organic cation transporter 3 (SLC22A3) expression for the cytotoxic effect of oxaliplatin in colorectal cancer.* Drug Metabolism and Disposition, 2008. **36**(11): p. 2299-2306.

17. Zhang, S.Z., Lovejoy, K.S., Shima, J.E., Lagpacan, L.L., Shu, Y., Lapuk, A., Chen, Y., Komori, T., Gray, J.W., Chen, X., Lippard, S.J., and Giacomini, K.M., *Organic cation transporters are determinants of oxaliplatin cytotoxicity.* Cancer Research, 2006. **66**(17): p. 8847-8857.

18. Hollis, L.S., Amundsen, A.R., and Stern, E.W., *Chemical and biological properties of a new series of cis-diammineplatinum(II) antitumor agents containing 3 nitrogen donors - cis-[Pt(NH3)2(N-donor)Cl]+*. Journal of Medicinal Chemistry, 1989. **32**(1): p. 128-136.

19. Lovejoy, K.S., Todd, R.C., Zhang, S.Z., McCormick, M.S., D'Aquino, J.A., Reardon, J.T., Sancar, A., Giacomini, K.M., and Lippard, S.J., *Cis-diammine(pyridine)chloroplatinum(II), a monofunctional platinum(II) antitumor agent: Uptake, structure, function, and prospects.* Proceedings of the National Academy of Sciences of the United States of America, 2008. **105**(26): p. 8902-8907.

20. Lau, W.Y. and Lai, E.C.H., *Hepatocellular carcinoma: Current management and recent advances.* Hepatobiliary & Pancreatic Diseases International, 2008. **7**(3): p. 237-257.

21. Gruendemann, D., Koester, S., Kiefer, N., Breidert, T., Engelhardt, M., Spitzenberger, F., Obermueller, N., and Schoemig, E., *Transport of monoamine transmitters by the organic cation transporter type 2, OCT2.* Journal of Biological Chemistry, 1998. **273**(47): p. 30915-30920.

22. Fernandez, F.G., Ritter, J., Goodwin, J.W., Linehan, D.C., Hawkins, W.G., and Strasberg, S.M., *Effect of steatohepatitis associated with irinotecan or oxaliplatin pretreatment on resectability of hepatic colorectal metastases.* Journal of the American College of Surgeons, 2005. **200**(6): p. 845-853.

23. Rubbia-Brandt, L., Audard, V., Sartoretti, P., Roth, A.D., Brezault, C., Le Charpentier, M., Dousset, B., Morel, P., Soubrane, O., Chaussade, S., Mentha, G., and Terris, B., *Severe hepatic sinusoidal obstruction associated with oxaliplatin-based chemotherapy in patients with metastatic colorectal cancer.* Annals of Oncology, 2004. **15**(3): p. 460-466.

24. Shu, Y., Brown, C., Castro, R.A., Shi, R.J., Lin, E.T., Owen, R.P., Sheardown, S.A., Yue, L., Burchard, E.G., Brett, C.M., and Giacomini, K.M., *Effect of genetic variation in the organic cation transporter 1, OCT1, on metformin pharmacokinetics.* Clinical Pharmacology & Therapeutics, 2008. **83**(2): p. 273-280.

25. Shu, Y., Sheardown, S.A., Brown, C., Owen, R.P., Zhang, S.Z., Castro, R.A., Ianculescu, A.G., Yue, L., Lo, J.C., Burchard, E.G., Brett, C.M., and Giacomini, K.M., *Effect of genetic variation in the organic cation transporter 1 (OCT1) on metformin action.* Journal of Clinical Investigation, 2007. **117**(5): p. 1422-1431.

26. Wang, D.S., Jonker, J.W., Kato, Y., Kusuhara, H., Schinkel, A.H., and Sugiyama, Y., *Involvement of organic cation transporter 1 in hepatic and intestinal distribution of metformin.* Journal of Pharmacology and Experimental Therapeutics, 2002. **302**(2): p. 510-515.

27. Kalow, W., Endrenyi, L., and Tang, B.K., *Repeat administration of drugs as a means to assess the genetic component in pharmacological variability.* Pharmacology, 1999. **58**(6): p. 281-284.

Publishing Agreement

It is the policy of the University to encourage the distribution of all theses, dissertations, and manuscripts. Copies of all UCSF theses, dissertations, and manuscripts will be routed to the library via the Graduate Division. The library will make all theses, dissertations, and manuscripts accessible to the public and will preserve these to the best of their abilities, in perpetuity.

Please sign the following statement:

I hereby grant permission to the Graduate Division of the University of California, San Francisco to release copies of my thesis, dissertation, or manuscript to the Campus Library to provide access and preservation, in whole or in part, in perpetuity.

Shuaylian Li
Author Signature

June, 01, 2010
Date